Atmospheric pressure plasmas for surface modification

Ward, Luke John

ATMOSPHERIC PRESSURE PLASMAS FOR SURFACE MODIFICATION

Luke John Ward

Ph.D. Thesis

Department of Chemistry
University of Durham

JANUARY 2001

For Mum and Dad

STATEMENT OF COPYRIGHT

DECLARATION

The work in this thesis was carried out in the Chemistry Department at the University of Durham between October 1997 and September 2000. It is the original work of the author, except where otherwise acknowledged, and has not been submitted previously for a degree at this or any other University.

Atomic force microscopy was performed by Stephen Ebbens (Chapter 2) and Iain Woodward (Chapters 2 and 4). Argon ion depth profiles were obtained by Jonathan Crowther and Christos Spanos (Chapter 2). Spectrophotometric thickness measurements were carried out by Wayne Schofield (Chapters 5 and 6).

LIST OF PUBLICATIONS

Work in this thesis has been published or will be submitted for publication as follows:

"Solventless Coupling of Perfluoroalkyl Chlorosilanes to Polymer Surfaces", Ward, L.J.; Badyal, J.P.S., in preparation.

"Atmospheric Growth of Polysilane Layers and Their Conversion to SiO_x", Ward, L.J.; Badyal, J.P.S., in preparation.

"Atmospheric Pressure Plasma Oxidation of Polydimethylsiloxane-Polyethylene Blend Surfaces", Ward, L.J.; Woodward, I.S.; Badyal, J.P.S., in preparation.

"Atmospheric Pressure Glow Discharge Deposition of Polysiloxane and SiO_x Films", Ward, L.J.; Schofield, W.C.E.; Badyal, J.P.S., in preparation.

"Atmospheric Pressure Plasma Deposition Of Structurally Well-Defined Polyacrylic Acid Films", Ward, L.J.; Schofield, W.C.E.; Badyal, J.P.S., in preparation.

ACKNOWLEDGEMENTS

I wish to express my gratitude to Professor Jas Pal Badyal, my supervisor, for three years of help, guidance and tolerance of property damage. Andy Goodwin and Patrick Merlin, my industrial sponsors at Dow Corning, are also thanked for their advice and perspective.

Hearty thanks go to everyone in lab 98 for their willingness in matters primarily social and to the staff of the "chem caff" for their tireless purveyance of pasties to hung-over chemists.

Thanks also to those who helped build a seemingly unending series of ever more ludicrous and dangerous pieces of equipment: George, Kelvin and Barry in the electrical workshop, Jim and Neil in the mechanical workshop and Gordon, Ray, Malcolm and Peter, the glassblowers. I am indebted to your patience.

And to everyone else who has helped in any way, cheers.

ABSTRACT

Many methods are currently used for the production of silicon oxide films, most have drawbacks associated with high temperatures and the requirement for a vacuum. Atmospheric pressure plasma treatment can address some of these difficulties.

Air silent discharge treatment of spin-coated organo-silicon compounds resulted in substantial oxidation. The depth and morphology of the oxidised region was found to depend on the structure of the precursor.

Condensation of substituted chlorodisilanes (SCDS) onto polymer surfaces yielded polysiloxane-like layers. Upon atmospheric pressure plasma oxidation these gave rise to SiO_x rich films which exhibited gas barrier, and readily underwent reaction with conventional chlorosilane coupling reagents.

Dielectric barrier discharge and atmospheric pressure glow discharge (APGD) modification of polydimethylsiloxane (PDMS) containing polyethylene blends led to the formation of wettable, SiO_X rich coatings. The hydrophobic recovery, SiO_x content, reactivity and topography of the oxidised films was found to depend on the architecture of the PDMS additive.

The limited depth penetration of plasma oxidation was thought to limit its potential as a gas barrier technology. The development of a novel APGD plasma reactor equipped with an ultrasonic nozzle enabled the creation of thick coatings from cyclotetrasiloxane monomers. Control of the feed gas allowed the rapid deposition of both hydrophobic polysiloxane-like films and hydrophilic SiO_x gas barrier coatings.

The APGD deposition methodology was extended to the creation of organic plasma polymers. The resultant polyacrylic acid and 1H, 1H, 2H,-perfluoro-1-octene films were highly functionalised and exhibited properties comparable with their conventionally manufactured counterparts.

"Nothing blinds quite so much as wishful thinking"

Richard Feynman

CONTENTS

CHAPTER 1 INTRODUCTION TO SILICON DIOXIDE FILMS AND HIGH PRESSURE NON-EQUILIBRIUM PLASMAS

1.1 THIN SILICON DIOXIDE FILMS 2

1.1.1 Introduction 2

1.1.2 Thin Silica Film Manufacture 2

1.2 HIGH PRESSURE NON-EQUILIBRIUM PLASMAS 6

1.2.1 Introduction 6

1.2.2 The Physics of Gas Breakdown 7

1.2.3 The Dielectric Barrier Discharge (DBD) 10

1.2.4 Atmospheric Pressure Glow Discharge (APGD) 13

1.2.5 High-Pressure Pulsed Volume Discharge. 14

1.2.6 Corona Discharge. 15

1.3 CHARACTERIZATION TECHNIQUES 17

1.3.1 X-Ray Photoelectron Spectroscopy (XPS) 17

1.3.2 Fourier Transform Infra-Red Spectroscopy 20

1.3.3 Contact Angle Analysis 20

1.3.4 Gas Barrier Characterization 22

1.3.5 Atomic Force Microscopy (AFM) 23

1.4 REFERENCES 24

CHAPTER 2 ATMOSPHERIC PRESSURE PLASMA OXIDATION OF ORGANO-SILICON COATINGS

2.1 INTRODUCTION 33

2.2 EXPERIMENTAL 35

2.3 RESULTS 37

2.3.1 The Discharge Frequency Dependence of PCHMS, PPSQ and PPSQ Oxidation 37

2.3.2 Argon Ion Depth Profiles of Oxidized PCHMS, PPSQ and PPSQ 45

2.3.3 Atomic Force Microscopy of Oxidized PCHMS, PPSQ and PPSQ 47

2.3.4 Power and Off-Time Dependence of PMSQ Oxidation 51

2.4 DISCUSSION 54

2.5 CONCLUSIONS 56

2.6 REFERENCES 57

CHAPTER 3 THE ATTACHMENT OF CHLOROSILANE COUPLING AGENTS TO POLYMER SURFACES

3.1 INTRODUCTION 61

3.2 SOLVENTLESS COUPLING OF PERFLUOROALKYL CHLOROSILANES TO POLYMER SURFACES 63

3.2.1 Introduction 63

3.2.2 Experimental 63

3.2.3 Results 64

3.2.4 Discussion 72

3.2.5 Conclusions 73

3.3 ATMOSPHERIC GROWTH OF POLYSILOXANE LAYERS AND THEIR CONVERSION TO SiO_x 74

3.3.1 Introduction 74

3.3.2 Experimental 75

3.3.3 Results 77

3.3.4 Discussion 88

3.3.5 Conclusions 90

3.4 REFERENCES 91

CHAPTER 4 ATMOSPHERIC PRESSURE PLASMA OXIDATION OF POLYDIMETHYLSILOXANE-POLYETHYLENE BLEND SURFACES

4.1 INTRODUCTION 96

4.2 EXPERIMENTAL 97

4.3 RESULTS 98

4.3.1 Surface Segregation of PDMS Segments Upon Annealing 98

4.3.2 Atmospheric Pressure Plasma Oxidation of PDMS Enriched Polymer Blend Surfaces 99

4.3.3 Chlorosilane Coupling to Plasma Oxidized PDMS Blend Surfaces 107

4.4 DISCUSSION 111

4.5 CONCLUSIONS 113

4.6 REFERENCES 114

CHAPTER 5 ATMOSPHERIC PRESSURE GLOW DISCHARGE DEPOSITION OF POLYSILOXANE AND SiO_x FILMS

5.1INTRODUCTION 117

5.2 EXPERIMENTAL 118

5.3 RESULTS 120

5.3.1 Octamethylcyclotetrasiloxane Deposition 120

5.3.2 Tetramethylcyclotetrasiloxane Deposition 125

5.4 DISCUSSION 129

5.5 CONCLUSIONS 129

5.6 REFERENCES 131

CHAPTER 6 ATMOSPHERIC PRESSURE PLASMA DEPOSITION OF STRUCTURALLY WELL-DEFINED POLYACRYLIC ACID AND 1H, 1H, 2H - PERFLUORO- 1 -OCTENE FILMS

6.1 INTRODUCTION 135

6.2 EXPERIMENTAL 136

6.3 RESULTS 138

6.3.1 APGD Polymerization of Acrylic Acid 138

6.3.2 APGD Polymerization of 1H, 1H, 2H-Perfluoro-1-octene 142

6.4 DISCUSSION 146

6.5 CONCLUSIONS 148

6.6 REFERENCES 149

7.0 CONCLUSIONS AND FUTURE WORK

7.1 CONCLUSIONS 153

7.2 FUTURE WORK 155

APPENDIX

Colloquia and Seminars from Invited Speakers.....157

Examined Lecture Courses.....160

Conferences Attended.....160

Presentations.....160

PROJECT AIM

The long-term goal of this project was an industrially viable means of converting low cost polyethylene feedstocks into oxygen-impermeable packaging materials. A thin, surface coating of silicon dioxide appeared to be the ideal means of achieving this. The extended, immobile, structure imparting gas barrier characteristics without adversely effecting polymer processibility or transparency (the latter in contrast to traditional metallic coatings).

Unfortunately, polyethylene's incompatibility with high temperature processing excluded many traditional methods for producing siliceous coatings. Of the remaining low-temperature means of oxidation atmospheric-pressure non-equilibrium plasmas appeared the most environmentally friendly and cost effective; requiring neither solvents nor expensive vacuum maintenance.

Initial investigations focused upon the atmospheric-pressure plasma surface oxidation of organo-silicon systems such as spin-coated polysilsesquioxanes, annealed polydimethylsiloxane / polyethylene blends and condensed layers of substituted-chlorodisilanes. Unfortunately, the resultant films whilst rich in siliceous material, and in some cases possessing useful hydrophobic recovery and reactivity properties, were too thin and defective to prevent oxygen transmission without a tedious reiterative approach. In response to this a deposition methodology was developed which combined an atmospheric pressure plasma with a novel gas-phase monomer delivery system. The resultant films were SiO_x rich and thick enough for gas barrier enhancement. The plasma deposition methodology also merited extension to organic monomers, yielding highly functionalised polymeric films similar to those produced with low-pressure plasmas.

CHAPTER 1

INTRODUCTION TO SILICON DIOXIDE FILMS AND HIGH PRESSURE NON-EQUILIBRIUM PLASMAS

1.1 THIN SILICON DIOXIDE FILMS

1.1.1 INTRODUCTION

Thin films of silicon dioxide are characterized by their high thermal and chemical stability, transparency, high surface energy, high dielectric strength, and barrier properties.[1,2,3] These attributes have lead to widespread application in packaging, microelectronics,[4] and wettability and adhesion modification. For these reasons the production of thin silica films is of considerable commercial importance.

1.1.2 THIN SILICA FILM MANUFACTURE

There are many techniques currently used to manufacture silicon dioxide films and the preferred methodology depends upon the demands of the application.

In microelectronics the films must be of the highest possible quality. In the drive for smaller device sizes ever thinner films have to meet stringent electrical requirements leading to a need for increased purity and step-coverage (the ability of a film to follow substrate features).

Gas barrier coatings must also meet rigorous standards, typically having to possess 10^4-10^5 times better barrier properties than the polymer substrate.[1] This requires that the films are virtually defect free, restricting their production to processes which result in no cracking, surface roughness or particle formation.

1.1.2.1 Chemical Vapour Deposition (CVD)

CVD is a high temperature (usually > 873 K) methodology which may be performed at high or low pressure. In CVD the feed gases are thermally decomposed and the decomposition products diffuse onto the substrate to form the film.[5] At low pressure (30-90 Torr) the source gas reacts near the surface and creates the film directly. At high pressures (760 Torr) gas phase reactions form intermediate products which may form particles prior to deposition.[5]

CVD is normally performed using binary mixtures of a silicon source and either N_2O or O_2. The silicon source is usually silane (SiH_4) or a siloxane. The toxicity and flammability hazards associated with silane have made siloxanes such as tetraethoxysiloxane (TEOS) increasingly popular.[6]

The high substrate temperatures traditionally required for CVD can result in wafer warpage, dopant redistribution, defect generation and the deformation of predeposited metal lines.[7] In addition many semiconductors such as amorphous silicon (a-:Si), gallium arsenide (GaAs) and indium phosphide (InP) are temperature sensitive.[8] A variant of CVD which addresses this problem is the low temperature atmospheric pressure CVD method in which the source gas is reacted with ozone. The use of ozone, a reactive ground state oxidant, allows pure, conformal films to be deposited from siloxane precursors at temperatures of around 673 K.[9,10,11,12]

1.1.2.2 Plasma Enhanced Chemical Vapour Deposition (PECVD)

The PECVD method uses a plasma to promote the reaction of the silicon source with excited oxygen species, usually derived from O_2 or N_2O.[13] The silicon containing feed gases are those used in CVD (silane and siloxanes such as TEOS) and the plasmas are generally low pressure RF glow or microwave discharges.[14]

PECVD is a relatively low temperature technique, able to coat polymeric substrates, making it popular for producing gas barriers.[13,15,16] However, to produce coatings of sufficient quality for microelectronics substrate heating ($\geq$ 573 K) is necessary to completely remove the residual carbon and hydrogen.[17,18]

Silica films deposited by PECVD are often more porous and contain more hydrogen than those deposited by thermal methods.[19] Film quality is strongly dependent on deposition conditions with complex correlations between parameters making optimization difficult.[19,20] Deposition can be rapid and the accompanying ion bombardment is thought to improve film density and decrease Si-OH content.[21,22] However, the high energy species present in plasmas can damage the substrate and the growing film. The positive plasma potential accelerates ions into the chamber wall, sputtering impurities and reducing film quality.[4,7] A means of avoiding these problems is for the silicon

source to be introduced downstream from the plasma (Remote PECVD).[23,24] As the substrate is outside the discharge region deposition occurs without plasma or radiation damage.[25,26] Typically the plasma is generated from O_2 or N_2O, sometimes with a diluent gas such as He or Ar.[27,28] Films have also been fabricated from N_2 and Ar plasmas but oxygen radicals are thought to be necessary to ensure the complete removal of hydrogen and organic contamination.[29]

1.1.2.3 Photo Chemical Vapour Deposition

Photo CVD utilises high energy photons (VUV) to dissociate the gaseous precursors. This approach avoids the thermal exposure and particle bombardment inherent in many methods with the added advantage that the deposition area can be selected by local irradiation of the substrate.[30]

A popular source of intense VUV radiation are silent discharge excimer lamps. These are efficient, reliable, easily scaled up and, unlike mercury lamps, do not require a sensitiser, thus avoiding contamination.[31,32] The most commonly used excimer lamps contain Xe_2^* excimers which produce radiation at a wavelength of 172 nm. This corresponds to a photon energy of 7.2 eV: sufficient to break C-O and C-H bonds (bond energies 3.8 and 4.2 eV respectively) but insufficient to break Si-O bonds (bond energy 8.3 eV), making them ideal for SiO_2 deposition.[33]

Photo CVD is performed at low pressure (~8 Torr) using SiH_4 and either N_2O or O_2. Adequate films can be produced at temperatures as low as 573 K, but the deposition rate is very low and the film purity is inferior to thermally produced oxides.[8,30,34]

1.1.2.4 Reactive Evaporation

Films containing Si, SiO and SiO_2 result when a silicon monoxide source is evaporated in the presence of oxygen using an electron beam (generated by a hot filament, typically tungsten).[1] Deposition speeds are high and the Si is thought to be present as free atoms, conferring additional potential in luminescent devices.[13,35] However, low pressures are required to maintain the electron beam and capital costs are expensive.

1.1.2.5 *Modification of Precursor Films*

Silica coatings can be generated by modifying existing silicon containing precursor layers. The thermal degradation of polydimethylsiloxane (PDMS) yields silicon oxide, although the high treatment temperature (> 1073 K) makes it unsuitable for most systems.[36]

UV exposure of spin coated TEOS films in an inert atmosphere results in SiO_x formation.[37] Alternatively a combination of UV and oxygen can be used to generate ozone at the sample surface. Silicon wafers and PDMS Langmuir Blodgett films develop silica over-layers when oxidized by this method.[38,39,40] Both UV methods are slow, taking up to 30 minutes to completely remove the organic component of the precursor.

Low pressure glow discharge and corona oxidation of PDMS and polysilanes rapidly yield wettable, siliceous surfaces.[41,42,43,44,45] However, these techniques rapidly create thin SiO_X layers which block further reaction, restricting oxide thickness. This makes surface plasma oxidation of limited use, best suited to circumstances where only the topmost surface needs to be oxidized (e.g. in wettabilty and adhesion applications).

1.1.2.6 *Solution Phase Methods*

Silica layers may be generated at low temperatures (< 373 K) by solution phase methods. Sol gel and aero gel techniques utilise the hydrolysis and condensation of alkoxysiloxanes (e.g. TEOS) in acidic solutions. Coating properties range from dense and mechanically resilient films to porous membranes depending on the conditions.[46,47]

1.2 HIGH PRESSURE NON-EQUILIBRIUM PLASMAS

1.2.1 INTRODUCTION

A plasma is defined as a volume of quasi-neutral ionized gas in which local concentrations of charge dominate particle motion, giving rise to collective behaviour.[48,49]

There are two main categories of plasma: equilibrium and non-equilibrium. In an equilibrium plasma the electron and gas temperatures are approximately equal. Their high energy density has led to use in the reduction and smelting of ores and the treatment of industrial wastes.[50] However, the high temperatures of equilibrium discharges make them unsuitable for direct treatment of most substrates.

Non-equilibrium plasmas are characterized by the absence of thermodynamic equilibrium between the discharge species. The electron temperature (T_e= 10^4-10^5 K) is much higher than that of the ions and neutrals (T_g~300 K).[51] The high electron energy enables energetic reactions to proceed whilst the gas temperature does not rise significantly above that of the ambient environment, allowing the treatment of heat sensitive materials such as polyolefins. Most plasmas of this type (DC glow, RF glow, microwave glow) operate at pressures below 10 Torr and require pumping systems. This makes them expensive, difficult to scale up and more suited to batch processing. In contrast, high pressure non-equilibrium plasmas, such as corona and dielectric barrier discharge, do not require expensive vacuum maintenance and are more suited to continuous processing.[52]

1.2.2 THE PHYSICS OF GAS BREAKDOWN

1.2.2.1 Townsend Breakdown

Due to the effects of naturally occurring ionization sources, such as cosmic rays or radioactivity, gases always contain some free electrons. When an electric field is applied across a volume of gas these electrons are accelerated. As electrons are light only a small fraction of their kinetic energy is transferred in elastic collisions with atoms and molecules. Hence the energy of the electrons rapidly increases under the influence of the applied field. Ultimately the electrons have sufficient energy to cause inelastic collisions, resulting in ionization and excitation. This results in a cascade effect, wherein one electron can give rise to an avalanche of free electron production which spreads throughout the discharge space. Eventually secondary electron creation is sufficient to maintain the discharge at a steady state where electron production and loss are equal. The impact of positive ions and photons on the cathode is thought to be the main source of secondary electrons.[53,54,55,56] This leads to the Paschen breakdown law, Equation 1.1, where P is the pressure, d the electrode gap, α the Townsend first ionization coefficient for the gas, and γ the Townsend second ionization coefficient for the cathode surface.

$$Pd = \frac{1}{\alpha / P} \ln\left(1 + \frac{1}{\gamma}\right) \qquad \textbf{Equation 1.1}$$

The Townsend mechanism is prevalent at low pressures and controls the early stages of glow discharge development.[53,57] Multiple primary avalanches build-up until secondary emission is sufficient to counter electron loss. However, due to the effects of space charge (local regions of net positive charge[55]) most low pressure plasmas actually possess fairly complicated structures and are comprised of different regions with quite different properties.

1.2.2.2 *Streamer Breakdown*

The streamer breakdown mechanism is most probable when the Pd product is larger than 10 Torr cm, such as at atmospheric pressure with a discharge gap greater than 0.1 mm.[57]

An applied electric field causes electron avalanches to propagate from the cathode to the anode. Because electrons are much more mobile than ions a positive space charge develops behind the cascade heads. The high Pd value can result in the space charge of an avalanche creating a self induced field comparable to that of the applied field. The resultant field enhancement occurs along the direction of avalanche propagation and accelerates the tail electrons of the avalanche to high velocities, leading to the rapid propagation of a breakdown channel towards the anode. UV photons produced within the primary cascade assist this process by generating secondary electron cascades which converge on the primary avalanche (as a result of its high space charge). Once the streamer reaches the anode its field is reflected, resulting in a backwards wave of ionization being propagated towards the cathode, bridging the electrode gap. Hence the rapid development of a filamentary conducting channel (or micro-discharge) can result from the passage of just one electron avalanche across the discharge gap, Figure 1.1.[53,57,58,59,60]

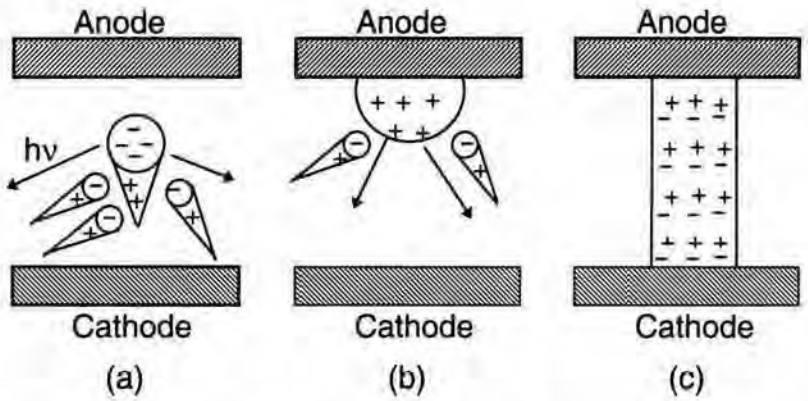

Figure 1.1 Three stages of micro-discharge production, (a) streamer development around a single primary electron avalanche, (b) backward propagation of a cathode-directed plasma streamer after the arrival of the primary avalanche head at the anode, (c) bridging of the electrode gap by the plasma streamer.[61]

1.2.2.3 The Glow to Arc Transition

High pressure plasmas are fundamentally unstable, an atmospheric Townsend discharge can develop a spatial instability causing its homogenous current distribution to collapse into an arc. This transition from a glow to an arc discharge occurs over a timescale characteristic of the gas, gas pressure, discharge gap length and state of the overvoltage.[61,62,63] The development of an atmospheric pressure discharge with time is illustrated by the 'Kekez curve', Figure 1.2.[64]

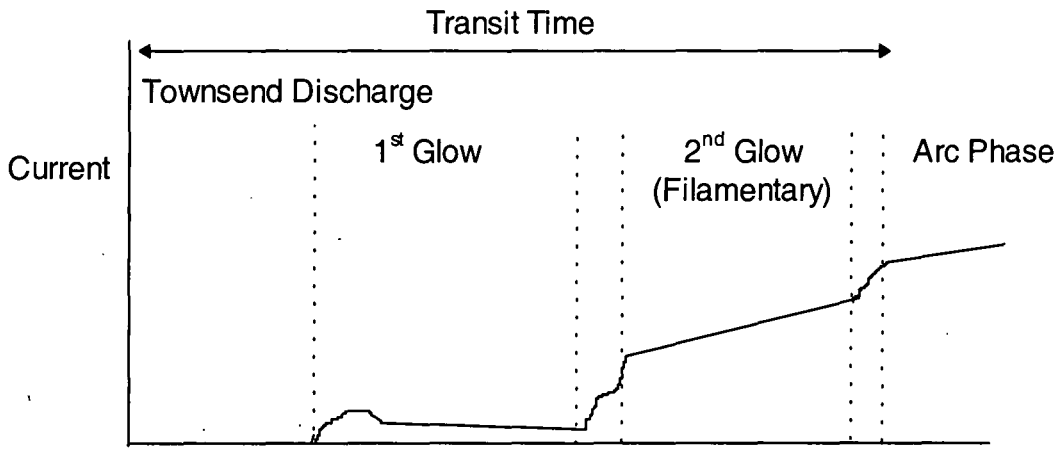

Figure 1.2 The Kekez curve.[64]

An atmospheric pressure plasma starts as a Townsend discharge, changes into a glow discharge (first glow), develops into a filamentary discharge (second glow) and finally forms an arc. In some situations the transition to an arc can be suppressed through the use of current-limiting devices in an external circuit. Unfortunately this technique is not generally applicable to the atmospheric pressure discharges currently under investigation.[53] A useful, stable discharge can only be obtained by manipulating the discharge conditions so as to control the breakdown mechanism.

1.2.3 THE DIELECTRIC BARRIER DISCHARGE (DBD)

1.2.3.1 Discharge Characteristics

Dielectric barrier discharge (or silent discharge) is a non equilibrium plasma operated at pressures from 75 to 7500 Torr.[58] It is characterized by the presence of at least one dielectric barrier in the inter-electrode gap (a few mm).

When a rising voltage (in excess of the breakdown or Paschen voltage of the system) is applied between the electrodes current is carried across the discharge gap by numerous micro-discharges. The formation of these micro-discharges is a result of the high Pd product favouring the streamer breakdown mechanism, Section 1.2.2.2.

When a streamer reaches the electrode, charge build-up occurs on the dielectric, producing a field directed against the applied field. This reduces the total field in the neighbourhood of the dielectric until the flow of current is choked and the current drops to zero.[58,59,60,65]. Other micro-discharges initiated by the still rising applied voltage will then preferentially strike at different locations with higher electric fields.[59,60] The role of the dielectric is hence twofold: it ensures the random spatial distribution of the micro-discharges across the entire electrode surface and it extinguishes them, preventing the transition to an arc, Section 1.2.2.3.

Total charge	10^{-10} A s
Current density	10^{3} A cm^{-2}
Electron density	10^{14} cm^{-3} (c.f. RF discharge: 10^{10} cm^{-3})
Electron energy	>5 eV
Streamer diameter	100 μm
Micro-discharge duration	100 ns

Table 1.1 The properties of a typical micro-discharge.[4,60]

1.2.3.2 Discharge Chemistry

The short lifetime of micro-discharges enables high gas pressures to be used without causing significant sputtering of the electrodes, eliminating the corrosion and contamination problems associated with traditional arc processes.[31] The high energy electrons within a micro-discharge deposit almost all of their energy into the excited states of species within the discharge channel resulting in little interaction with atoms and molecules outside the filament.[66]

The vast majority of charged species with a micro-discharge decay before they can react so the chemistry of silent discharge is ostensibly that of radicals and excited ground state neutral species.[58] An approximate time-scale for the processes that occur after the application of the voltage is given in Table 1.2.

ps	Electrons reach equilibrium (Boltzmann energy distribution) corresponding to applied field)
ns	Micro-discharge formation (breakdown, excitation, dissociation and ionization)
μm-ms	Free radical chemistry
s	Ground state chemistry

Table 1.2 Time-scales for dielectric barrier discharge processes.

1.2.3.3 Applications

(a) Ozone Generation

The first step in the production of ozone is the electron-impact dissociation of oxygen molecules. The high electron energies required for this reaction (> 6 eV) necessitate a high reduced field. Hence ozonizers operate with kV alternating applied voltages and small gap widths (≤ 1 mm).[59,60,67]

The gas feed is also of great importance. Air fed ozonizers, in comparison with oxygen-fed ozonizers, require twice as much energy to produce the same quantity of ozone and can reach only half the ozone concentration. This enhancement (air-fed ozonizers would be expected to produce a fifth of the ozone of those using pure oxygen) is thought to be due to reactions involving excited nitrogen species and N_xO_y yielding O atoms.[68] Ozonizers also have to be very dry (a few ppm H_2O) otherwise water coats the

dielectric, increasing its dielectric constant and resulting in the production of fewer, but excessively strong, micro-discharges.[58,69,70]

(b) Excimer Lamps

The energy and electron densities within micro-discharges are comparable to those of discharge pumped excimer lasers. It is hence possible to use silent discharge to produce excimers, providing an intense, efficient source of UV and VUV light. The gas mixture (75 to 750 Torr) is usually sealed within a quartz envelope which acts as the dielectric. The outer electrode is a wire mesh to permit the passage of emitted photons.[8,31,71]

Many excimers and exciplexes have been discovered, mainly noble gas dimers and noble gas / halogen complexes, their emission covering the range 50 - 600 nm. Silent discharge lamps can therefore provide radiation over the range most important for photo-induced bond breaking.[58,59,71] This makes them ideal for rapid UV curing, photo-etching, photochemical vapour deposition of dielectrics and the pollutant destruction.[7,30,31,33,34,71,72]

(c) Other Applications

Air atmospheric pressure discharges are often used to enhance the wettability and adhesion properties of polymeric substrates.[59,73] This action is believed to arise from surface oxidation and / or topographical surface alteration of the substrate.

The ions and radicals produced by dielectric barrier discharge, especially $O(^3P)$, $O(^1D)$ and in wet air HO_2 and OH, are capable of rapid and sometimes highly selective chemical reactions.[59] This reactivity is a potential means of pollution control with the reduction of NO_x and SO_x and the treatment of volatile organic compounds (VOCs) having been investigated.[74,75]

Film deposition by dielectric barrier discharge has received relatively little attention. Isolated examples are the plasma polymerization of acetylene into homogenous hydrocarbon films and the production of amorphous $Si_{1-x}C_x$ from mixtures of silane and methane.[76,77,78]

1.2.4 ATMOSPHERIC PRESSURE GLOW DISCHARGE (APGD)

1.2.4.1 Discharge Characteristics

The atmospheric pressure glow discharge (APGD) is a non-filamentary, high pressure pulsed discharge, stable across interelectrode gaps of several cm.[62] Stable APGDs result when high flow rates of helium are used in a dielectric barrier discharge configuration with a voltage source of frequency greater than 1 kHz.

The first stage of APGD formation is controlled by the Townsend mechanism, section 1.2.2.1.[57] However, at Pd products of over 10 Torr cm the streamer mechanism soon becomes the dominant process. The conditions which maintain an APGD prevent this transition by suppressing the formation of electron avalanches with sufficient space-charge to attract secondary cascades. Experiments with dielectric barrier discharges show that the formation of seed electrons by UV irradiation increases discharge homogeneity (micro-discharges become weaker but more numerous) by creating multiple initial electron avalanches (The Joshi Effect).[70] In APGD this effect is achieved by the very low breakdown voltage of helium. The high energy metastable states of helium may also help to maintain the APGD by ionizing species on the dielectric and extending the discharge points.[63]

The precise nature of APGD not yet fully understood. Whether they are a true glow or more akin to a great number of coupled filaments is a basic question that has not yet been answered. The observation of regions within a helium APGD similar to the negative glow, Faraday dark space and positive column of a low-pressure glow discharge, and ion and electron density measurements suggest that the plasma is a true glow discharge.[57]

1.2.4.2 Discharge Chemistry

Although APGDs consist largely of helium, small quantities (<5%) of any other gas can be added, enabling the plasma to exhibit a range of chemistries.

The principle activation mechanism within an APGD is a Penning reaction with metastable helium.[79] These excited species possess high internal

energies (2^3S: 19.8 eV, 2^1S: 20.7 eV)[79] and are capable of activating most reactions as molecular dissociation typically requires 5-10 eV.[63]

$$He\ (2^3S) + A \rightarrow He + A^+ + e$$
$$He\ (2^1S) + A \rightarrow He + A^+ + e$$

Scheme 1.1 Penning Ionization.[56]

1.2.4.3 Applications

In principle APGDs have huge commercial potential as they combine the homogeneity of low pressure plasma processing with the convenience of an atmospheric system. Plasma polymerization has been found to produce films very similar in quality to those generated by low pressure glow discharges, despite the dissimilar excitation mechanism.[79,80,81] Other applications include wettability enhancement,[82,83] sterilisation,[84] and metal reduction.[85]

1.2.5 HIGH-PRESSURE PULSED VOLUME DISCHARGE.

1.2.5.1 Discharge Characteristics

A volume discharge reactor consists of two parallel metal plates and a very high voltage (>> 10 kV) power supply, capable of producing fast rising pulses of the order of 10^{-8} s duration. An external pre-ionization source, e.g. UV, X-rays, γ-rays, α particles, electron beam or corona discharge, is also required to create the initial conditions required for the formation of a homogenous discharge. The pre-ionization provides an initial electron density such that when the external voltage is applied a large number of primary avalanches are created. Subsequent overlapping of the secondary ionization generated by the primary avalanches then homogenises the resulting discharge. This smoothing prevents the formation of the strong local gradients in space charge which lead to streamer formation.[53,61,86] The use of pre-ionization thus compensates for the absence of the strong electronic and ionic diffusion effects responsible for the homogenisation and stability of low pressure glow discharges.[61] The use of

fast rising voltage pulses of short duration also prevents arcing as the electric field is not on long enough to allow the transition to an arc.

1.2.5.2 Applications

Pulsed homogenous volume discharges have been used for some time in Transversely Excited Atmospheric-Pressure (TEA) lasers where they are used to pump CO_2, N_2 and HF. More recently they have been used in rare-gas halide and metal halide excimer lasers.[53,61]

Pulse volume discharges also have potential use as ozonizers, theoretical calculations indicate that they are capable of greater ozone yield and higher generation efficiency than conventional silent discharge models.[87]

1.2.6 CORONA DISCHARGE

1.2.6.1 Discharge Characteristics

The corona is a high-pressure discharge stabilised by the use of an inhomogeneous electrode geometry: a point and a plate, a point and a ring or a coaxial wire and tube. Two basic discharges are possible depending on which electrode is the point: a positive corona results if the anode is the point and a negative corona if the cathode is the point. In both cases, at sufficiently high voltages the plasma takes the form of a small localised glow around the point. The field decreases rapidly away from this region and reaches a minimum near the plate, largely preventing the movement of charge carriers to the plate.[88]

Electric field	0.5-50 kV/cm variable
Electron energy	5 eV variable
Electron density	10^{13} cm^{-3}
Degree of ionization	small, variable

Table 1.3. Characteristic parameters of corona discharges.[88]

1.2.6.2 Applications

The utility of corona discharge is limited by the low degree of excitation and small discharge volume, Table 1.3.[89] It has hence been largely superseded by dielectric barrier discharge in most applications.

Corona discharges are however useful in applications where only a small quantity of excited species are required. Typical examples are electrostatic precipitators and copying machines where corona discharge is used to provide charged particles.[90,91]

Another application is the surface treatment of polymers. Polymer wettability and adhesion are increased by corona treatment, an effect thought to be due to oxidation and electrostatic charging.[92] Corona discharge can also be used to generate peroxide functionalities which are then capable of initiating graft polymerization.[93]

Coronas have received revived interest for pollution control due to the development of the pulsed corona discharge (PCD) which uses a DC power supply to produce fast rising pulses of less than 1 μs duration. This allows much higher electric fields to be applied without causing an arc breakdown.[94] PCDs resemble the micro-discharges produced by DBD and are hence a highly effective means of reducing NO_x,[95] producing ozone,[96] and destroying volatile organic compounds.[97]

1.3 CHARACTERIZATION TECHNIQUES

1.3.1 X-RAY PHOTOELECTRON SPECTROSCOPY (XPS)

XPS is a surface specific characterization technique which probes the uppermost 5 nm of a sample. Analysis is carried out in ultra-high vacuum (UHV) to minimise sample contamination and prevent scatter of the photo-electrons prior to analysis.[98]

In an XPS experiment the sample is irradiated by high energy photons (typically soft X-rays) resulting in the ejection of core electrons by the photoelectron effect. The kinetic energies of these electrons are measured and their binding energies calculated from Equation 1.2, where E_K and E_B are the kinetic and binding energies of the photo-emitted electron, $h\nu$ the energy of the exciting photon and ϕ the spectrometer work function.[99]

$$E_K = h\nu - E_B - \phi \qquad \textbf{Equation 1.2}$$

The binding energies derived from this analysis are unique for every element, enabling the composition of a material to be ascertained. In addition, binding energies are sensitive to an element's oxidation state, allowing limited chemical information to be deduced.[99] Generally the presence of electron withdrawing substituents results in decreased nuclear screening by the valence electrons, typically raising the binding energy by a few eV. XPS spectra of elements exhibiting a range of oxidation states often appear as complex envelopes which can be deconvoluted into their component environments by a peak fitting procedure.[100]

X-ray photons are usually derived from the impact of thermionic electrons with either a magnesium or aluminium coated anode. The radiation produced by this mechanism is sufficiently energetic (1253.6 eV and 1486.6 eV for Mg Kα and Al Kα sources respectively) to eject core electrons from a wide range of elements and possesses a line width narrow enough (Mg Kα: 0.7 eV, Al Kα: 0.85 eV) to permit high energy resolution analysis.[98]

Energy analysis of the photo-emitted electrons in XPS is normally accomplished using a concentric hemispherical analyser (CHA). These devices utilise two negatively charged, hemispherical plates to filter electrons prior to detection by a secondary electron multiplier.[98]

The surface sensitivity of XPS derives from the energy dependence of the inelastic mean free path for electrons within a solid, Figure 1.3.[101,102] Low kinetic energy electrons possess insufficient energy to participate in energy loss processes so their inelastic mean free path is large. High energy electrons possess similarly low cross sections for inelastic interactions, again resulting in a large inelastic mean free path. In contrast, electrons of medium kinetic energy (100-1000 eV), such as those generated by XPS, have a high cross section for inelastic events. The resultant low escape depth gives XPS its surface sensitivity.

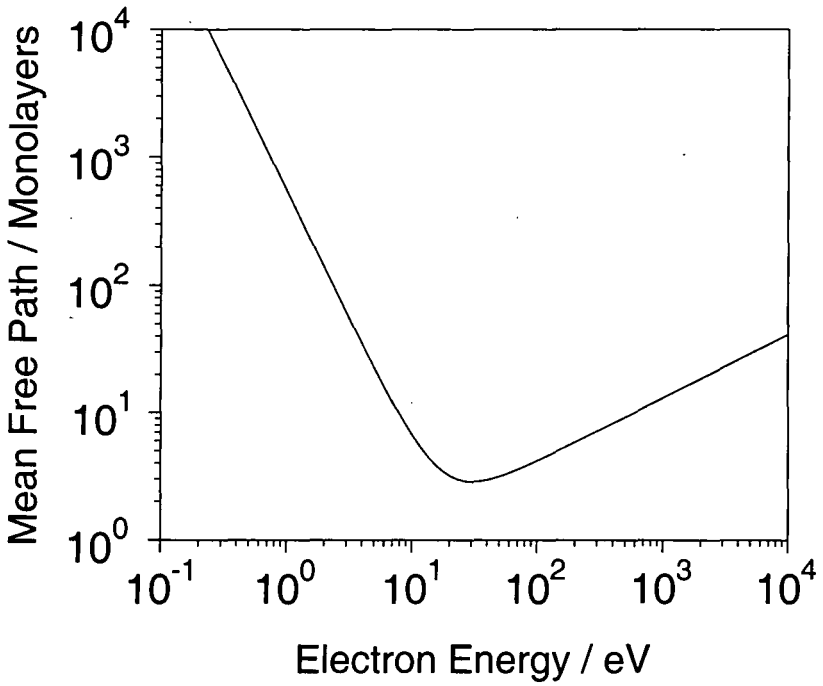

Figure 1.3 The dependence of inelastic mean free path upon emitted electron energy

All XPS analysis in this thesis was performed using Kratos ES300 electron spectrometers equipped with an unmonochromated Mg $K\alpha_{1,2}$ X-ray source and

a concentric hemispherical analyser. The photo-electrons were collected at a take off angle of 30° from the substrate normal and the spectra accumulated on an interfaced personal computer. The relative abundancies of C, F, O, Si and Cl at the sample surfaces were calculated from the areas of the XPS envelopes. Unless otherwise stated sensitivity factors, experimentally determined using chemical standards, were taken as C(1s) : F(1s) : O(1s) : Si(2p) : Cl(2p) equals 1.00 : 0.67 : 0.57 : 0.72 : 0.42. These sensitivity factors take into account the kinetic energy dependence of the inelastic mean free path of emitted electrons, Figure 1.3, and the differing photoelectron cross sections of the elements.[103,104] Each percentage elemental abundance result presented in this thesis is the mean of several, separately prepared, samples and the error quoted is their standard deviation.

The C(1s) XPS spectra were fitted with Gaussian peaks of equal full width at half-maximum (FWHM) using a Marquart minimization computer program. The binding energies of oxidized carbon functionalities were referenced to the hydrocarbon (-**C**$_x$H$_y$-) and **C**-Si peaks at 285.0 eV: carbon next to a carboxylate group (**C**-CO_2) at 285.7 eV, carbon singly bonded to one oxygen atom (**C**-O) at 286.6 eV, carbon singly bonded to two different oxygen atoms or doubly bonded to one oxygen atom (>**C**=O or -O-**C**-O-) at 287.9 eV, carboxylate groups (O-**C**=O) at 289.0 eV, and carbonate carbons (-O-**C**O-O-) at 290.0 eV.[105,106,107] Similarly the Si(2p) spectra were referenced to the -**C**$_x$H$_y$-/**C**-Si environment at 285.0 eV: **Si**-C set at 100.4 eV, **Si**-O functionality at 102.0 eV, **Si**$_2$O$_3$ at 103.0 eV and **Si**O_2 at 104.O eV.[108,109,110] In Chapter 4 and Chapter 5 the total amount of SiO_x material (%SiO_x) was estimated by summing the amounts of silicon and oxygen in the Si_2O_3 and SiO_2 environments:

$$\%SiO_x = \frac{(2.5 \times \%Si \times \%Si_2O_3) + (3 \times \%Si \times \%SiO_2)}{100} \qquad \textbf{Equation 1.3}$$

%Si: The overall percentage of surface silicon

%Si_2O_3: The percentage of Si_2O_3, derived from the Si(2p) peak-fit, expressed as a percentage of the total silicon content.

%SiO_2: The percentage of SiO_2, derived from the Si(2p) peak-fit, expressed as a percentage of the total silicon content.

1.3.2 FOURIER TRANSFORM INFRA-RED SPECTROSCOPY

The basis of infra-red spectroscopy is the vibrational excitation of molecules by the absorption of infra-red radiation (wavelength 1-100 μm). This occurs at characteristic photon energies, enabling structural analysis. For a vibrational transition to be infra-red active there must be a change in the dipole moment.[111]

IR spectroscopy is normally performed in transmission mode, i.e. radiation is passed through the sample. This is a bulk technique, inappropriate for detecting surface change. A more surface sensitive method is attenuated total reflectance fourier transform infra-red spectroscopy (ATR-FTIR). Here the sample is held in intimate contact with an IR transparent crystal (e.g. KRS-5 or diamond) into which infra-red radiation is directed. The difference in refractive indices between the optically dense crystal and the sample result in internal reflection at their interface. However, the beam is not completely reflected at this junction: some propagates a short way into the sample, where it can excite vibrations and be absorbed.[112] The penetration of this phenomena is dependent upon the incident wavelength but is typically about 0.1 - 10 μm, providing information complementary to that of XPS.[113]

1.3.3 CONTACT ANGLE ANALYSIS

The wettability of a sessile droplet upon a surface is sensitive to changes in surface free energy and roughness. Contact angle, a common means of measuring wetting behaviour, is hence an extremely surface sensitive (0.5-1 nm) means of characterizing a solid.[114]

The theory behind the contact angle technique is as follows. A sessile droplet upon a surface creates a three phase boundary between liquid, solid, and vapour, Figure 1.4. This can be described by three vector quantities: γ_{SV}, γ_{SL} and γ_{LV} where γ is the surface tension and the subscripts SV, SL and LV refer to the solid-vapour, solid-liquid and liquid-vapour interfaces respectively. The resolution of these interfacial tensions creates the balance of forces described by Young's equation, Equation 1.4, where $\gamma_{LV}\cos\theta$ is the projection of γ_{LV} upon the surface plane.[115]

$$\gamma_{SV} = \gamma_{SL} + \gamma_{LV}\cos\theta$$ **Equation 1.4**

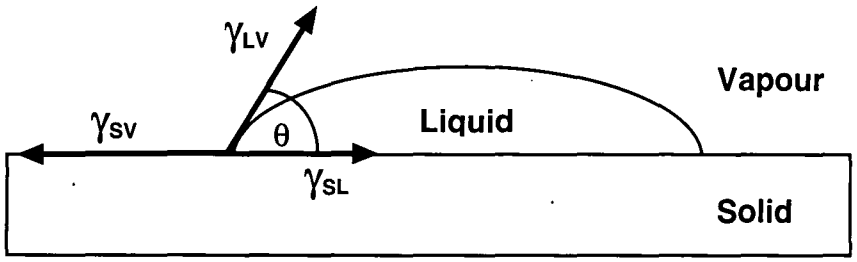

Figure 1.4 The three phase boundary created by a liquid droplet upon a solid surface

Young's equation assumes a perfectly flat, homogenous solid that remains unperturbed by the liquid and its vapour. This is seldom the case and a common departure from ideality occurs when the sample is rough. A basic relation which takes this into account is Wenzel's equation, Equation 1.5:

$$\cos\theta_{ROUGH} = r\cos\theta$$ **Equation 1.5**

where r is the ratio of the actual area of the surface to the apparent area (i.e. projected area) and θ_{ROUGH} is the contact angle of the real solid. It follows that contact angles greater than 90° are accentuated by roughness whilst for θ less than 90° the contact angle decreases.[116]

A useful empirical method of summarizing contact angle data is the Zisman plot. Ordinarily the contact angle of a given solid (cosθ) is a linear function of γ_L for a homologous series of liquids (e.g. n-alkanes), Equation 1.6.[116]

$$\cos\theta = a - b\gamma_L$$ **Equation 1.6**

Extrapolation of a graph of cosθ against γ_L to cosθ=1 yields the value of γ_L at which the surface becomes completely wetted (i.e. θ=0°). This quantity, termed the critical surface tension γ_c, is characteristic of a surface and considered to be

a measure of its surface free energy.[115] The critical surface tension is a useful concept for classifying surfaces, allowing the correlation of wettability with related properties such as adhesion.

For this work contact angle analysis was performed using a video contact angle (VCA) instrument (AST Products VCA2500XE). A motorised syringe deposited a droplet of known volume (2 μl) onto the sample surface. A snapshot of the droplet was then captured using a CCD camera and displayed on the interfaced PC. Accompanying image analysis software would then compute the contact angle. Each of the results presented herein is the average of multiple readings from several, separately prepared samples and the quoted error is the standard deviation.

1.3.4 GAS BARRIER CHARACTERIZATION

The gas permeability of a film is dependent upon a number of factors, including crystallinity, the cohesive energy of the polymer chains, the number of defects (e.g. pinholes, cracks, roughness), and the free volume. It can hence provide useful information on coating structure and integrity.[117]

In this thesis oxygen gas barrier ability was determined using a mass spectrometric device[118] of a type previously used to evaluate the permeability of common elastomers.[119,120] A polymer film sample was placed into the partition cell, which comprised two drilled-out stainless steel flanges on either side of a copper gasket. This was attached to a UHV chamber (base pressure of 5×10^{-10} Torr) via a gate valve. The coated side of each polymer film sample was then exposed to an oxygen (BOC, 99.998%) pressure of 1000 Torr. A quadrupole mass spectrometer (Vacuum Generators SX200) interfaced to a PC computer was used to carry out compositional analysis of the permeant species and the permeant pressure across the substrate monitored with a UHV ion gauge (Vacuum Generators, VIG 24). Upon the attainment of a steady state, where the concentration of permeant upon either side of the sample was constant, the intensity of the permeant signal was measured with the QMS. This value was then correlated with the amount of permeant by introducing oxygen directly into the chamber via a leak valve and recording the mass spectrum at a predetermined pressure of 4×10^{-7} Torr (taking into account ion

gauge sensitivity factors[121]) thus determining the QMS's response per unit pressure. The value calculated by this method was the mean equilibrium permeant partial pressure (MEPPP) measured in the steady state flow regime,[122] a quantity proportional to the permeability of the sample (a measure of permeant flux). The barrier improvement factor (BIF) of each sample was then calculated with reference to the MEPPP of the untreated polyethylene substrate.

1.3.5 ATOMIC FORCE MICROSCOPY (AFM)

AFM is part of the scanning probe microscopy (SPM) family of techniques which use a sharp, finely controlled tip to provide atomic resolution images of surfaces.[123]

In tapping mode AFM a sharp tip (5-50 nm radius of curvature) is attached to a piezoelectrically controlled cantilever and oscillated at, or near to, its resonant frequency. As the tip intermittently contacts the surface its oscillation amplitude changes, an effect detected by laser interferometry of the cantilever.[124] The compensatory adjustments made by a constant oscillation amplitude feedback loop are then used to form a height image of the sample.

A further source of information in tapping mode AFM is the phase shift of the oscillating tip, measured at its resonant frequency. Phase contrast has been attributed to adhesion,[125] hydrophobicity,[126] and elasticity[124] and the resulting images are extremely sensitive to surface heterogeneity.[127]

All AFM images subsequently presented were acquired in air using a Digital Instruments Nanoscope III fitted with an extender module. Tapping mode AFM was used to avoid damaging the silicon nitride tip or sample.[128] Phase and height images were collected simultaneously under operating conditions chosen so that the tip would not become trapped in the surface contamination layer.[129]

1.4 REFERENCES

[1] Regnier, C.; Tristant, P.; Demaison, J. *Surf. Coat. Technol.* **1996**, *80*, 18

[2] Chatham, H. *Surf. Coat. Technol.* **1996**, *78*, 1

[3] Da Silva Sobrinho, A.S.; Czeremuszkin, G.; Latreche, M.; Wertheimer, M.R. Study of Defect Numbers and Distributions in PECVD SiO_2 Transparent Barrier Coatings on PET. In *Plasma Deposition and Treatment of Polymers*; Lee, W.W.; d'Agostino, R.; Wertheimer, M.R., Eds.; Mater. Res. Soc. Symp. Proc. Vol. 544; Materials Research Society: Pittsburgh, PN, 1990, p 245

[4] Bergonzo, P; Patel, P.; Boyd, I.W.; Kogelschatz, U. *Appl. Surf. Sci.* **1992**, *54*, 424

[5] Fujimoto, T.; Okuyama, K.; Yamada, S.; Adachi, M. *J. Appl. Phys.* **1999**, *85*, 4196

[6] Barron, A.R. *Adv. Mater. Opt. Elec.* **1996**, *6*, 101

[7] Gonzalez, P.; Fernandez, D.; Pou, J.; Garcia, E.; Serra, J.; Leon, B.; Perez-Amor, M. *Thin Solid Films*, **1992**, *218*, 170

[8] Bergonzo, P.; Kogelschatz, U.; Boyd, I.W. *Appl. Surf. Sci.* **1993**, *69*, 393

[9] Fujino, K.; Nisimoto, Y.; Tokumasu, N.; Maeda, K. *J. Electrochem. Soc.* **1991**, *138*, 3727

[10] Fujino, K.; Nisimoto, Y.; Tokumasu, N.; Maeda, K. *Jpn. J. Appl. Phys.* **1994**, *33*, 2019

[11] Ikeda, K.;Maeda, M. *Jpn. J. Appl. Phys.* **1996**, *35*, 1573

[12] Fujino, K.; Nisimoto, Y.; Tokumasu, N.; Maeda K. *J. Electrochem. Soc.* **1990**, *137*, 2883

[13] Benmalek, M.; Dunlop, H.M. *Surf. Coat. Technol.* **1995**, *76-77*, 821

[14] Alexander, M.R.; Short, R.D.; Jones, F.R.; Michaeli, W.; Blomfield, C.J. *Appl. Surf. Sci.* **1999**, *137*, 179

[15] Agres, L.; Segui, Y.; Delsol, R.; Raynaud, P. *J. Appl. Polym. Sci.* **1996**, *61*, 2015

[16] Erlat, A.G.; Spontak, R.J.; Clarke, R.P.; Robinson, T.C.; Haaland, P.D.; Tropsha, Y.; Harvey, N.G.; Vogler, E.A. *J. Phys. Chem. B* **1999**, *103*, 6047

[17] Bogart, K.H.A.; Ramirez, S.K.; Gonzales, L.A.; Bogart, G.R. *J. Vac. Sci. Technol., A* **1998**, 3175

[18] Inagaki, N.; Tasaka, S.; Makino, M. *J. Appl. Polym. Sci.* **1997**, *64*, 1031

[19] Adams, A.C.; Alexander, F.B.; Capio, C.D.; Smith, T.E. *J. Electrochem. Soc.* **1981**, *128*, 1545

[20] Batey, J.; Tierney, E. *J. Appl. Phys.* **1986**, *60*, 3136

[21] Hsieh, J.J.; Ibbotson, D.E.; Mucha, J.A.; Flamm, D.L. Directional Deposition of Silicon Oxide by a Plasma Enhanced TEOS Process. In *Characterisation of Plasma-Enhanced CVD Processes*; Lucovsky, G.; Ibbotson, D.E.; Hess, D.W., Eds.; Mater. Res. Soc. Symp. Proc. Vol. 165; Materials Research Society: Pittsburgh, PN, 1990, p 107

[22] Rats, D.; Hajek, V.; Martinu, L. *Thin Solid Films* **1999**, *340*, 33

[23] Rudder, R.A.; Fountain, G.G.; Hattangady, S.V.; Posthill, J.B.; Markunas, R.J. Development of Remote Plasma Enhanced Chemical Vapor Deposition precesses Through the Use of In Vacuo Electron Diffraction and Electron Spectroscopy In *Characterisation of Plasma-Enhanced CVD Processes*; Lucovsky, G.; Ibbotson, D.E.; Hess, D.W., Eds.; Mater. Res. Soc. Symp. Proc. Vol. 165; Materials Research Society: Pittsburgh, PN, 1990, p 151

[24] Tsu, D.V.; Kim, S.S.; Theil, J.A.; Wang, C.; Lucovsky, G. Formation of Multilayer SiO_2-SiO_x Heterostructures by Control of Reaction Pathways in Remote CVD In *Characterisation of Plasma-Enhanced CVD Processes*; Lucovsky, G.; Ibbotson, D.E.; Hess, D.W., Eds.; Mater. Res. Soc. Symp. Proc. Vol. 165; Materials Research Society: Pittsburgh, PN, 1990, p 209

[25] Bayer, C.; Bapin, E.; Rudolf von Rohr, P. *Surf. Coat. Technol.* **1999**, *116-119*, 874

[26] Wrobel, A.M.; Pietrzykowska, A.; Wickramanayaka, S.; Hatanaka, Y. *J. Electrochem. Soc.* **1998**, *145*, 2866

[27] Park, Y.-B.; Kang, J.K.; Rhee, S.W. *Thin Solid Films* **1996**, *280*, 43

[28] Pai, C.S.; Miner, J.F.; Foo, P.D. *J. Electrochem. Soc.* **1992**, *139*, 850

[29] Wickramanayaka, S.; Matsumoto, A.; Nakanishi, Y.; Hosokawa, N.; Hatanaka, Y. *Jpn. J. Appl. Phys.* **1994**, *33*, 3520

[30] Gonzalez, P.; Garcia, E.; Pou, J.; Fernandez, D.; Serra, J.; Leon, B.; Perez-Amor, M. *Thin Solid Films* **1993**, *421*, 348

[31] Usami, K.; Mochizukim, Y.; Minagawa, T.; Iida, A.; Gohshi, Y. *Jpn. J. Appl. Phys.* **1985**, *25*, 410

[32] Boyd, I.W. *Appl. Surf. Sci* **1997**, *109/110*, 538

[33] Yokotani, A.; Takezoa, N.; Kurosawa, K.; Igarashi, T.; Matsuno, H. *J. Appl. Phys.* **1996**, *69*, 1399

[34] Bergonzo, P.; Boyd, I.W. *J. Appl. Phys.* **1994**, *76*, 4372

[35] Zhang, S.; Fan, R.X.; Deng, X.Q. *J. Mater. Sci.: Mater. Lett.* **1998**, *17*, 1817

[36] Seyferth, D. *Adv. Chem. Ser.* **1990**, *224*, 565

[37] Niwano, M.; Kinashi, K.; Kazuhiko, S.; Miyamoto, N. *J. Electrochem. Soc.* **1994**, *141*, 1556

[38] Cui, Z.; Madsen, J.M.; Takoudis, C.G. *J. Appl. Phys.* **2000**, *87*, 8181

[39] Nakamura, K.; Kurokawa, A.; Ichimura, S. *Thin Solid Films* **1999**, *343-344*, 361

[40] Muisener, R.J.; Koberstein, J.T. *Abstracts of Papers of the Am. Chem. Soc.* **1997**, *214*, 56

[41] Hillborg, H.; Gedde, U. W. *Polymer* **1998**, *39*, 1991.

[42] Klee, D.; Breuers, W.; Bilo-Jung, M.; Mittermayer, C.; Hocker, H. *Die Angewandte Makromolekulare Chemie* **1989**, *166/167*, 179.

[43] Namatsu, H. *J. Electrochem. Soc.* **1989**, *136*, 2676.

[44] Smolinsky, G.; Reichmanis, E.; Wilkins, C.W. In *Proc. Regional Technical Conf. Photopolymers: Principals, Processes and Materials*, Ellenville, NY, 1985; Soc. Plastic Engin., 1985, p167

[45] Gokan, H.; Saotome, Y.; Saigo, K.; Watanabe, F.; Ohnishi, Y. Oxygen Ion Etching Resistance of Organosilicon Polymers. In *Polymers For High Technology: Electronics and Photonics*. Bowden, M.J.; Turner, S.R., Eds.; ACS Symposium Series 346; ACS: Washington, DC, 1987; p 358

[46] Vautey, C.; Burgos, M.; Langlet, M. *Thin Solid Films* **1999**, *347*, 184

[47] Kusakabe, K.; Sakamoto, S.; Saie, T.; Morooka, S. *Separation and Purification Technology* **1999**, *16*, 139

[48] Coburn, J.W. *IEEE Trans. Plasma Sci.* **1991**, *19*, 1048

[49] Grill, A. *Cold Plasma In Materials Fabrication*; IEEE Press: New York, 1994; Chapter 1

[50] Aguirre, P. Treatment of industrial wastes by plasma technology, IEE Colloquium on Atmospheric Dicharges for Chemical Synthesis, ; IEE: London, 1998

[51] Hollahan, J.R., Bell, A.T., Eds. *Techniques and Applications of Plasma Chemistry*; Wiley: New York, 1974

[52] Pochner, K.; Neff, W.; Lebert, R. *Surf. Coat. Technol.*, **1995**, *74-75*, 394-398

[53] Palmer, A.J. *Appl. Phys. Lett.* **1974**, *25*, 138

[54] Penning, F. M. *Electrical Discharges in Gases*; Philips' Technical Library: The Netherlands, 1957.

[55] Chapman, B. *Glow Discharge Processes*; Wiley: New York, 1981

[56] Meek, J.M.; Craggs, J.D. *Electrical Breakdown of Gases*; Wiley: Chichester, U.K., 1978.

[57] Massines, F.; Rabehi, A.; Decomps, P.; Gadri, R.B; Ségur, P; Mayoux, C. *J. Appl. Phys.* **1998**, *83*, 2950

[58] Eliasson, B.; Kogelschatz, U. *IEEE Trans. Plasma Sci.* **1991**,*19*, 309

[59] Eliasson, B.; Egli, W.; Kogelschatz, U. *Pure & Appl. Chem.* **1994,** *66*, 1275

[60] Eliasson, B.; Hirth, M.; Kogelschatz, U. *J. Phys. D: Appl. Phys.*, **1987**, *20*, 1421

[61] Levatter, J.I.; Lin, S.-C. *J. Appl. Phys.* **1980**, *51*, 210

[62] Okazaki, S.; Kogoma, M.; Uehara, M.; Kimura, Y. *J. Phys. D: Appl. Phys.* **1993**, *26*, 889

[63] Yokoyama, T.; Kogoma, M.; Moriwaki, T.; Okazaki, S. *J. Phys. D: Appl. Phys.* **1990**, *23*, 1125

[64] Kekez, M.M; Barrault, M.R.; Craggs, J.D. *J. Phys. D: Appl. Phys.* **1970**, *3*, 1886

[65] Braun, D.; Kuchler, U.; Pietsch, G. *J. Phys. D: Appl. Phys.*, **1991**, *24*, 564

[66] Eliasson B.; Gellert, B *J. Appl. Phys.* **1990**, *68*, 2025

[67] Pashaie, B.; Dhali, S.K.; Honea, F.I. *J. Phys. D: Appl. Phys.* **1994**, *27,* 2107

[68] Kitayama, J.; Kuzumoto, M. *J. Phys. D: Appl. Phys.* **1997**, *30*, 2453

[69] Eliasson, B.; Kogelschatz, U.; Baessler, P. *J. Phys. B: At. Mol. Phys.* **1984**, *17*, L797

[70] Falkenstein, Z. *J. Appl. Phys.* **1997**, *81,* 5975

[71] Kogelschatz, U. *Appl. Surf. Sci.* **1992**, *54*, 410

[72] Kessler, F.; Bauer, G.H. *Appl. Surf. Sci.* **1992**, *54*, 430

[73] Greenwood, O.D.; Boyd, R.D.; Hopkins, J.; Badyal, J.P.S. *J. Adhesion Sci. Technol.* **1995**, *9,* 311

[74] Sardja, I.; Dhali, S.K. *Appl. Phys. Lett.* **1990**, *56*, 21

[75] Chang, M.B.; Balbach, J.H.; Rood, M.J.; Kushner, M.J. *J. Appl. Phys.* **1991**, *69*, 4409

[76] Salge, J. *Journal De Physique IV* **1995**, *C5*, 583

[77] Reitz, U.; Salge, J.G.H.; Schwarz, R. *Surf. Coat. Technol.* **1993**, *59*, 144

[78] Segers, M.; Dhali, S.K. *J. Electrochem. Soc.* **1991**, *138,* 2741

[79] Sawada, Y.; Ogawa, S.; Kogoma, M. *J. Phys. D: Appl. Phys.* **1995**, *28*, 1661

[80] Kanazawa, S.; Kogoma, M.; Moriwaki, T.; Okazaki, S. *Nucl. Instrum. Methods Phys. Res., Sect. B* **1989**, *37/38*, 842

[81] Okazaki, S.; Kogoma, M. *Proc. Jpn. Symp. Plasma Chem.* **1989**, *2*, 95

[82] Tsai, P.P.; Wadsworth, L.C.; Roth, J.R. *Textile Res.* **1997**, *67*, 359

[83] Lynch, J.B.; Spence, P.D.; Baker, D.E.; Postlethwaite, T.A. *J. Appl. Polym. Sci.* **1999**, *71*, 319

[84] Kelly-Wintenburg, K.; Montie, T.C.; Brickman, C.; Roth, J.R.; Carr, A.K.; Sorge, K.; Wadsworth, L.C.; Tsai, P.P.Y. *Journal of Industrial Microbiology & Biotechnology* **1998**, *20*, 69

[85] Sawada, Y.; Tamura, H.; Kogoma, M.; Kawase, M.; Hashimoto, K. *J. Phys. D.: Appl. Phys.* **1996**, *29*, 2539

[86] Brenning, N.; Axnäs, I.; Nilsson, J.O.; Eniger, J.E. *IEEE Trans. Plasma Sci.* **1997**, *25*, 83

[87] Nilsson, J.O.; Eninger, J.E. *IEEE Trans. Plasma Sci.* **1997**, *25*, 73

[88] Elliasson, B.; Kogelschatz, U. *IEEE Trans. Plasma. Sci.* **1991**, *19*, 1063

[89] Mizuno, A.; Shimizu, K.; Chakrabarti, A.; Dascalesu, L.; Furuta, S. *IEEE Trans. Ind. Applicat.* **1995**, *31*, 957

[90] Williams, E.M. *The Physics and Technology of Xerographic Processes,* Wiley: New York, 1984

[91] Hays, D.A. *J. Adhesion* **1995**, *51*, 41

[92] Sapieha, S.; Cerny, J.; Klemberg-Sapieha, J.E.; Martinu, L. *J. Adhesion* **1993**, *42*, 91

[93] Iwata, H.; Kishida, A.; Suzuki, M.; Hata, Y.; Ikada, Y. *J. Polym Sci. Polym Chem.* **1988**, *26*, 3309

[94] Chang, J.S.; Lawless, P.A.; Yakamoto, T. *IEEE Trans. Plasma. Sci.* **1991**, *19*, 1152

[95] Penetrante, B.M.; Hsia, M.C.; Merritt, B.T.; Vogtlin, G.E.; Wallman, P.H.; Neiger, M.; Wolf, O.; Hammer, T.; Broer, S. *Appl. Phys. Lett.* **1994**, *68*, 3719

[96] Popescu, S.; Vaju, D. *J. Anal. At. Spectrom.* **1997**, *12*, 1091

[97] Shvedchikov, A.P.; Belousova, E.V.; Polyakova, A.V.; Ponizovskii, A.Z.; Goncharov, V.A. *High Energy Chemistry* **1992**, *26*, 364

[98] Rivière, J.C. Instrumentation. In *Practical Surface Analysis Volume 1 - Auger and X-ray Photoelectron Spectroscopy*, 2nd ed.; Briggs, D., Seah, M.P., Eds.; Wiley: Chichester, U.K., 1990; Chapter 2

[99] Briggs, D.; Rivière, J.C. Spectral Interpretation. In *Practical Surface Analysis Volume 1 - Auger and X-ray Photoelectron Spectroscopy*, 2nd ed.; Briggs, D., Seah, M.P., Eds.; Wiley: Chichester, U.K., 1990; Chapter 3

[100] Evans, J.F.; Gibson, J.H.; Moulder, J.F.; Hammond, J.S.; Goretzhi, H. *Fresenius Z. Anal. Chemie* **1984**, *319*, 841

[101] Seah, M.P.; Dench, W.A. *Surf. Interface Anal.* **1979**, *1*, 2

[102] Seah, M. Quantification of AES and XPS. In *Practical Surface Analysis Volume 1 - Auger and X-ray Photoelectron Spectroscopy*, 2nd ed.; Briggs, D., Seah, M.P., Eds.; Wiley: Chichester, U.K., 1990; Chapter 5

[103] Briggs, D.; Seah, M.P. Practical Surface Analysis Vol. 1, 2nd Ed., John Wiley & Sons, 1990

[104] Bhatia, Q.S.; Burrel, M.C. *Polymer* **1991**, *32*, 1948

[105] Beamson, G.; Briggs, D. High Resolution XPS of Organic Polymers, John Wiley & Sons, 1992

[106] Clark, D.T.; Shuttleworth, D. *J. Polym. Sci. Chem. Ed.* **1980**, 18, 27

[107] Clark, D.T.; Dilks, A. *J. Polym. Sci., Polym. Chem. Ed.* **1979**, *17*, 957

[108] Greenwood, O.G. Ph.D. Thesis, University of Durham, 1997

[109] Alfonsetti, R. *Appl. Surf. Sci.* **1993**, *70/71*, 222

[110] Laoharojanaphand, P.; Lin, T.; Stoffer, J.O. *J. Appl. Polym. Sci.* **1990**, *40*, 369

[111] Banwell, C.N. *Fundamentals of Molecular Spectroscopy*; McGraw-Hill: Maidenhead, U.K., 1966

[112] Hoflund, G.B.; Rivière, J.C. Less Commonly Used Techniques for Analysis of Surfaces and Interfaces. In *Handbook of Surface and Interface Analysis*; Rivière, J.C., Myhra, S., Eds.; Marcel Dekker: New York, 1998; Appendix 3

[113] Gaboury, S. R.; Urban, M. W. Analysis of Gas -Plasma Modified Poly(dimethylsiloxane) Elastomer Surfaces. Attenuated-Total-Reflectance-Fourier Transform Infrared Spectrscopy In *Structure-Property Relations in Polymers*; Urban, M. W., Craver, D.C, Eds.; A.C.S., 1993; Vol. 236, pp 778.

[114] Domingue, J. *American Laboratory* **1990**, *22*, 50

[115] Good, R.J. Contact angle, wetting, and adhesion: a critical review. In *Contact Angle, Wettability and Adhesion*; Mittal, K.; Ed.; VSP: Utrecht, The Netherlands, 1993; pp 3-36

[116] Adamson, A.W.; Gast, A.P. *Physical Chemistry of Surfaces*, Wiley: New York, 1997; Chapter 10

[117] *Polymer Permeability*; Comyn, J., Ed.; Elsevier Applied Science: Barking, U.K., 1985

[118] Westover, L.B.; Tou J.C.; Mark, J.H. *Anal. Chem.* **1974**, *46*, 568.

[119] Laurenson, L.; Dennis, N.T.M. *J. Vac. Sci. Technol. A* **1985**, *3*,1707.

[120] Tou, J.C.; Rulf D.C.; DeLassus, P.T. *Anal. Chem.*, **1990**, *62*, 592.

[121] *Pressure Measurement Technical Information*, Vacuum Generators.

[122] Crank, J.; Park, G.S. In *Diffusion in Polymers*, Crank J., Park G. S., Eds.; Academic Press: London, 1968; Chapter 1.

[123] Adamson, A.W.; Gast, A.P. *Physical Chemistry of Surfaces*, Wiley: New York, 1997; Chapter 8

[124] Brandsch, R.; Bar, G. *Langmuir* **1997**, *13*, 6349

[125] Finot, M.O.; McDermott, M.T. *J. Am. Chem. Soc.* **1997**, *119*, 8564

[126] Chen, X.; Davies, M.C.; Roberts, C.J.; Tendler, S.J.B.; Williams, P.M.; Davies, J.; Dawkes, A.C.; Edwards, J.C. *Ultramicroscopy* **1998**, *75*, 171

[127] Bar, G.; Thomann, Y.; Brandsch, R.; Cantow, H.J.; Whangbo, M.-H. *Langmuir* **1997**, *13*, 3807

[128] Zhong, Q.; Innis, D.; Kjoller, K.; Elings, V.B. *Surf. Sci.*, **1993**, *290*, L688

[129] Magonov, S.N.; Elings, V.; Whangbo, M-H. *Surf. Sci.* **1997**, *375*, L385

CHAPTER 2

ATMOSPHERIC PRESSURE PLASMA OXIDATION OF ORGANO-SILICON COATINGS

2.1 INTRODUCTION

The stability and impermeability of silica have made it invaluable in the microelectronics and packaging industries where it finds application in passivation and gas barrier coatings.[1,2,3,4] In addition to its bulk attributes, silica exhibits surface characteristics that are useful where enhanced adhesion and frictional properties are required. This combination of qualities makes thin silica film manufacture of considerable commercial interest.

A widely used means of depositing silica coatings is to oxidize a silicon containing precursor in the gas phase. Chemical vapour deposition (CVD)[5,6,7,8] and plasma enhanced CVD[9,10] of silane (SiH_4) and siloxanes (e.g. tetraethoxysiloxane and hexamethyldisiloxane) routinely produce high purity silica coatings possessing excellent electrical and barrier properties. However, the high substrate temperatures required for these processes make them unsuitable for treating heat sensitive materials such as polyolefin films. A low temperature approach is to plasma oxidize a solid organo-silicon precursor film. Low pressure plasma oxidation is frequently used to improve the hydrophilicity of polysiloxane biomaterials[11] (e.g. cell culture surfaces[12] and contact lens coatings[13]) by imparting a silica-like surface layer. In this study inorganic silica-like layers have been produced by the atmospheric pressure plasma oxidation of alternative organo-silicon precursors: polycyclohexylmethylsilane (PCHMS), polymethylsilsesquioxane (PMSQ) and polyphenylsilsesquioxane (PPSQ), Figures 2.1, 2.2 and 2.3.

Polysilanes such as PCHMS consist of a Si-Si backbone with pendant organic groups. The weak Si-Si bonds are easily cleaved by UV irradiation,[14] and the resultant chain scission causes the loss of material as volatile fragments.[15] The UV sensitivity of polysilanes has led to their widespread use as photo-lithographic resists[16,17,18] and photo-initiators for vinyl polymerization.[19] Polysilanes also react rapidly with excited oxygen species, forming a thin layer of SiO_x which blocks further reaction, an attribute which finds commercial application in oxygen reactive ion etching (O_2-RIE).[20,21] When utilised in conjunction with photo-lithography this technique can be used to construct micropatterned arrays such as multilayer resists.[17,19,22]

Polysilsesquioxanes such as PMSQ and PPSQ consist of stable Si-O-Si

cross-linked structures, mainly in a ladder or cage morphology, with an empirical formula of $RSiO_{1.5}$. The 3-dimensional bonding arrangement impedes degradation by chain scission and when pendant organic groups are removed by oxidative attack they tend to be replaced by additional siloxane bonds.[23] Polysilsesquioxanes have a variety of applications including microlithographic resists, gas separation membranes, ceramic precursors (SiC and silicon oxycarbide), anti reflective coatings[24] and cores for dendrimer synthesis.[23,25]

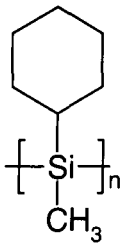

Figure 2.1 Polycyclohexylmethylsilane.

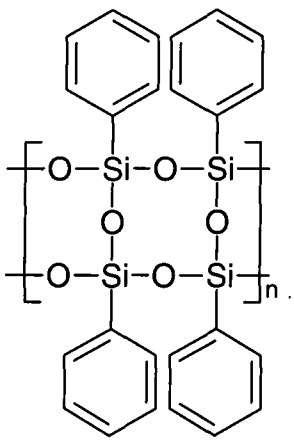

Figure 2.2 Polyphenylsilsesquioxane.

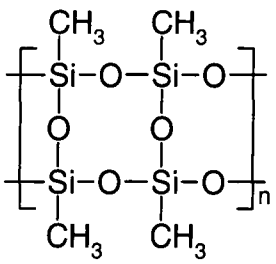

Figure 2.3 Polymethylsilsesquioxane.

The chosen means of oxidation was air dielectric barrier discharge (DBD). These atmospheric pressure plasmas, also known as silent discharges, are primarily used for generating ozone but have been used to purify flue gases,[26,27] in high intensity VUV excimer lamps[28,29,30] and to improve the wettability and adhesive properties of polymer surfaces.[31,32] The ease of scaling up dielectric barrier discharge reactors, and their suitability for continuous roll-to-roll polymer processing,[33] confers a degree of industrial viability upon a process utilizing them.

2.2 EXPERIMENTAL

Nylon 6,6 (Goodfellow, 0.15 mm thick) substrates were ultrasonically cleaned in a 1:1 mixture of isopropylalcohol (BDH, Analar) and cyclohexane (BDH, Analar) for 30 seconds.

Polycyclohexylmethylsilane (ABCR) and polymethylsilsesquioxane (Fluorochem) were dissolved in 10% w/v toluene solutions. A 1.1% w/v saturated solution of polyphenylsilsesquioxane (Fluorochem, high ladder content) was prepared by heating an excess of solute in toluene at 363 K for 4 hours. The organo-silicon films were deposited from solution using a spin-coater (Cammax Precima) operating at a rotation speed of 1500 rpm for 20 seconds with a jet of nitrogen used to aid solvent evaporation.

Oxidation was effected using an in-house built, parallel-plate, silent discharge apparatus, Figure 2.4. This device uses a high-voltage, thyristor-switched power supply to generate dampened sinusoidal pulses of variable voltage (up to a maximum of 11 kV). The power supply was triggered by an external signal generator enabling variable pulse repetition rate (frequency) experiments. The voltage characteristics of the discharge output were monitored using a passive probe attached to an oscilloscope. The aluminium electrodes were chemically polished and degreased with isopropyl alcohol. The earthed lower electrode was covered with a polymer dielectric.

Dielectric barrier discharge treatment consisted of placing a sample upon the lower electrode and operating the discharge in air for 60 s with a 2 mm inter-electrode gap. An exception to this procedure was the plasma off-time experiments performed upon PMSQ. Here a change in discharge frequency was accompanied by a compensating change in treatment duration. As the total number of pulses was held constant the only variable was the amount of time between each pulse (plasma off-time).

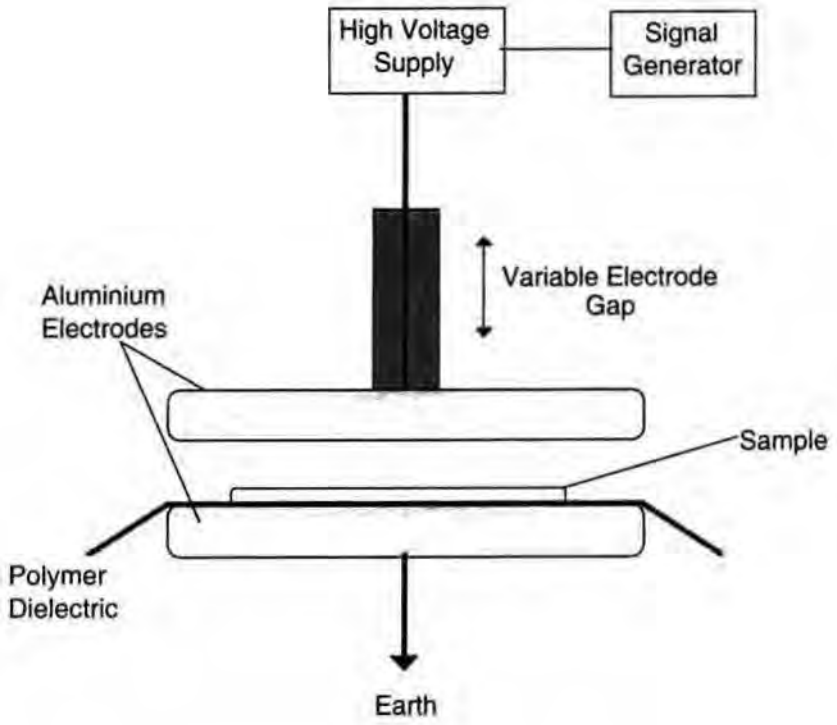

Figure 2.4 The dielectric barrier discharge apparatus.

XPS was performed using the equipment and peak-fitting procedure described in Section 1.3.1. However, the sensitivity factors for this particular Kratos ES300 spectrometer were C(1s) : O(1s) : Si(2p) equals 1.00 : 0.62 : 1.02. Etching through the coating was monitored by checking for the presence of nitrogen from the underlying nylon substrate.

The homogeneity of the oxidized SiO_x layer was evaluated by argon-ion depth profiling. A VG CLAM 100 XPS spectrometer equipped with a VG AG21 cold cathode ion gun operating at 3 keV energy with a background argon (BOC 99.9 % purity) pressure of 2×10^{-6} mbar and an ion current of 1.5 μA was used to incrementally sputter away the surface of the sample. XPS analysis of the eroded surface was regularly performed and the change in surface composition related to sputter time to provide an overall depth profile.

AFM images were acquired using the apparatus and conditions described in Section 1.3.5.

2.3 RESULTS

2.3.1 THE DISCHARGE FREQUENCY DEPENDENCE OF PCHMS, PPSQ AND PPSQ OXIDATION

Total dielectric barrier discharge treatment time was kept constant, whilst the frequency of the discharge was varied. The increase in discharge frequency effectively corresponds to an increase in plasma on-time. The aim of this approach was to maximize the degree of modification within the shortest possible treatment time.

Native films of polycyclohexylmethylsilane (PCHMS), polyphenylsilsesquioxane (PPSQ) and polymethylsilsesquioxane (PMSQ) displayed elemental abundances close to those predicted by their theoretical structures, Table 2.1.

Silent discharge treatment of all three organo-silicon precursors effected a large increase in the concentration of surface oxygen with a concomitant decrease in surface carbon. No nitrogen was detected, confirming that etching through to the substrate had not occurred and that no nitrogenous functionalities were generated on the film surface. The extent of these changes was found to rise with increasing discharge frequency; demonstrating that oxidation efficiency is directly related to plasma on-time, Figures 2.5a, 2.7a and 2.9a. However, the level of chemical modification appeared to reach saturation at higher frequencies.

The most silicon and oxygen rich films were those derived from PPSQ and PMSQ, Table 2.1. Oxidized PCHMS, whilst possessing a less silica-like surface than the silsesquioxanes, had undergone the most impressive transformation, changing from a virtually oxygen free structure (C=86%, O=3%, Si=11%) to one possessing elemental abundances of C=22%, O=57%, Si=20%. The degree of oxygen incorporation / carbon removal was significantly greater than that previously reported for the treatment of PCHMS with a low pressure oxygen glow discharge plasma (elemental abundancies observed for PCHMS spin coated onto polyethylene treated with a 50 W O_2 glow discharge plasma were 30 % C, 35 % Si and 35 % O).[34]

A shift in Si(2p) binding energy was observed upon plasma exposure,

indicating that the silicon in the coatings had been converted to a more oxidized inorganic phase. Figures 2.6, 2.8 and 2.10.[12,35,36,37] As the discharge frequency was increased the high binding energy component grew at the expense of the lower binding energy peaks associated with the precursor. This was investigated quantitatively by peak fitting the Si(2p) XPS spectra, Figures 2.5b, 2.7b and 2.9b. It was found that the silicon content of PCHMS and PPSQ became most oxidized with a silicon composition of ~25% Si_2O_3 and ~75% SiO_2 being attained (corresponding to a modal Si(2p) Binding Energy of ~103.8 eV). PMSQ films, whilst containing the least organic material, both before and after oxidation, contained significantly less oxidized silicon (~45% Si_2O_3 and ~55% SiO_2, Si(2p) B.E. = 103.5 eV).

Sample	% C	% O	% Si
PCHMS, theoretical	87.5	0	12.5
PCHMS, untreated	85.8 ±0.2	2.8 ±0.3	11.4 ±0.1
PCHMS, 328 Hz DBD	22.4 ±2.0	57.3 ±1.0	20.3 ±1.1
PPSQ, theoretical	70.6	17.6	11.8
PPSQ, untreated	64.8 ±3.0	21.5 ±2.1	13.7 ±1.0
PPSQ, 328 Hz DBD	16.3 ±1.9	61.1 ±0.5	22.7 ±2.4
PMSQ, theoretical	28.6	42.9	28.6
PMSQ, untreated	27.1 ±0.4	44.9 ±0.9	28.0 ±0.6
PMSQ, 328 Hz DBD	12.8 ±1.0	63.3 ±2.0	23.9 ±0.6

Table 2.1 Surface elemental abundances of PCHMS, PPSQ and PCHMS before and after 328 Hz dielectric barrier discharge treatment.

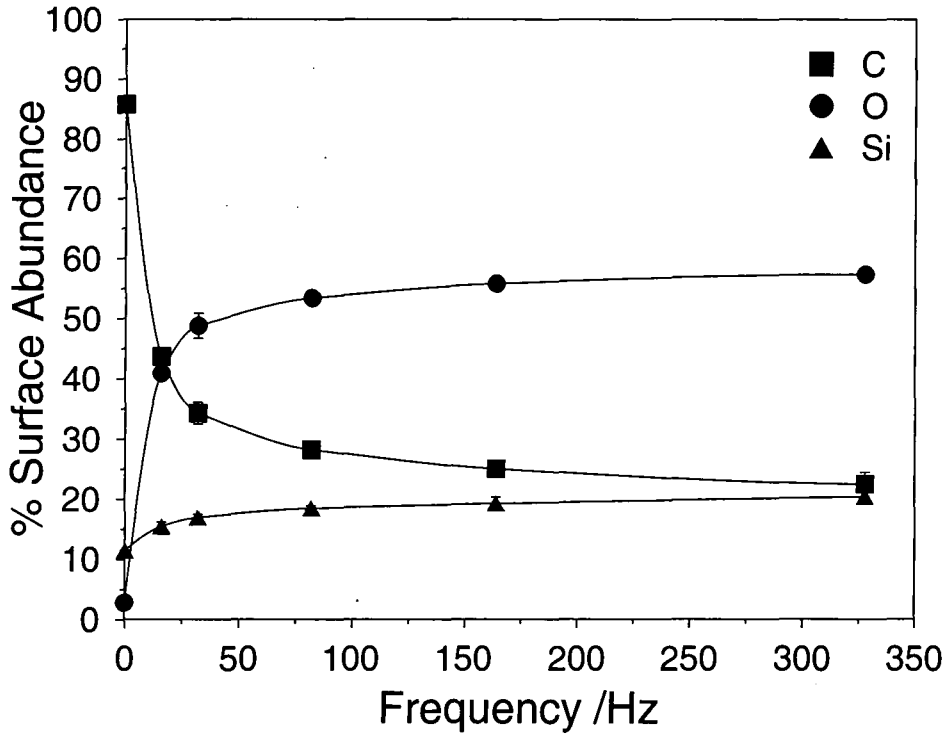

Figure 2.5a Surface elemental abundances of PCHMS oxidized with DBD treatments of varying frequencies.

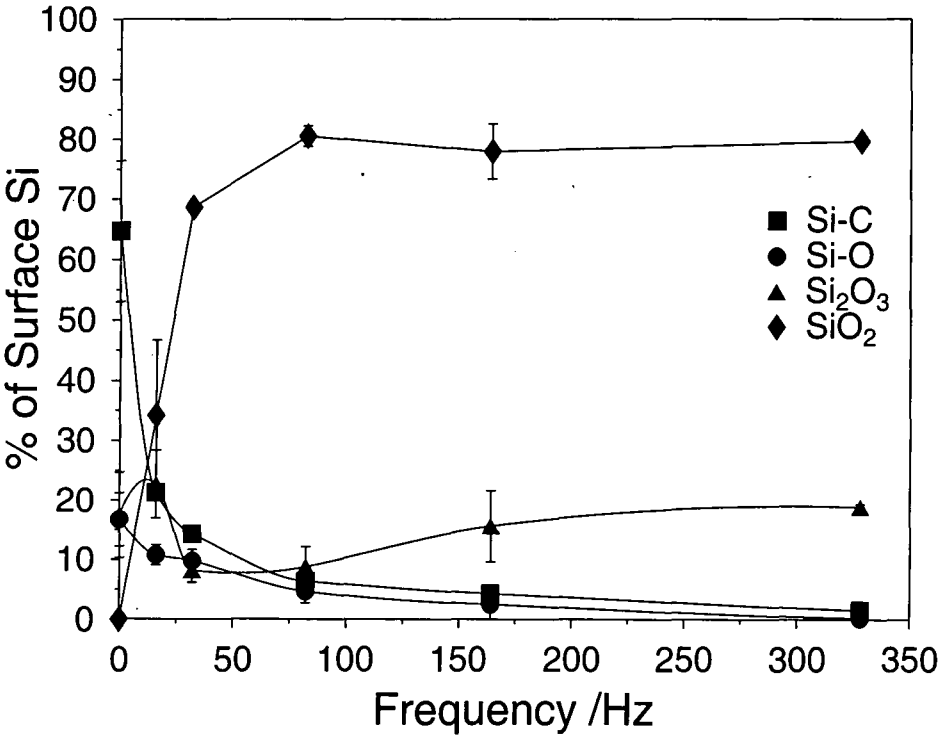

Figure 2.5b Silicon oxidation state distribution of PCHMS oxidized with DBD treatments of varying frequencies.

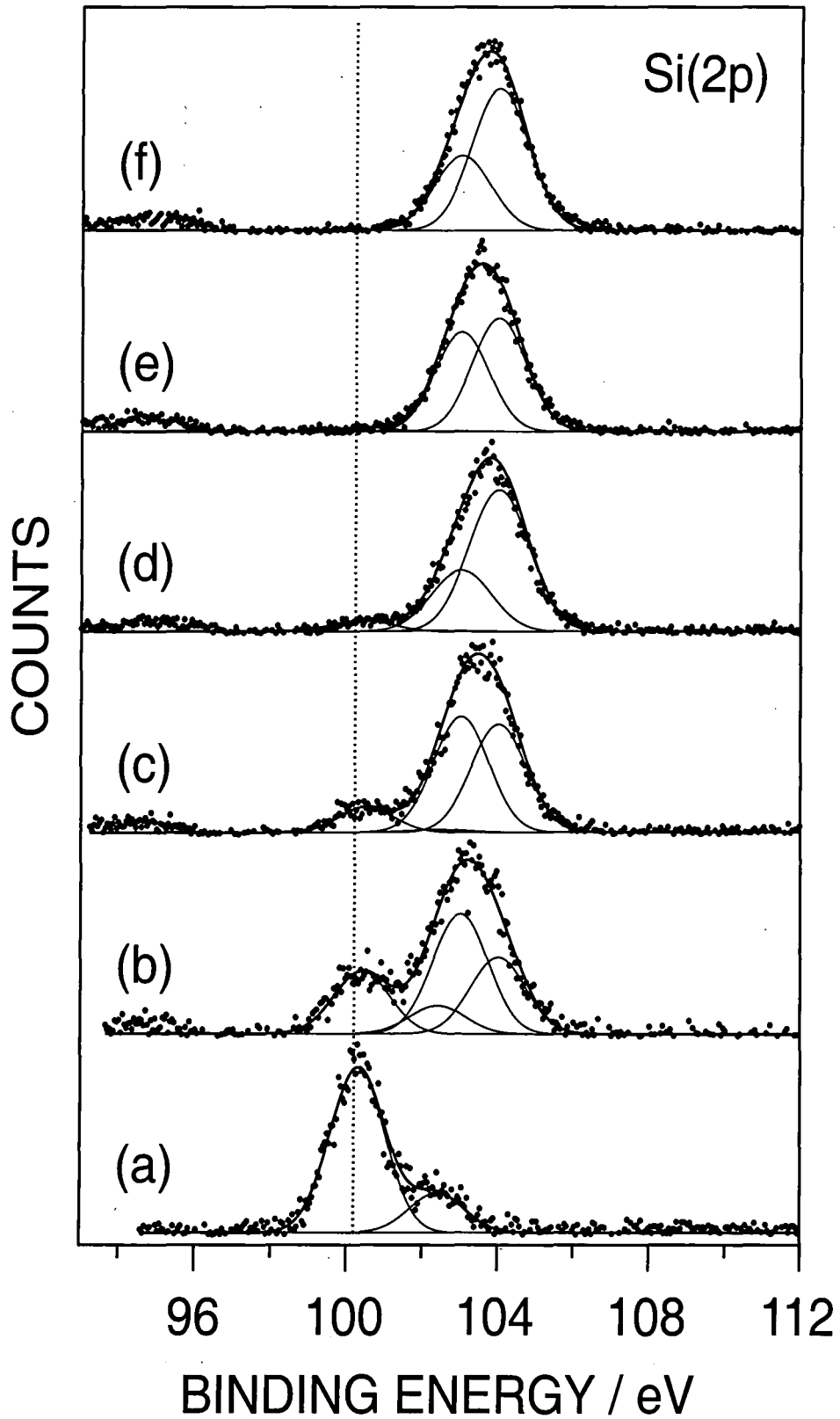

Figure 2.6 Si(2p) XPS spectra of DBD oxidized PCHMS (a) untreated, (b) 16 Hz, (c) 32Hz, (d) 82 Hz, (e) 164 Hz, (f) 328 Hz.

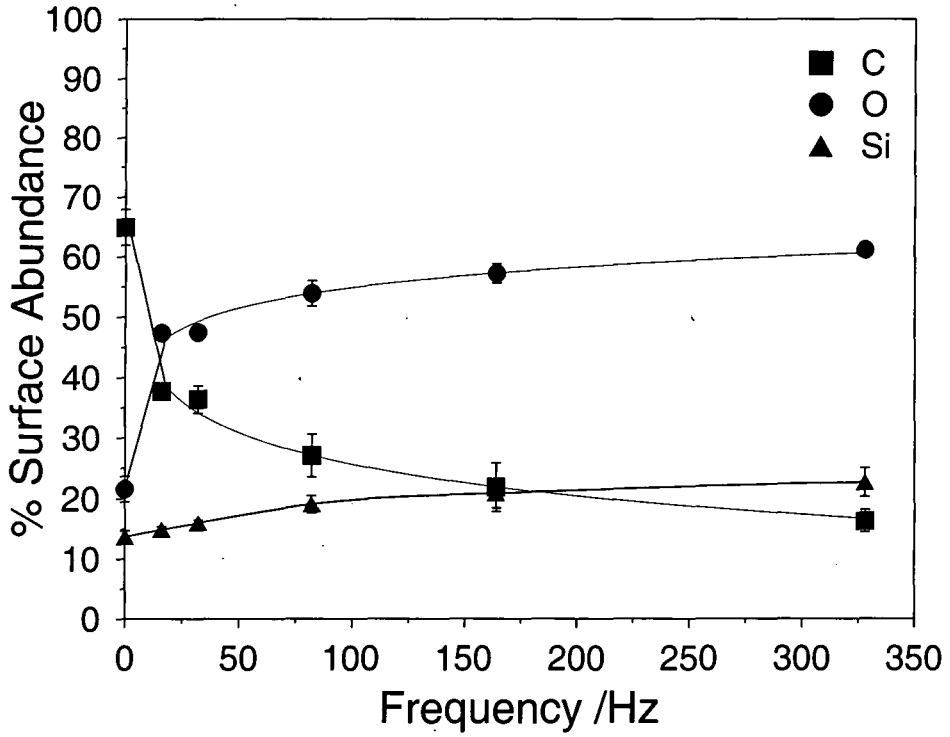

Figure 2.7a Surface elemental abundances of PPSQ oxidized with DBD treatments of varying frequencies.

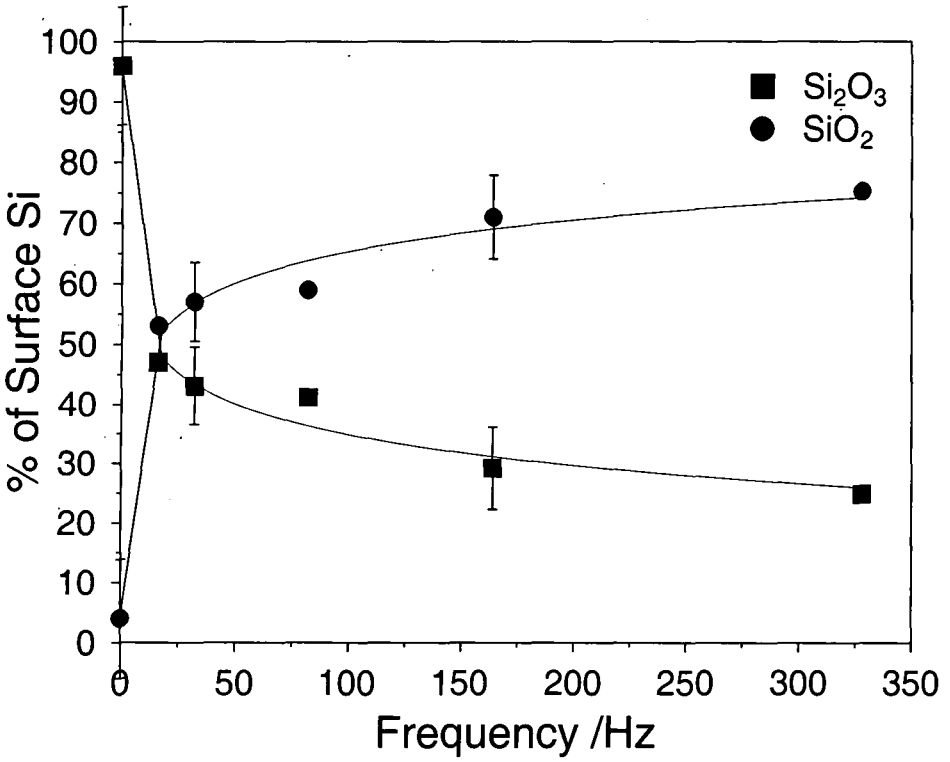

Figure 2.7b Silicon oxidation state distribution of PPSQ oxidized with DBD treatments of varying frequencies.

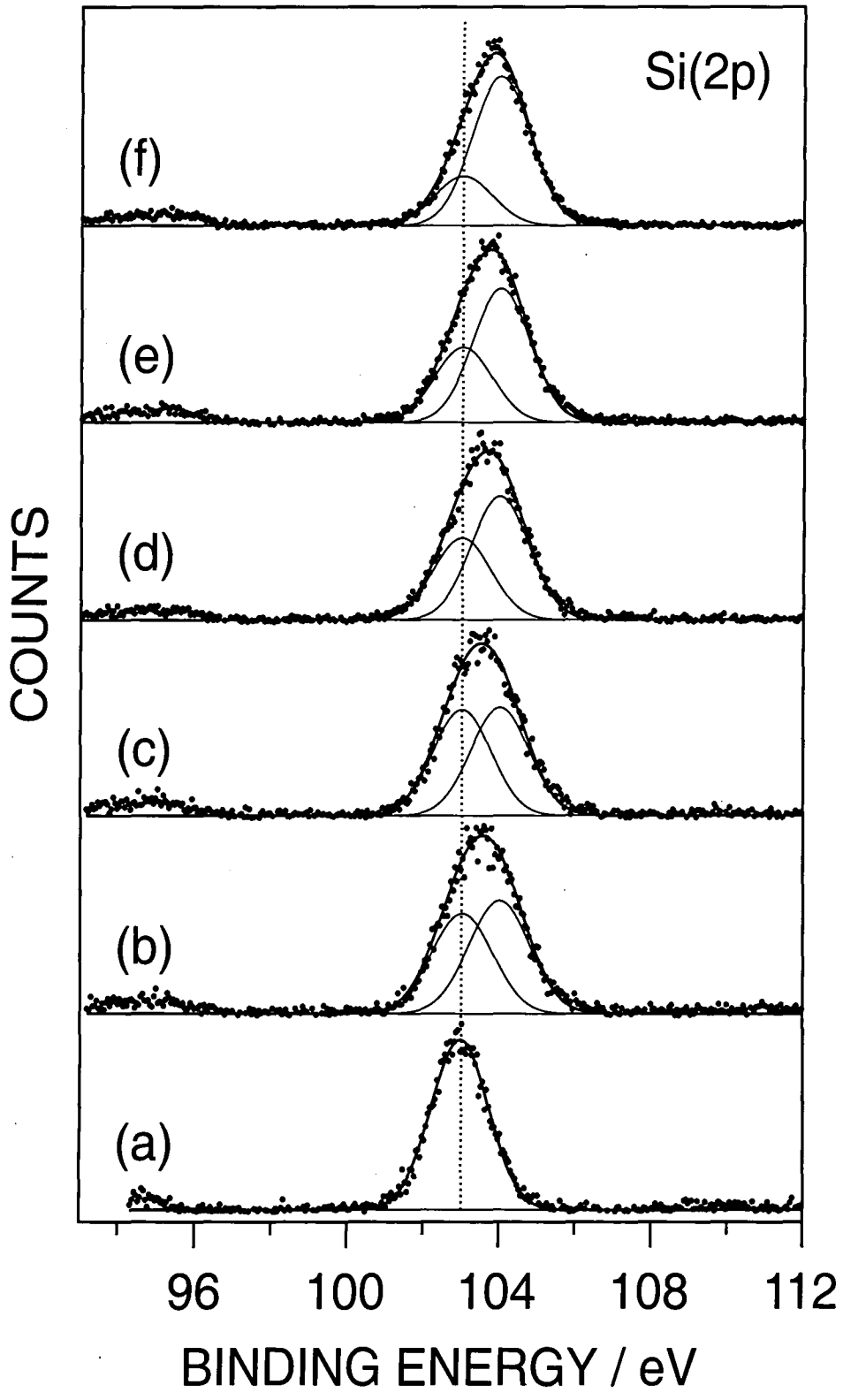

Figure 2.8 Si(2p) XPS spectra of DBD oxidized PPSQ (a) untreated, (b) 16 Hz, (c) 32Hz, (d) 82 Hz, (e) 164 Hz, (f) 328 Hz.

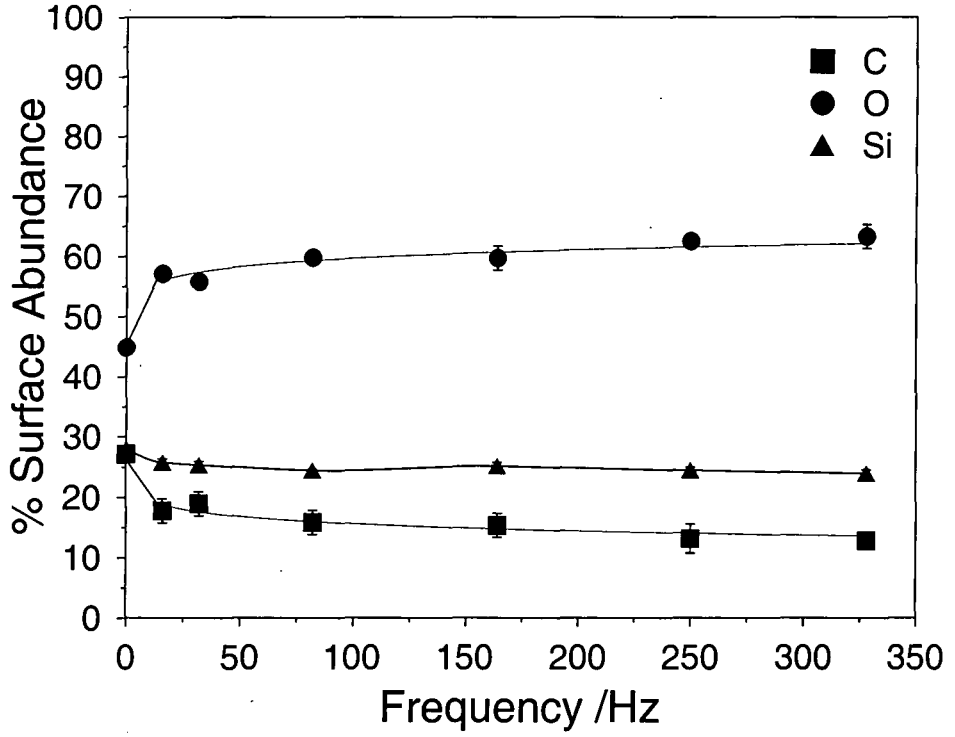

Figure 2.9a Surface elemental abundances of PMSQ oxidized with DBD treatments of varying frequencies.

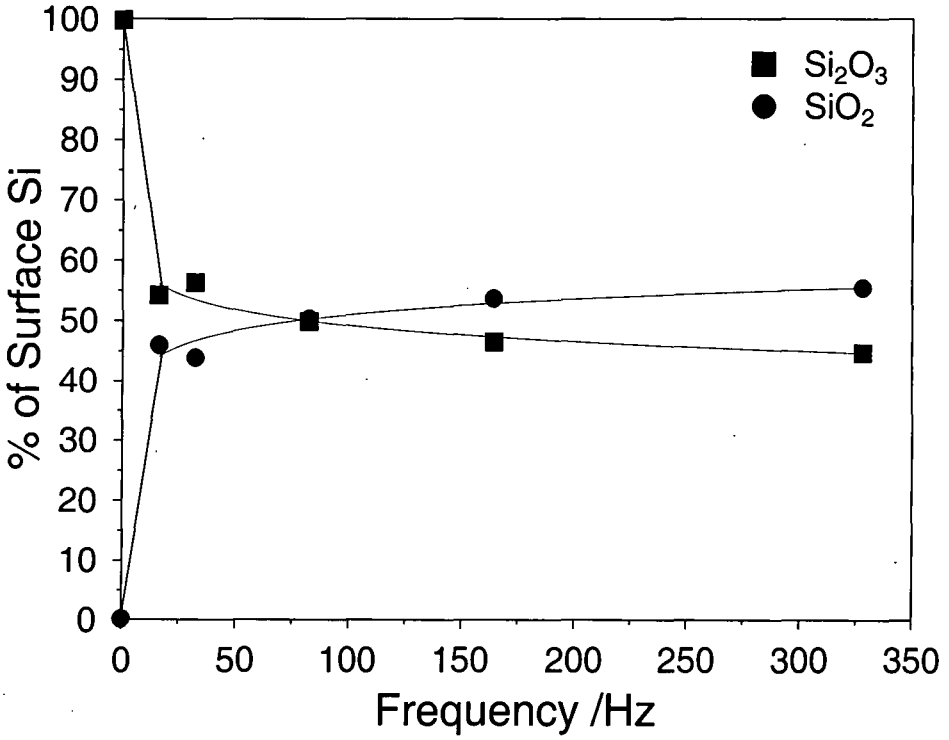

Figure 2.9b Silicon oxidation state distribution of PMSQ oxidized with DBD treatments of varying frequencies.

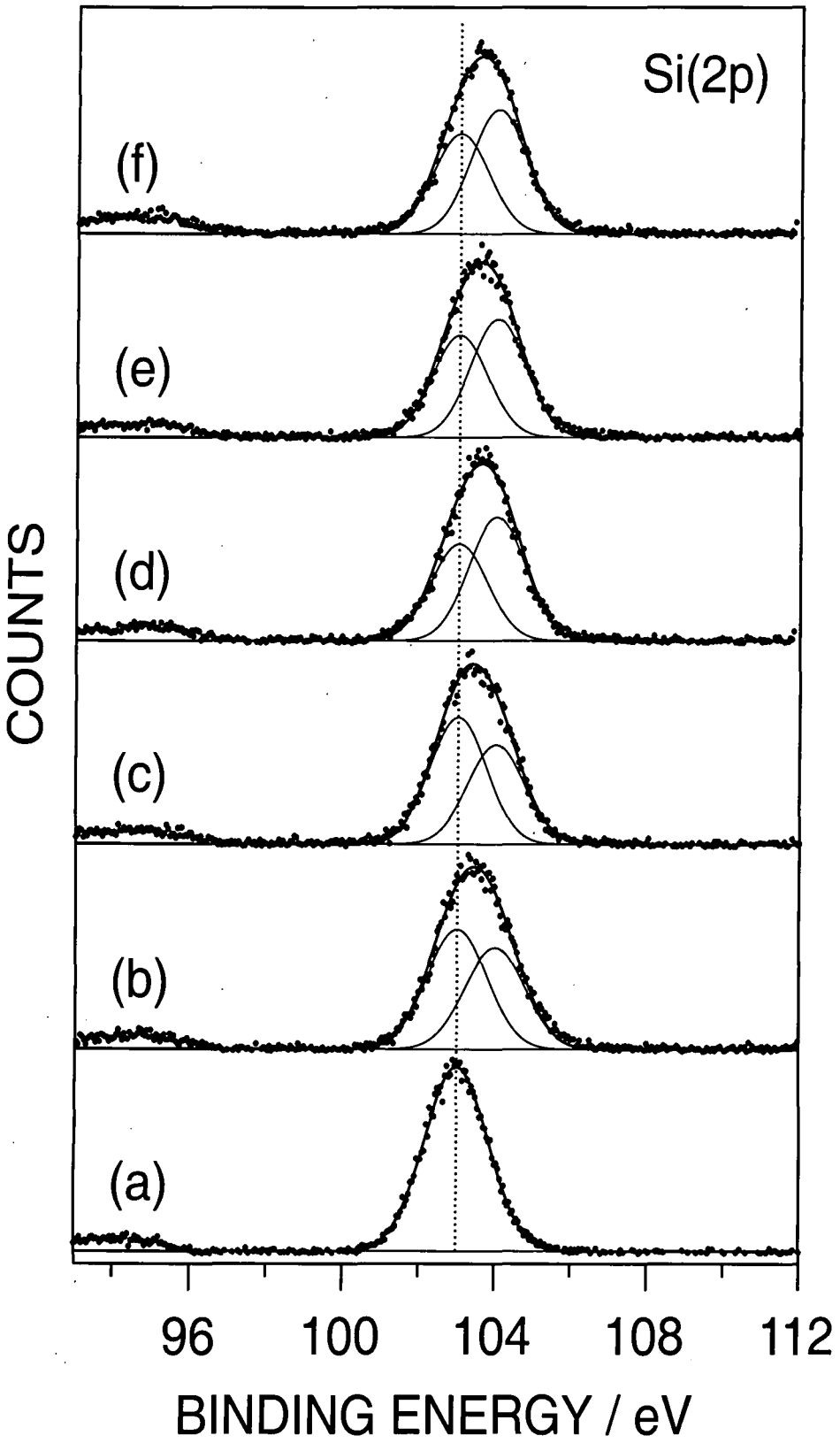

Figure 2.10 Si(2p) XPS spectra of DBD oxidized PMSQ (a) untreated, (b) 16 Hz, (c) 32Hz, (d) 82 Hz, (e) 164 Hz, (f) 328 Hz.

2.3.2 ARGON ION DEPTH PROFILES OF OXIDIZED PCHMS, PPSQ AND PMSQ

Argon ion depth profiling was performed upon 328 Hz air dielectric barrier discharge oxidized PCHMS, PPSQ and PMSQ.

The depth profile of oxidized PCHMS revealed the presence of a shallow layer of adventitious carbon upon an oxidized region rich in silicon and oxygen but depleted in carbon, Figure 2.11. Further etching gradually gave way to a material with elemental abundances resembling those of the unmodified polysilane. A small amount of nitrogen was evident for longer sputtering times. This may result from dissolution of the nylon substrate into the polysilane during / after spin coating or be genuine subsurface functionality introduced by the plasma treatment. Since the level remains constant with increasing sputter time it is unlikely to be due to the film having been etched through to the substrate (Nylon 6,6 contains 12.5% N).

The depth profiles of oxidized PPSQ and PMSQ exhibited similar features: a carbon rich layer over a silicon oxide rich zone, subsiding to unoxidized material underneath, Figures 2.12 and 2.13. However, the oxidized regions of the polysilsesquioxanes, especially PMSQ, were shallower and better delineated than that of oxidized PCHMS.

Estimated depths for dielectric barrier discharge oxidation were obtained by calibrating the sputter procedure. A sputter rate of 0.008 nm min^{-1} for siliceous material was determined by argon ion depth profiling a silicon wafer possessing a 20 nm thick overlayer of silicon dioxide. The thickness of the oxidized region was calculated from the sputter time where the elemental abundances reached a plateau representative of the unmodified material. This analysis indicated that the oxidation depths for PCHMS, PPSQ and PMSQ were approximately 12.2 nm, 5.0 nm and 1.2 nm respectively.

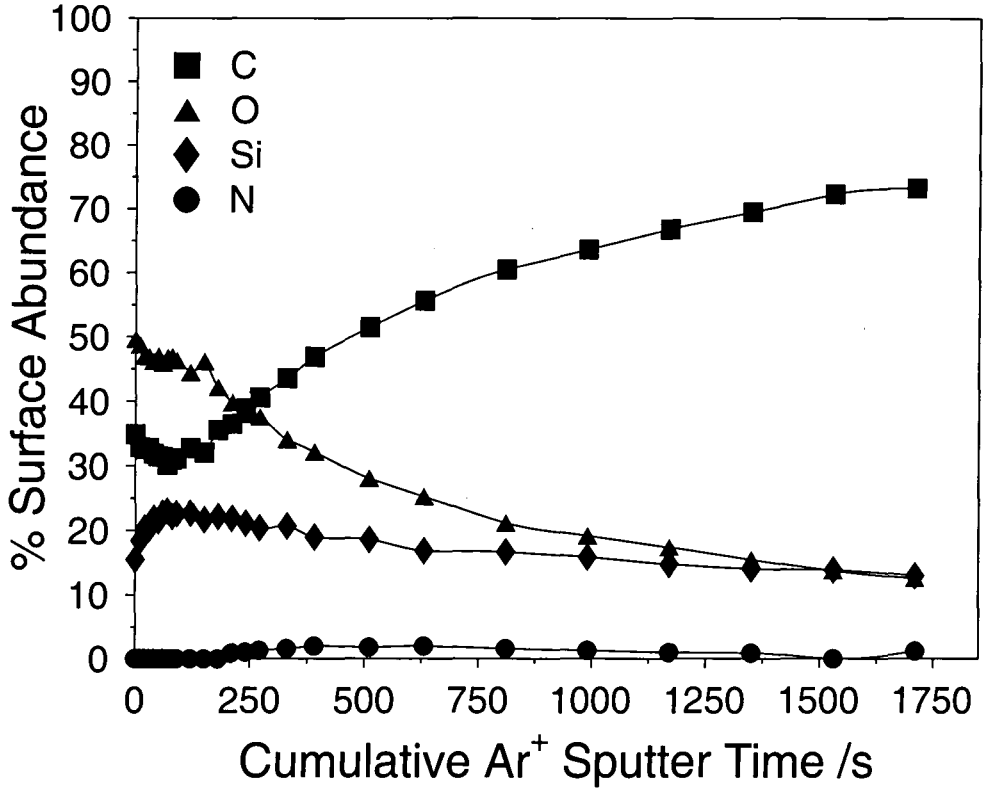

Figure 2.11 Depth profile of DBD oxidized PCHMS.

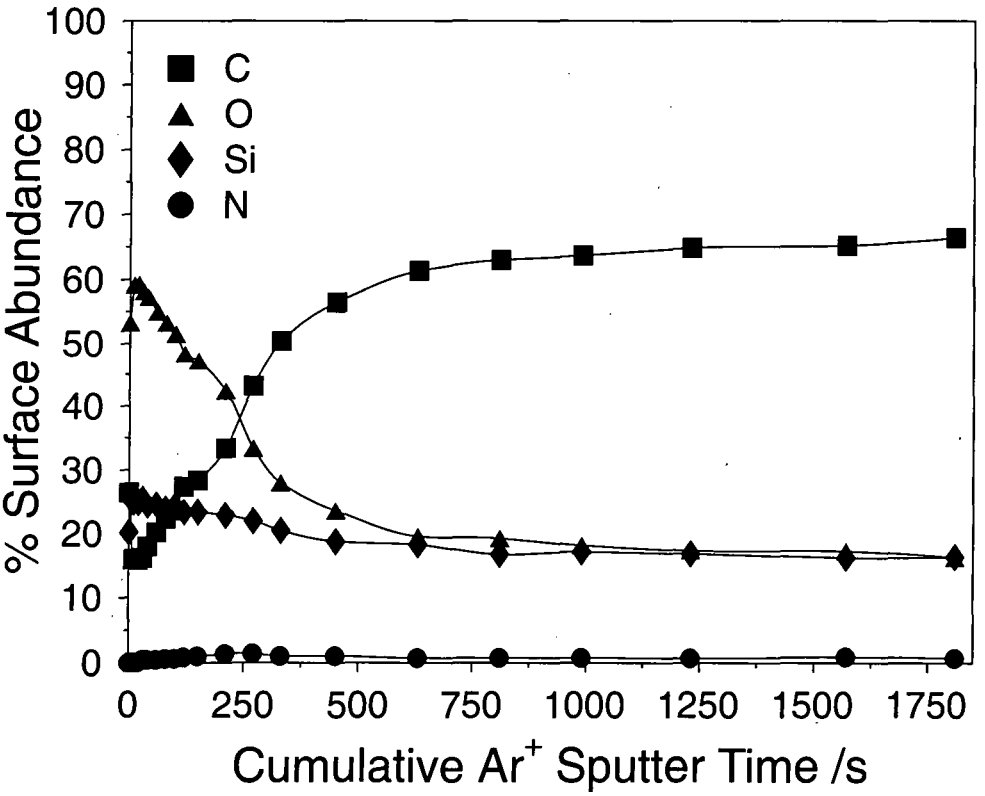

Figure 2.12 Depth profile of DBD oxidized PPSQ.

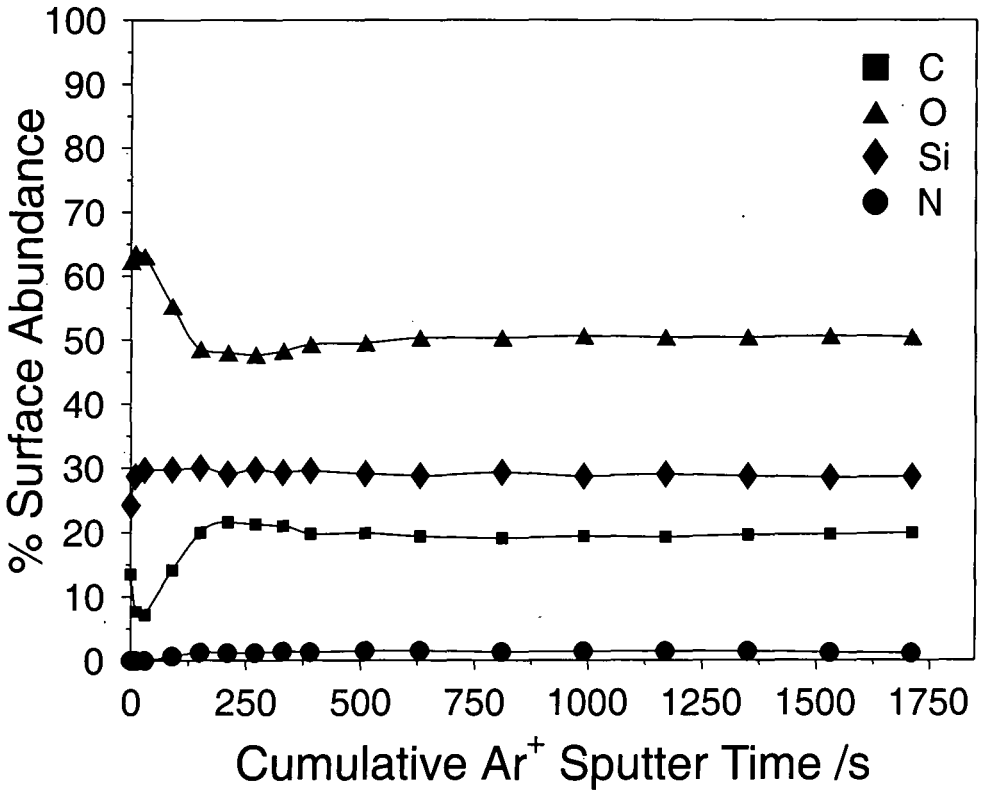

Figure 2.13 Depth profile of DBD oxidized PMSQ.

2.3.3 ATOMIC FORCE MICROSCOPY OF OXIDIZED PCHMS, PPSQ AND PMSQ

Atomic force microscopy was used to detect changes in surface morphology and homogeneity upon silent discharge treatment. Light and dark regions in the height image are indicative of high and low areas respectively.

The images of the untreated films were generally flat and homogenous, although the height images of the silsesquioxanes did possess some spherulitic features, Figures 2.14, 2.16 and 2.18.

Air dielectric barrier discharge treatment of PCHMS resulted in a surface covered in a network of cracks, Figure 2.15. Oxidation of PPSQ also yielded a heterogeneous surface, although with a morphology distinct from that of the polysilane, Figure 2.17. In contrast, PMSQ experienced a negligible degree of surface disruption, Figure 2.19.

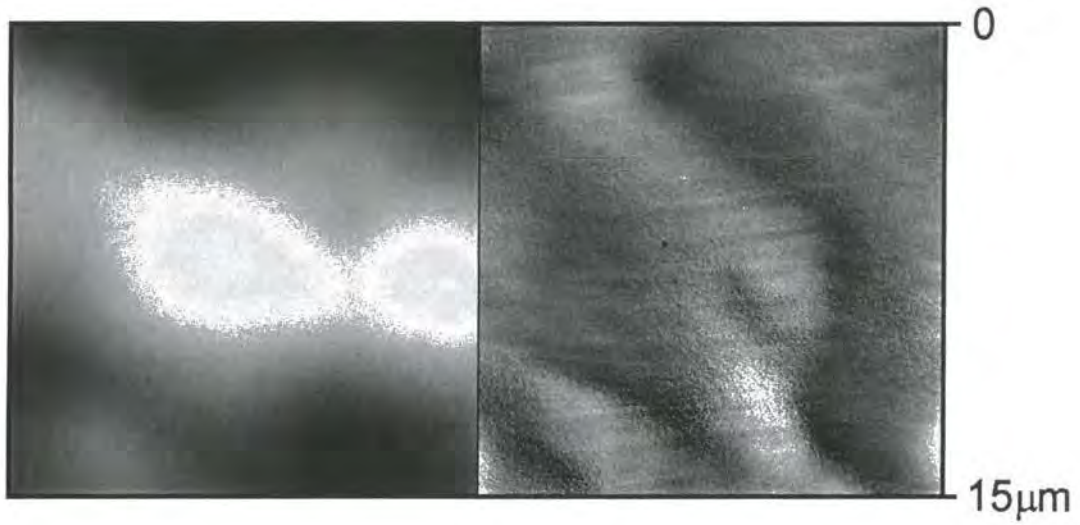

Figure 2.14 AFM image of an untreated PCHMS film (height LHS, phase RHS).

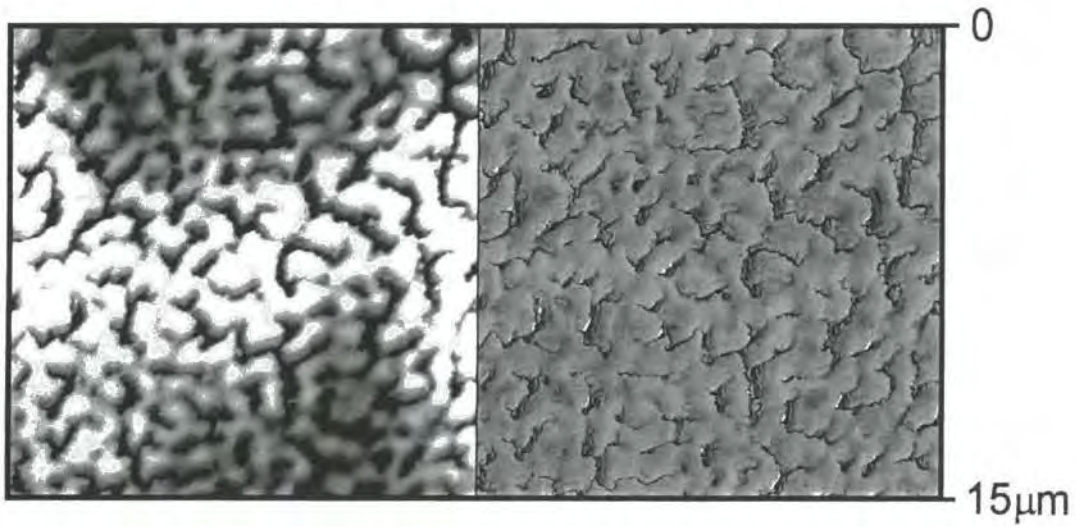

Figure 2.15 AFM image of a DBD oxidized PCHMS film (height LHS, phase RHS).

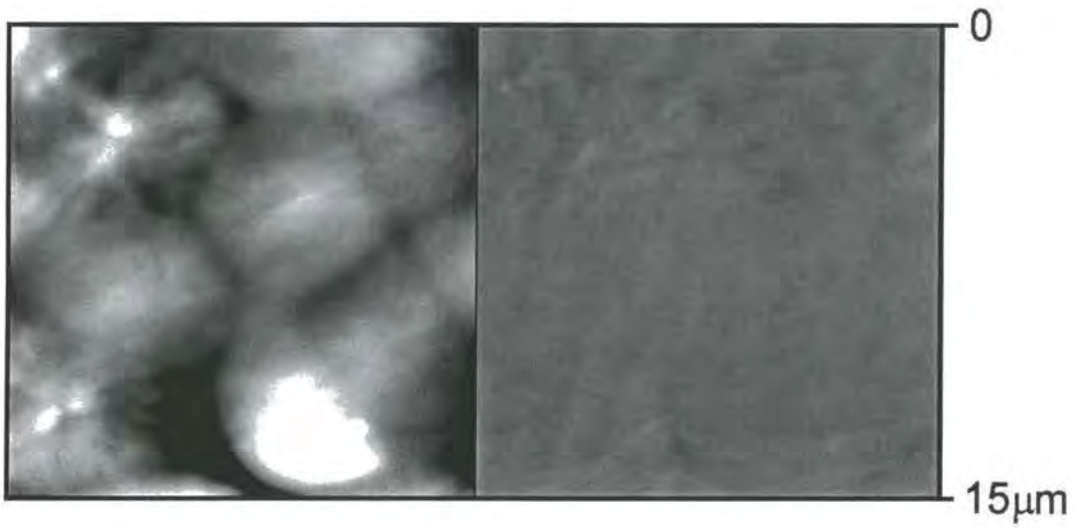

Figure 2.16 AFM image of an untreated PPSQ film (height LHS, phase RHS).

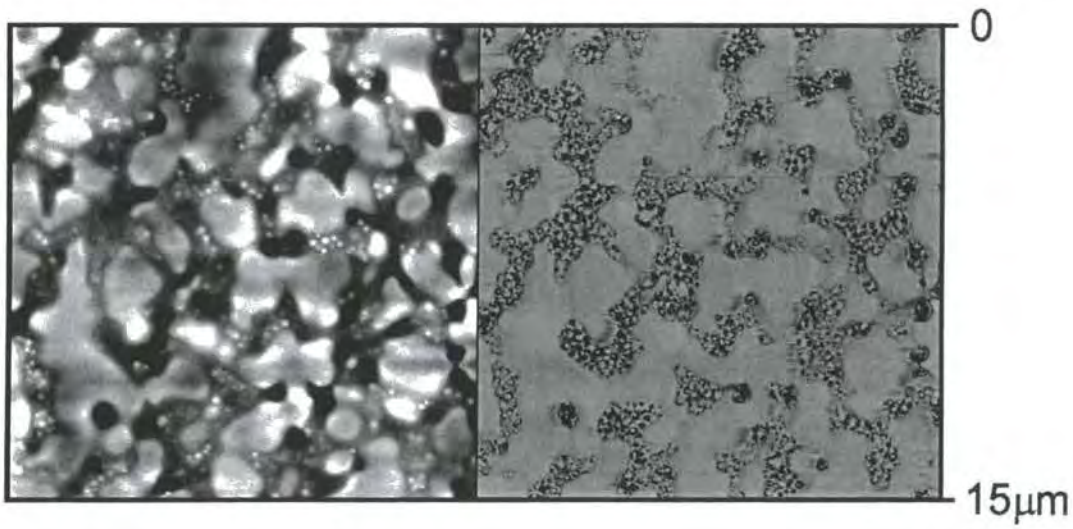

Figure 2.17 AFM image of a DBD oxidized PPSQ film (height LHS, phase RHS).

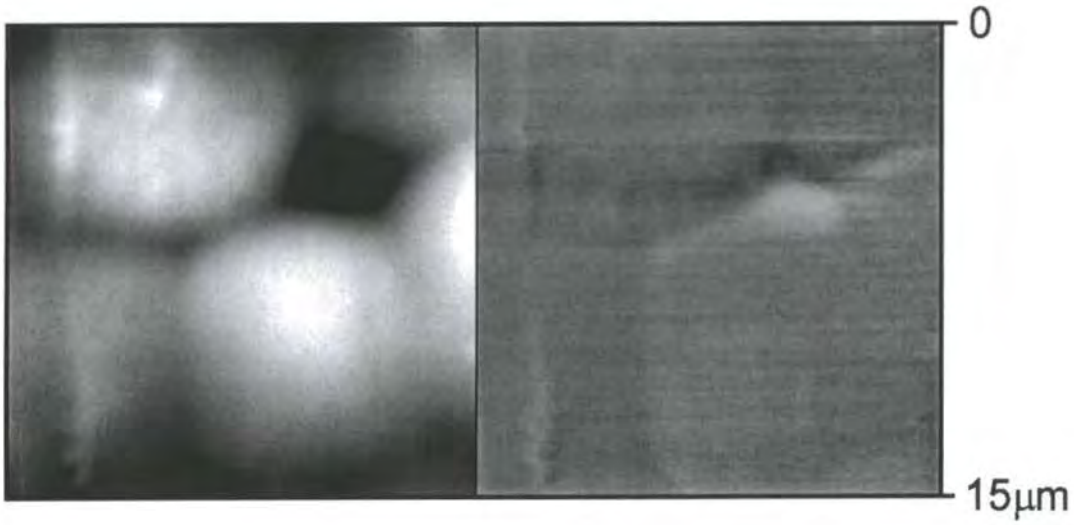

Figure 2.18 AFM image of an untreated PMSQ film (height LHS, phase RHS).

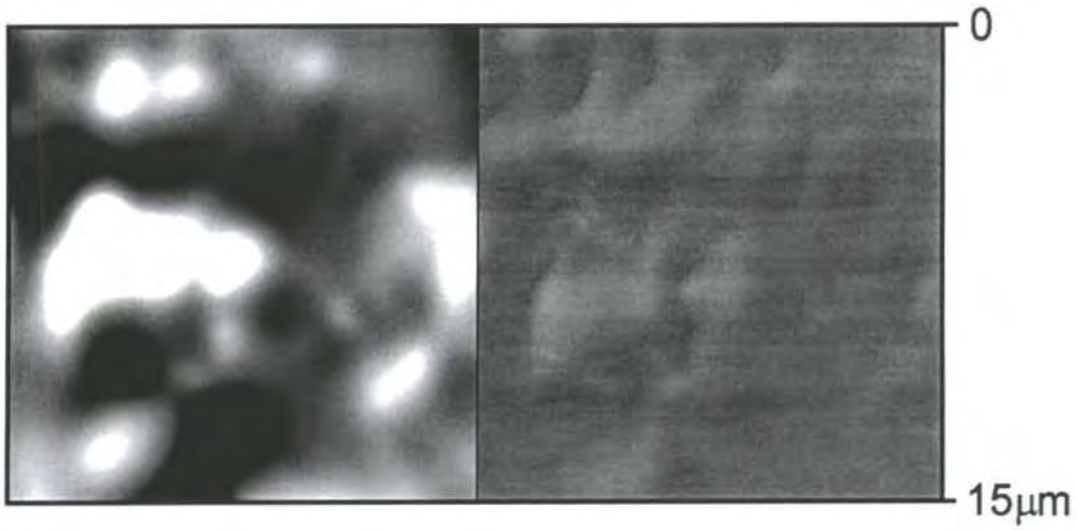

Figure 2.19 AFM image of a DBD oxidized PMSQ film (height LHS, phase RHS).

2.3.4 POWER AND OFF-TIME DEPENDENCE OF PMSQ OXIDATION

As the treatment of PMSQ showed the most potential with regard to producing an organic, carbon free surface the oxidation dependence upon discharge parameters was subject to further investigation.

In the first study the power of the discharge was varied by using different voltages. Investigations were carried out for 60 second treatments at a frequency of 50 Hz. At below approximately 55 % of maximum output there was no breakdown within the discharge gap and films exhibited the elemental characteristics of untreated samples. Above this threshold the degree of substrate oxidation was found to have a linear dependence on discharge power, Figures 2.20a and 2.20b.

In the second study the discharge frequency and treatment time were set so that the total number of pulses delivered to the substrate was constant but the "off-time" between pulses varied between $4 \leq \tau_{off} \leq 100$ ms. It was found that the surface abundancies of carbon, oxygen and silicon remained constant for the range of treatments performed, Figure 2.21a. However, the off-time did have an appreciable effect on the oxidation state of the silicon. Films treated with long off-times had a greater degree of silicon oxidation than those produced by a discharge treatment with shorter off-times but the same total number of pulses, Figure 2.21b.

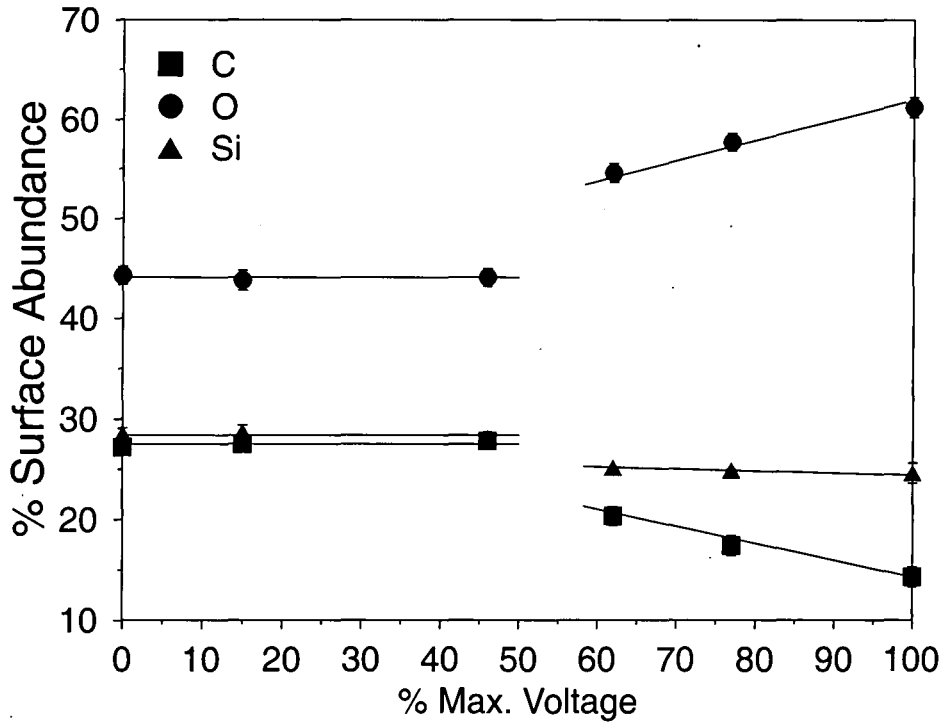

Figure 2.20a The effect of applied voltage upon the DBD treatment of PMSQ.

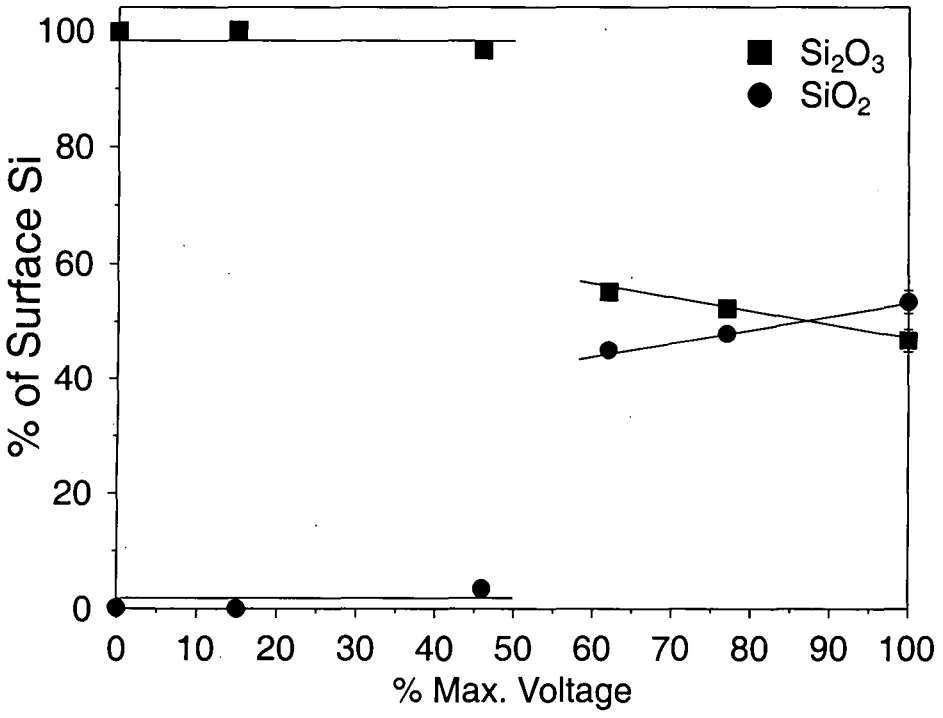

Figure 2.20b The effect of applied voltage upon the silicon oxidation state of DBD treated PMSQ.

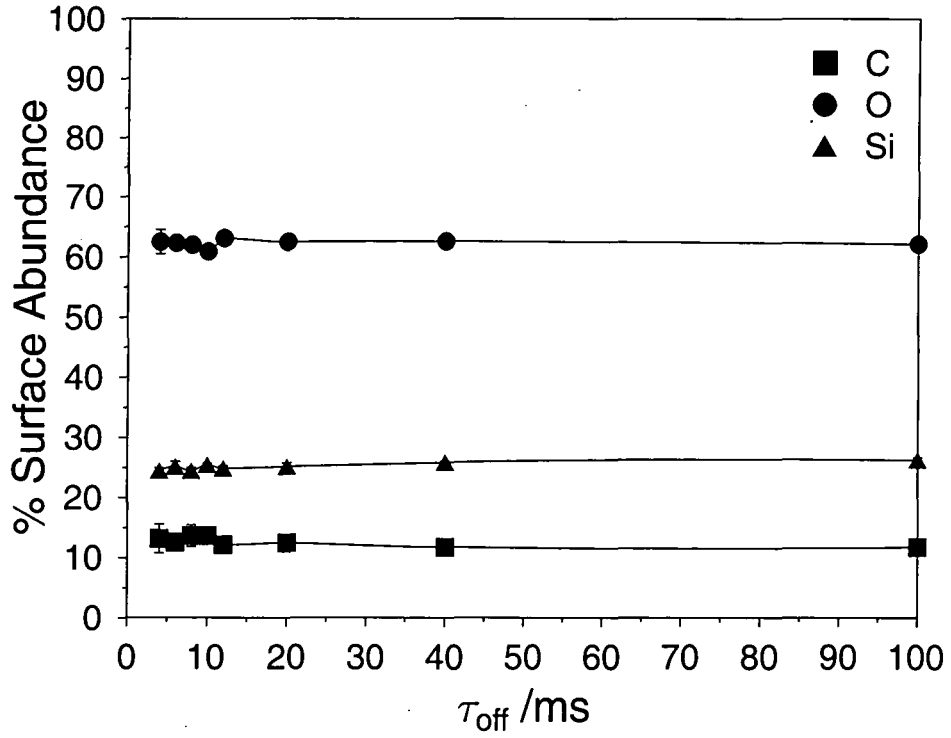

Figure 2.21a Surface elemental abundances of PMSQ oxidized with DBD treatments of varying plasma off-times.

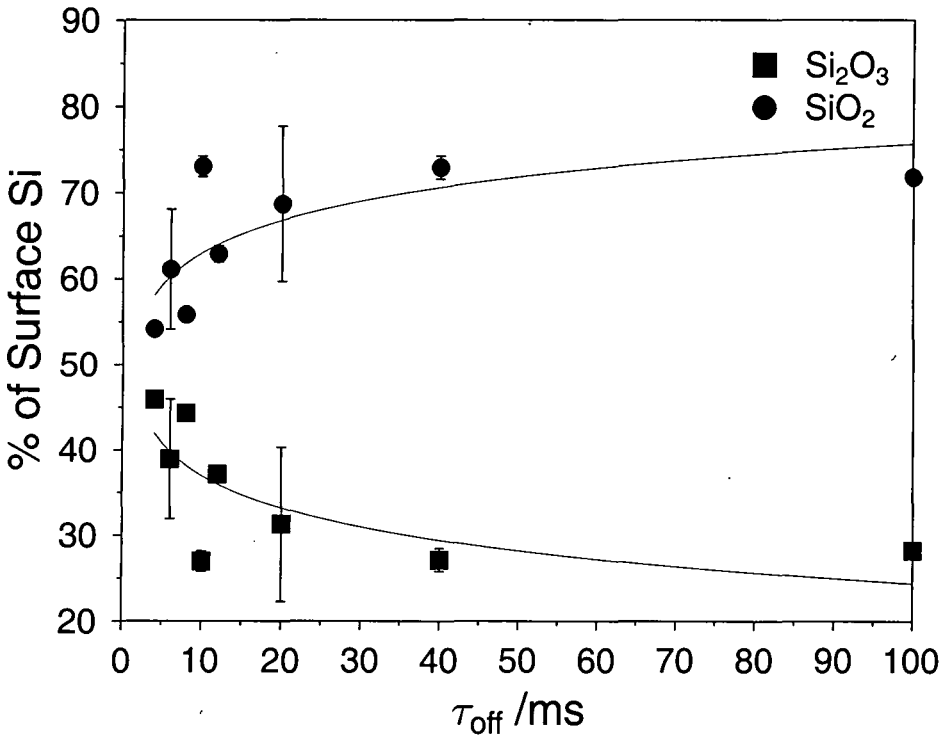

Figure 2.21b Silicon oxidation state distribution for PMSQ oxidized with DBD treatments of varying plasma off-times.

2.4 DISCUSSION

Air dielectric barrier discharge treatment of organo-silicon precursor layers was found to result in the loss of carbon with the concomitant incorporation of oxygen. The net effect was the formation of a SiO_x rich phase, intimated by the high Si(2p) binding energies (>103.5 eV), characteristic of high oxidation state silicon. The plasma oxidation of siloxanes has previously been shown to occur via the preferential attack of silicon by excited oxygen species.[37] This leads to the formation of Si-O bonds and the loss of pendant organic groups as non-condensing volatile species such as carbon dioxide and water.[38] Polysilanes in addition undergo chain scission and oxidation subsequent to UV absorption[14,15,16,17,18] and electron irradiation.[39] The net effect of these phenomena, the formation of SiO_x, may also be predicted on thermodynamic grounds: the average bond dissociation enthalpies of Si-Si, Si-C and C-C bonds are 226, 307 and 346 kJ mol^{-1} respectively.[40] The formation of stronger Si-O and C-O bonds, with energies of 466 and 358 kJ mol^{-1} respectively, is made possible by exposure to excited oxygen species. Therefore one would anticipate that treatment with a source of oxidative species, such as air dielectric barrier discharge, would result in weak Si-Si and Si-C bonds being broken and replaced by strong Si-O bonds, facilitating the loss of the organic component.

The extent of oxidation was found to depend on the frequency of the applied discharge. The kinetics which produce the active components in the dielectric barrier air discharge: primarily ozone, radicals, excited molecular species, electrons and photons,[32,41] are initiated in micro-discharges formed across the electrode gap. These micro-discharges are created by applying a rising voltage in excess of the breakdown voltage across the electrodes.[32,42] The higher the frequency, the greater the number of micro-discharges formed during the plasma treatment. This results in a higher concentration of excited species in the discharge and hence the greater degree of substrate oxidation observed. The limit on the degree of further modification achievable by higher frequencies is attributable to the formation of a SiO_X rich surface region, as observed in O_2-RIE, preventing the further reaction of subsurface organic groups.[20,21]

Atomic force microscopy illustrated the dependence of surface

morphology upon the nature of the oxidized substrate. PMSQ, which underwent the least compositional change upon dielectric barrier discharge treatment, also displayed the least damage. PPSQ was noticeably more degraded than PMSQ. This may be because the bulky phenyl groups create a more open structure, facilitating the penetration of oxidants, resulting in a greater degree of modification and more morphological damage. The surface of dielectric barrier discharge treated PCHMS was also heavily disrupted. An additional potential cause of damage for this system being photo-degradation and ablation by UV/oxidant induced scission of the Si-Si polymer backbone.[14,15,16,17,18] The reticulation of plasma oxidized organo-silicon compounds has also been ascribed to surface destabilisation by the conversion from a non-polar surface to polar SiO_x[43] and the increase in density accompanying the transformation to silica.[44]

The oxide thickness of plasma treated siloxane films is limited by the diffusion of active species through the silica layer created by oxidation and their penetration into the siloxane.[45] Argon-ion depth profiling of the oxidized organo-silicon films revealed that silent discharge oxidation has a depth of treatment comparable with that achieved by glow discharge oxidation of PPSQ (<5 nm)[44] and silicon containing resist materials (1-20 nm).[19,20,21] The oxidized layer was especially thin for PMSQ (~1 nm). A possible explanation is that the low initial level of organic content allowed the especially rapid creation of a highly oxidized crust which blocked further oxidation of the underlying film. This may also explain the low Si(2p) binding energies observed: the oxidized zone is shallow compared to the depth scanned by Si(2p) analysis, hence allowing more unoxidized material to contribute to the spectra. The deeper oxidation observed for PCHMS and PPSQ is attributable to the penetration of oxidized species through the large number of cracks observed by AFM. Hence the depth of treatment is effected by the structure of the precursor, films which undergo a high degree of chemical and morphological disruption (PCHMS > PPSQ > PMSQ) produce the thickest oxides.

Increasing the applied voltage when treating PMSQ films was found to have a positive effect on the degree of substrate oxidation. Higher discharge powers are known to increase the ozone yield of dielectric-barrier-discharge ozonizers as the high field strength increases the efficiency of reactions within the discharge gap.[46]

Increasing the separation between pulses appeared to have a positive effect on the amount of high oxidation state silicon (whilst causing negligible change to the surface elemental abundances). A possible reason for this enhancement is that the longer off-time allows oxidants to penetrate deeper and modify unreacted subsurface material. As Si(2p) spectra analyse a greater depth,[47] by virtue of the high kinetic energy of the photo-emitted electrons (~1150 eV with a Mg K_α X-ray source[48]), they are more sensitive to this sub-surface change.

2.5 CONCLUSIONS

Dielectric barrier air discharge treatment of organo-silicon films, quickly leads to the formation of highly oxidized layers rich in SiO_x under atmospheric conditions. The structure of the precursor was found to influence the morphology, silica content and thickness of the resultant film by limiting the penetration of oxidative species. Discharge parameters such as frequency, applied voltage and off-time were also observed to have a positive effect on the extent of oxidation.

2.6 REFERENCES

[1] Regnier, C.; Tristant, P.; Demaison, J. *Surf. Coat. Technol.* **1996**, *80*, 18

[2] Chatham, H. *Surf. Coat. Technol.* **1996**, *78*, 1

[3] Da Silva Sobrinho, A.S.; Czeremuszkin, G.; Latreche, M.; Wertheimer, M.R. Study of Defect Numbers and Distributions in PECVD SiO2 Transparent Barrier Coatings on PET. In *Plasma Deposition and Treatment of Polymers*; Lee, W.W.; d'Agostino, R.; Wertheimer, M.R., Eds.; Mater. Res. Soc. Symp. Proc. Vol. 544; Materials Research Society: Pittsburgh, PN, 1990, p 245

[4] Bergonzo, P; Patel, P.; Boyd, I.W.; Kogelschatz, U. *Appl. Surf. Sci.* **1992**, *54*, 424

[5] Gill, W.N.; Ganguli, S. *J. Vac. Sci. Technol. B* **1997**, *15*, 948

[6] Fujino, K., Nishimoto, Y.; Tokumasu, N.; Maeda, K. *Jpn. J. Appl. Phys.* **1994**, *33*, 2019

[7] Ikeda, K,; Maeda, M. *Jpn. J. Appl. Phys.* **1996**, *35,* 1573

[8] Fujino, K.; Nishimoto, Y.; Tokumasu, N.; Maeda, N. *J. Electrochem. Soc.* **1990**, *137*, 2883

[9] Nguyen, S.; Dobuzinsky, D.; Harmon, D.; Gleason, R.; Fridman, S. *J. Electrochem. Soc.* **1990**, *7*, 2209

[10] Rats, D.; Hajek, V.; Martinu, L. *Thin Solid Films* **1999**, *340, 33*

[11] Hollahan, J. R.; Carlson, G. L. *J. Appl. Polym. Sci.* **1970**, *14*, 2499.

[12] Owen, M. J.; Smith, P. J. *J. Adhesion Sci. Technol.* **1994**, *8*, 1063.

[13] Hettlich, H.-J.; Otterbach, F.; Mittermayer, C.; Kaufmann, R.; Klee, D. *Biomaterials* **1991**, *12*, 521.

[14] Watanabe, A.; Matsuda, M. *Macromolecules* **1992**, 25, 484

[15] Zeigler, J.M.; Harrah, L.A.; Johnson, A.W. *SPIE Advances in Resist Technology and Processing* **1985**, *539*, 166

[16] Ban, H.; Sukegawa, K. *J. Appl. Polym. Sci.* **1987**, 33, 2787

[17] Taylor, G.N.; Hellman, M.Y.; Wolf, T.M. *SPIE Advances in Resist Technology and Processing* **1988**, *920*, 274

[18] Kunz, R.R.; Horn, M.W.; Wallraff, G.M.; Bianconi, P.A.; Miller, R.D.; Goodman, R.W.; Smith, D.A.; Eshelman, J.R.; Ginsberg, E.J. *Jpn. J.*

Appl. Phys. **1992**, *31*, 4327

[19] Miller, R.D. *Angew. Chem. Int. Ed. Engl. Adv. Mater.* **1989**, *28*, 1733

[20] Smolinsky, G.; Reichmanis, E.; Wilkins, C.W. In *Proc. Regional Technical Conf. Photopolymers: Principals, Processes and Materials*, Ellenville, NY, 1985; Soc. Plastic Engin., 1985, p167

[21] Gokan, H.; Saotome, Y.; Saigo, K.; Watanabe, F.; Ohnishi, Y. Oxygen Ion Etching Resistance of Organosilicon Polymers. In *Polymers For High Technology: Electronics and Photonics*. Bowden, M.J.; Turner, S.R., Eds.; ACS Symposium Series 346; ACS: Washington, DC, 1987; p 358

[22] Watanabe, A.; Fujitsuka, M.; Ito, O. *Thin Solid Films* **1999**, *354,* 13

[23] Baney, R.H.; Itoh, M.; Sakakibara, A.; Suzuki, T. *Chem. Rev.* **1995**, *95*, 1409

[24] Minami, S.; Dachi, E.; Adachi, H. *Jpn. J. Appl. Phys.* **1996**, *35*, L1257

[25] Jaffres, P.A.; Morris, R.E. *J. Chem. Soc., Dalton Trans.* **1998**, 2767

[26] Sardja, I.; Dhali, S.K. *Appl. Phys. Lett.* **1990**, *56*, 21

[27] Chang, M.B.; Balbach, J.H.; Rood, M.J.; Kushner, M.J. *J. Appl. Phys.* **1991**, *69*, 44

[28] Boyd, I.W. *Appl. Surf. Sci.* **1997**, *109/110*, 538

[29] Bergonzo, P.; Kogelschatz, U.; Boyd, I.W. *Appl. Surf. Sci.* **1993**, *69,* 393

[30] Kogelschatz, U *Appl. Surf. Sci.* **1992**, *54*, 410

[31] Greenwood, O.D.; Boyd, R.D.; Hopkins, J.; Badyal, J.P.S. *J. Adhesion Sci. Technol.* **1995**, *9*, 311

[32] Eliasson, B.; Egli, W.; Kogelschatz, U. *Pure & Appl. Chem.* **1994**, *66,* 1275

[33] Pochner, K.; Neff, W.; Lebert, R. *Surface and Coatings Technology* **1995**, *74-75*, 394

[34] Fonseca, J.L.C. Ph.D. Thesis, University of Durham, 1992

[35] Hillborg, H.; Gedde, U. W. *Polymer* **1998**, *39*, 1991.

[36] Murakami, T.; Kuroda, S.-I.; Osawa, Z. *J. Colloid Interface Sci.* **1998**, *202*, 37.

[37] Morra, M.; Occhiello, E.; Marola, R.; Garbassi, F.; Humphrey, P.; Johnson, D. *Journal of Colloid and Interface Science* **1990**, *137*, 11.

[38] Muisener, R.J.; Koberstein, J.T. *Abstracts of Papers from the American*

Chemical Society **1997**, *214*, 56-MACR

[39] Lovinger, A.J.; Padden, F.J.; Davis, D.D. *Polymer* **1991**, *32*, 3086

[40] Aylward, G.; Findly, T. SI Chemical Data, 3rd Ed, John Wiley and Sons

[41] Eliasson, B. *IEEE Trans. Plasma Sci.* **1991**, *19*, 309

[42] Eliasson, B.; Hirth, M.; Kogelschatz, U. *J. Phys. D: Appl. Phys.* **1987**, *20*, 1421

[43] Chan, V.Z.H.; Thomas, E.L.; Frommer, J.; Sampson, D.; Campbell, R.; Miller, D.; Hawker, C.; Lee, V.; Miller, R.D. *Chemistry of Materials* **1998**, *10*, 3895

[44] Greenwood, O.G. Ph.D. Thesis, University of Durham, 1997

[45] Jones, J.W. U.S. Patent 3,442,686 May 6, 1969

[46] Ishimaru, K.; Okazaki, K. *Microscale Thermophysical Engineering* **1997**, *1*, 159

[47] Briggs, D.; Seah, M.P. Practical Surface Analysis Vol. 1, 2nd Ed., John Wiley & Sons, 1990

[48] *Handbook of X-ray Photoelectron Spectroscopy*; Chastain, J., Ed.; Perkin-Elmer Corporation: Minnesota, 1992

CHAPTER 3

THE ATTACHMENT OF CHLOROSILANE COUPLING AGENTS TO POLYMER SURFACES

3.1 INTRODUCTION

Silane coupling agents are a group of compounds with general formula R_nSiX_{4-n}, where R is a non hydrolysable organic group and X a group active in condensation reactions (usually ethoxy, methoxy or chlorine). They are chiefly used to functionalize solid silica surfaces. Their suitability stems from a combination of the resistance of the Si-O-Si linkage to hydrolysis and the ease of its formation.[1] Silane coupling agents react via a silanol (Si-OH) intermediate which typically bonds to silica 1000 faster than the equivalent carbon based alcohol.[2]

The type of coating formed by a coupling agent depends on the number of labile groups it possesses. Monofunctional (n=1) silanes tend to form monolayer thick films, often of low stability. In comparison trifunctional (n=3) silanes can be used to form films with thicknesses up to ten times that of a monolayer.[7] This has been attributed to the ability of trifunctional silanes to polymerize under appropriate conditions, both in solution and after adsorption upon the silica surface.[3,8,9]

The nature of the coupled product is also affected by the attachment conditions. Alkoxysilane and chlorosilane coupling agents are generally used in the solution phase. A standard procedure is to prehydrolyse them in an aqueous or aqueous-alcoholic solution to an equilibrium mixture of oligomers and polymers.[4,5] The silanol functionalities formed by this hydrolysis step are then allowed to react with the silica surface under acidic or basic conditions.[6] The resultant films are often ill-defined multi-layers: a mixture of 3-dimensional covalent networks and chemisorbed material.[4,6] An approach which affords greater control is to use a dry, organic solvent such as cyclohexane, thus limiting self condensation and oligomer formation.[7,8,9] Here the layer of adsorbed water present the silica surface is thought to be responsible for the hydrolysis of the Si-Cl or Si-OR bond.[8,9,10] If required, post-attachment cross-linking can subsequently be achieved by rinsing with water.[7]

Chlorosilanes can also be used in the vapour phase. At 573-673 K chlorosilanes react directly with surface silanol groups.[11] The high temperature limits this process to silanizing agents with a high degree of thermal stability.

However, the presence of an adsorbed water layer has been reported to permit the low temperature reaction of chlorosilane vapour with surfaces.[12,13,14,15,16]

In addition to silica, chlorosilanes have been used to functionalize iron,[17] alumina,[18] titanium oxide,[19] oxidized PDMS,[20] and chemically derivatized PET[21] and PTFE.[22] In this chapter chlorosilane coupling agents have been used to functionalize polyethylene. Section 3.2 focuses upon an atmospheric pressure method of attaching a perfluorinated trichlorosilane directly to dielectric barrier discharge (DBD) oxidized polyethylene. In Section 3.3 a precursor layer of condensed chlorodisilanes is vapour phase grafted to polyethylene. The resultant solvent resistant layers resembled polydimethylsiloxane (PDMS) and were highly amenable to atmospheric pressure oxidation. In addition to providing a reactive substrate for conventional coupling agent chemistry these coatings also possessed superior post-oxidative stability to PDMS and permitted the assembly of multi-layer gas barriers.

3.2 SOLVENTLESS COUPLING OF PERFLUOROALKYL CHLOROSILANES TO POLYMER SURFACES

3.2.1 INTRODUCTION

Fluorinated polymer surfaces are renowned for their liquid repellency, chemical inertness, and low coefficient of friction.[22] These attributes find application in biomedical devices,[23] anti-fouling finishes, filter media[24] and release coatings.[25] Current methodologies for achieving such behaviour include F_2 gas treatment,[26] plasma polymerization,[27] sputter-deposition,[28] and solution-based coating of preformed polymers.[29] All of these approaches tend to suffer from either being expensive, restricted to batch processing, safety hazards, or the generation of solvent waste.

In this study, the direct vapour phase grafting of perfluoroalkyl chlorosilanes onto dielectric-barrier discharge activated polymer substrates is described. Potential benefits include the scope for continuous processing and low cost. Silane coupling agents have been previously used to functionalize silica,[1,7,13,15] titanium dioxide,[19] alumina,[18] mica,[3] iron,[17] plasma oxidized polymethlysiloxane,[14,20] and hydroxylated PTFE[22] and PET.[21] In all of these cases hydroxyl groups were a prerequisite for chlorosilane coupling chemistry to proceed. Here a comparison is made between the relative efficiencies of monochloro and trichloro silane coupling reactions onto atmospheric dielectric barrier discharge activated polymer substrates.

3.2.2 EXPERIMENTAL

Glass and polyethylene (ICI) substrates were ultrasonically cleaned in a 1:1 mixture of isopropyl alcohol (BDH, Analar grade) and cyclohexane (BDH, Analar grade) for 30 s and dried in air prior to usage.

The parallel-plate silent-discharge apparatus described in Section 2.2 was used to activate the polymer film. Surface activation entailed placing the substrate under investigation on top of the dielectric layer and operating the

electrical discharge in air at a frequency of 328 Hz for 10 s using a 2 mm inter-electrode gap.

1,H 1H, 2H, 2H - perfluorodecyltrichlorosilane, (PFDTCS, $CF_3(CF_2)_7(CH_2)_2SiCl_3$, Fluorochem) and 1H, 1H, 2H, 2H - perfluorodecyl dimethylchlorosilane, (PFDMCS, $CF_3(CF_2)_7(CH_2)_2SiMe_2Cl$, Fluorochem) were used as the coupling reagents. Vapour phase exposure comprised placing each substrate in a sealed 60 cm^3 container under a dry nitrogen atmosphere (13 ppm H_2O, 12 ppm O_2), in the presence of 0.02 ml of chlorosilane. Adhesion of the fluorinated overlayer to the substrate was tested by washing in 1,3 bis (trifluoromethyl) benzene (99%, Aldrich), which is capable of dissolving any loose coupling reagent entrapped on the surface.

XPS analysis was undertaken using the equipment and methods described in Section 1.3.1.

Contact angle measurements were performed as described in Section 1.3.3 using de-ionized water and decane (Aldrich, 99+%).

3.2.3 RESULTS

Glass was chosen as a reference substrate because chlorosilanes are often coupled to silica surfaces. PFDTCS vapour reacted with glass to yield a well adhered hydrophobic / oleophobic surface with elemental abundances corresponding to a complete coverage of the substrate, Table 3.1. In the case of polyethylene, PFDTCS was found to adsorb onto the surface, but could be easily removed by washing in 1,3 bis-trifluoromethylbenzene. However, silent discharge pre-treatment of polyethylene in air was found to significantly improve the attachment of PFDTCS onto the surface. In this case, solvent washing made very little difference, and elemental abundances closely matched those seen for the glass substrate (i.e. approaching the theoretical values for complete coverage). Therefore the film thickness must at least be comparable to the XPS sampling depth (2-5 nm).[30] The absence of a Cl(2p) signal from all the samples intimated complete hydrolysis of the Si-Cl bond.

The small drop in fluorinated functionality (%(CF_3+CF_2)) seen after solvent washing can be accounted for in terms of the loss of low-molecular-weight-oxidized polyethylene chains,[35] or the removal of a loosely bound layer

of chemisorbed coupling agent.[4,31] The latter explanation is more likely considering the fact that a similar decrease was observed for the glass substrate (where adhesion to the reactive silanol rich surface is not considered to be an issue).

Prior to plasma activation, the C(1s) XPS spectrum of polyethylene showed a single peak at 285.0 eV corresponding to $\underline{C}_xH_y$, Figure 3.1. Silent-discharge pre-treatment gave rise to a high binding energy shoulder attributable to oxidized moieties.[32] Exposure of this oxygenated surface to PFDTCS vapour dramatically changed the appearance of the C(1s) envelope, with the emergence of a distinct high binding-energy component attributable to fluorinated functionalities ($\underline{C}$-CF: 286.6 eV; $\underline{C}F_2$: 291.2 eV; $\underline{C}F_3$: 293.3 eV).[32] The concentration of these groups increased with exposure time in conjunction with percentage fluorine and water contact angle. A plateau was reached towards 18 hours, corresponding to thicknesses greater than the XPS sampling depth, Figure 3.2.

The mono-chlorosilane analogue of PFDTCS, PFDMCS was found to be not as effective at modifying the glass substrate, Table 3.2. From a theoretical perspective, at best, the coupled layer should only reach monomolecular coverage, (because of the mono-functional nature of the coupling agent) which will be less than the XPS sampling depth. Similar behaviour was noted for the dielectric barrier discharge treated polyethylene substrate, where prolonged monochlorosilane exposure produced only marginal improvement, Figure 3.2. Furthermore, the speed of reaction was much slower compared to glass (although it was quicker than the virgin polyethylene), Figure 3.3. This may be indicative of the greater reactivity of silanol groups on glass compared to activated sites of dielectric barrier treated polyethylene.

	% C	% F	% O	% Si	%(CF_3+CF_2) of total % C	Contact angle (H_2O) /°	Contact angle (decane) /°
Theoretical complete PFDTCS layer.	34.5	58.6	6.6	3.3	80.0	-	-
Glass	22.9 ±2.7	0	52.9 ±1.3	24.2 ±1.9	0	18.0 ±2.0	wets
Glass / PFDTCS	33.1 ±3.4	49.3 ±5.8	10.6 ±5.4	6.5 ±3.1	73.9 ±1.2	113.2 ±1.3	74.2 ±3.7
Glass / PFDTCS / washed	26.7 ±2.1	47.8 ±4.5	15.8 ±5.1	9.6 ±1.5	64.5 ±4.6	105.1 ±2.9	71.2 ±2.6
PE	100	0	0	0	0	112.8 ±2.1	wets
PE / PFDTCS	87.5 ±4.6	9.4 ±5.6	2.1 ±0.7	1.0 ±0.4	1.7 ±1.7	113.6 ±3.9	82.7 ±3.0
PE / PFDTCS / washed	83.4 ±3.2	1.3 ±0.1	9.4 ±1.9	5.8 ±1.2	~0	112.0 ±1.8	wets
DBD PE	82.5 ±1.5	0	17.5 ±1.5	0	0	65.8 ±1.4	0
DBD PE / PFDTCS	33.0 ±1.0	56.5 ±1.5	6.2 ±0.2	4.3 ±0.3	73.9 ±2.8	142.6 ±4.1	83.7 ±3.3
DBD PE / PFDTCS / washed	34.6 ±0.9	50.9 ±0.5	7.6 ±1.1	6.9 ±0.3	65.5 ±5.6	135.6 ±4.4	79.2 ±3.3

Table 3.1 Results for 18 hr PFDTCS exposure.

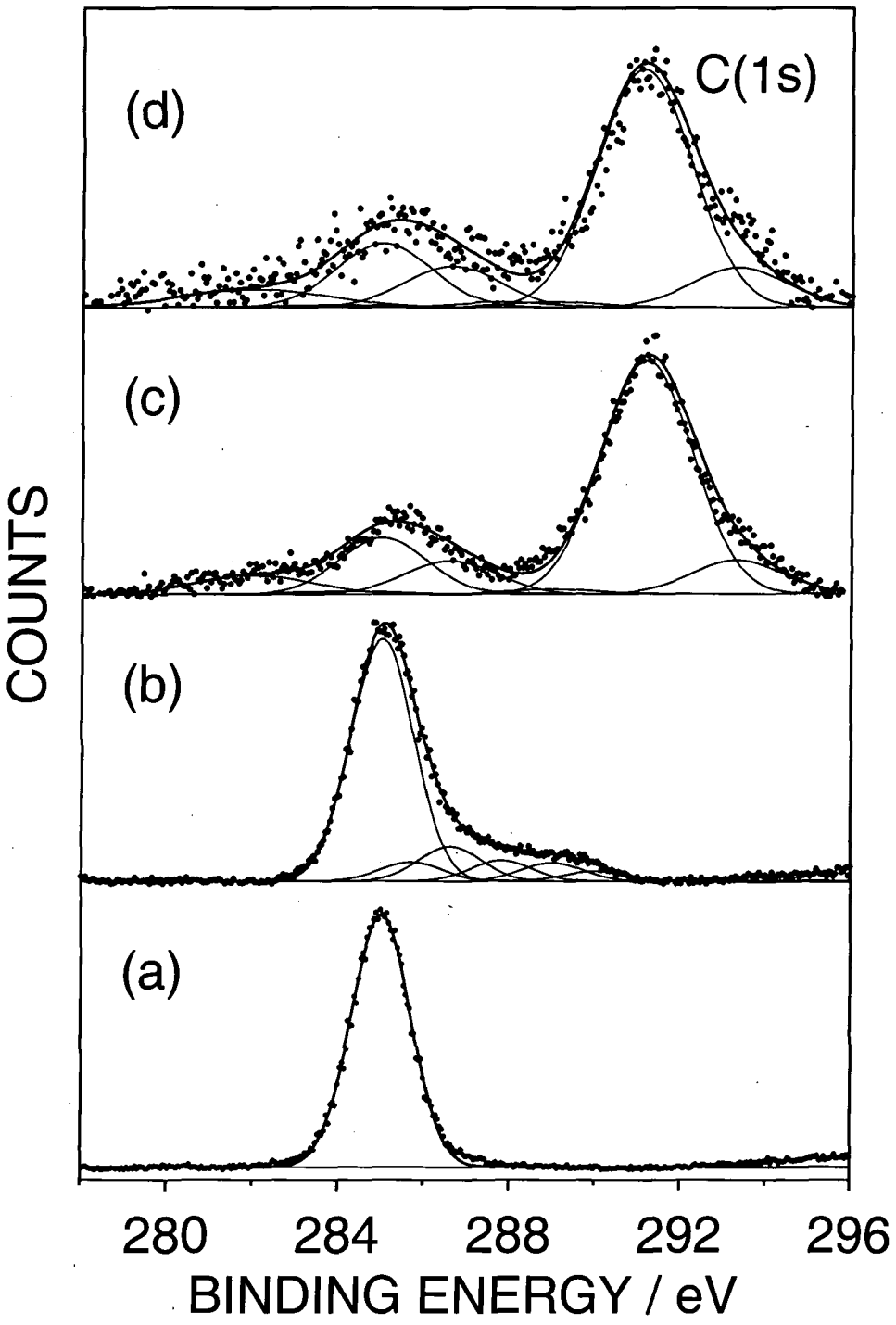

Figure 3.1 C(1s) XPS spectra of (a) clean PE; (b) 10 s silent discharge oxidized polyethylene; (c) 10 s silent discharge oxidized polyethylene exposed to PFDTCS; (d) solvent washed (c).

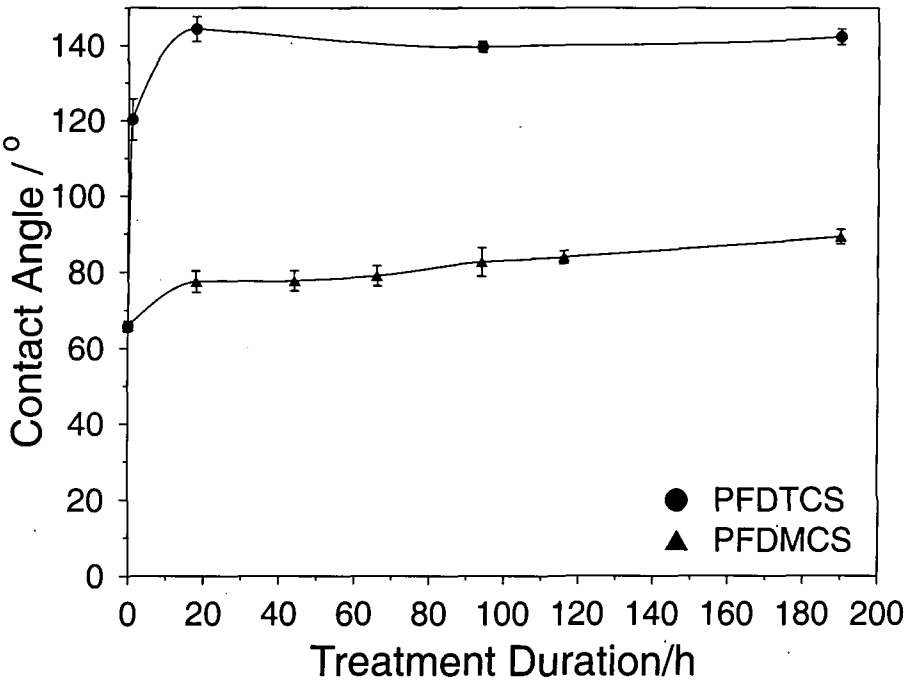

Figure 3.2a Time dependence of PFDTCS and PFDMCS coupling to 10 s silent discharge oxidized polyethylene: water contact angle.

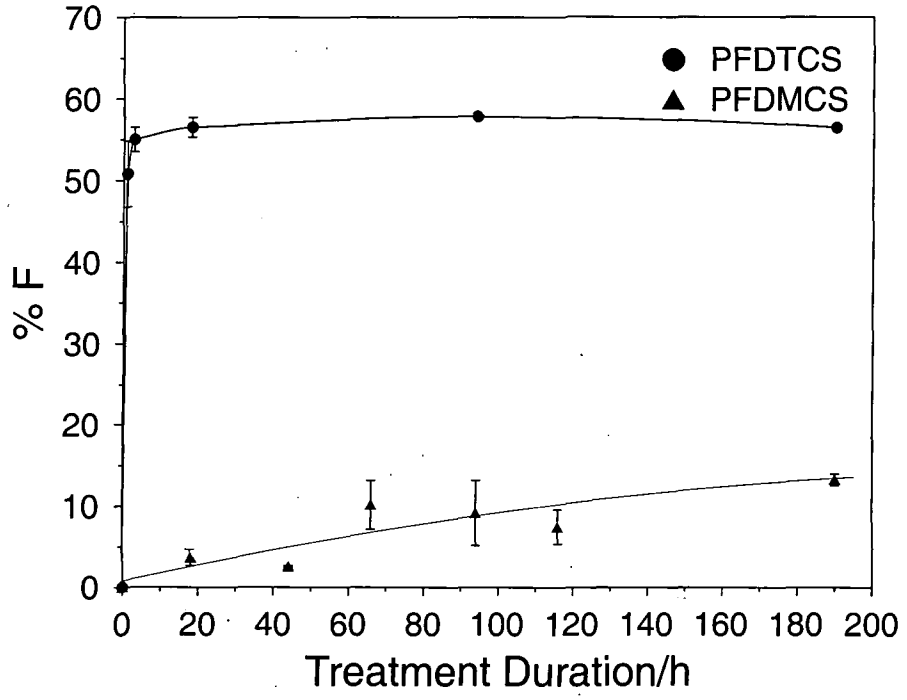

Figure 3.2b Time dependence of PFDTCS and PFDMCS coupling to 10 s silent discharge oxidized polyethylene: %F.

	% C	% F	% O	% Si	Contact angle (H_2O) /°	Contact angle (decane) /°
Glass / PFDMCS	16.3 ±1.0	19.5 ±1.2	43.4 ±0.4	20.9 ±0.1	96.0 ±4.7	47.6 ±4.1
Glass / PFDMCS / washed	23.7 ±2.8	18.2 ±3.0	39.4 ±2.8	18.7 ±1.2	91.4 ±2.2	49.9 ±4.3
Clean PE / PFDMCS	99.6 ±0.1	0	0.6 ±0.1	0	115.6 ±1.7	wets
Clean PE / PFDMCS / washed	99.4 ±0.6	0	0.6 ±0.4	0	108.8 ±3.6	wets
DBD PE / PFDMCS	80.0 ±0.9	3.7 ±1.0	15.2 ±0.9	1.1 ±0.7	77.5 ±2.8	wets
DBD PE / PFDMCS / washed	77.0 ±4.6	1.6 ±0.3	17.7 ±1.3	3.6 ±3.6	82.3 ±3.5	wets

Table 3.2 Results for 18 hr PFDMCS exposure.

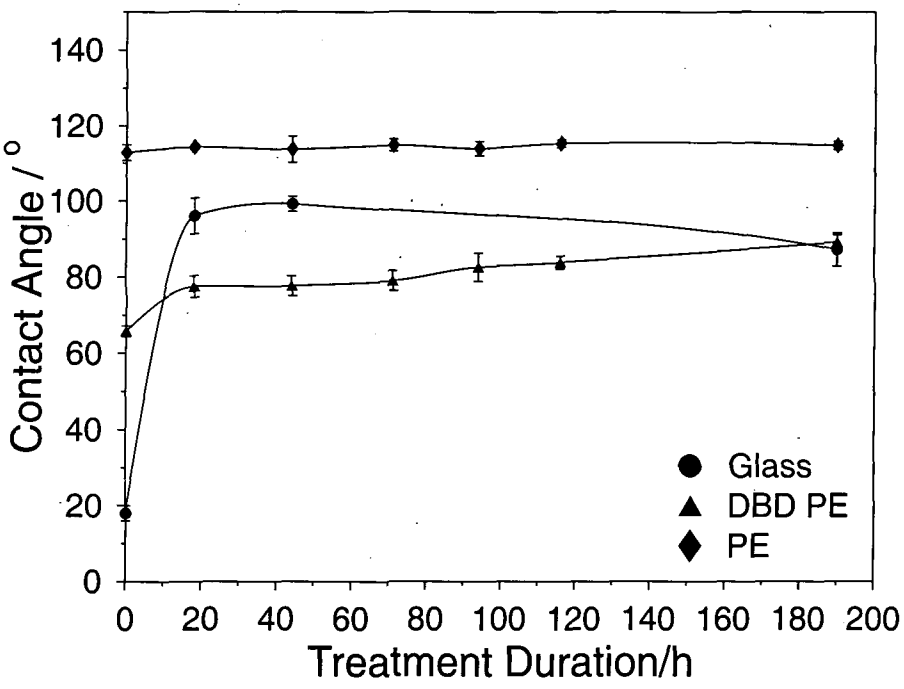

Figure 3.3a PFDMCS labelling onto polyethylene, silent discharge treated polyethylene and glass as a function of exposure time: water contact angle.

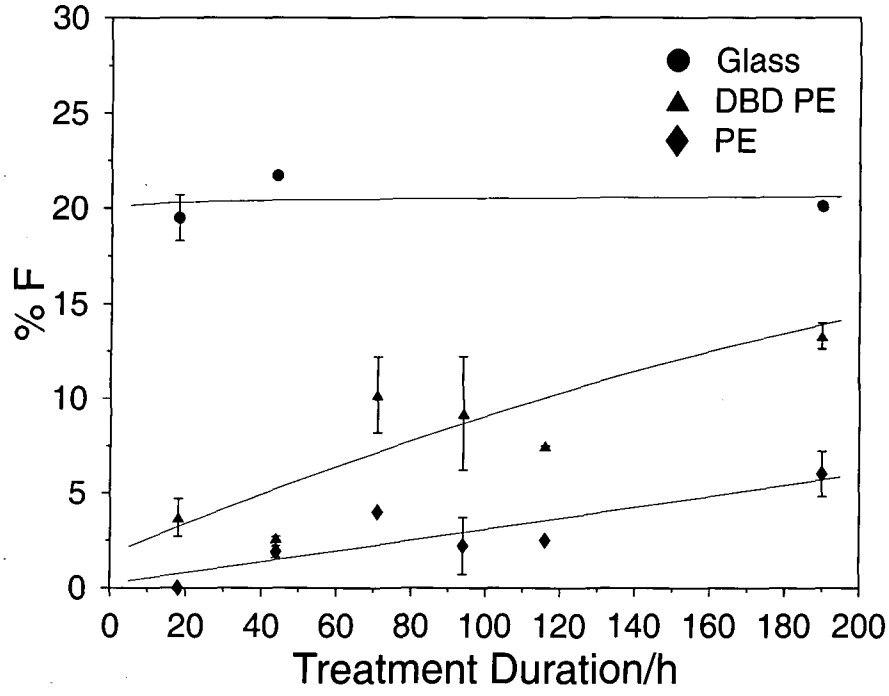

Figure 3.3b PFDMCS labelling onto polyethylene, silent discharge treated polyethylene and glass as a function of exposure time: %F.

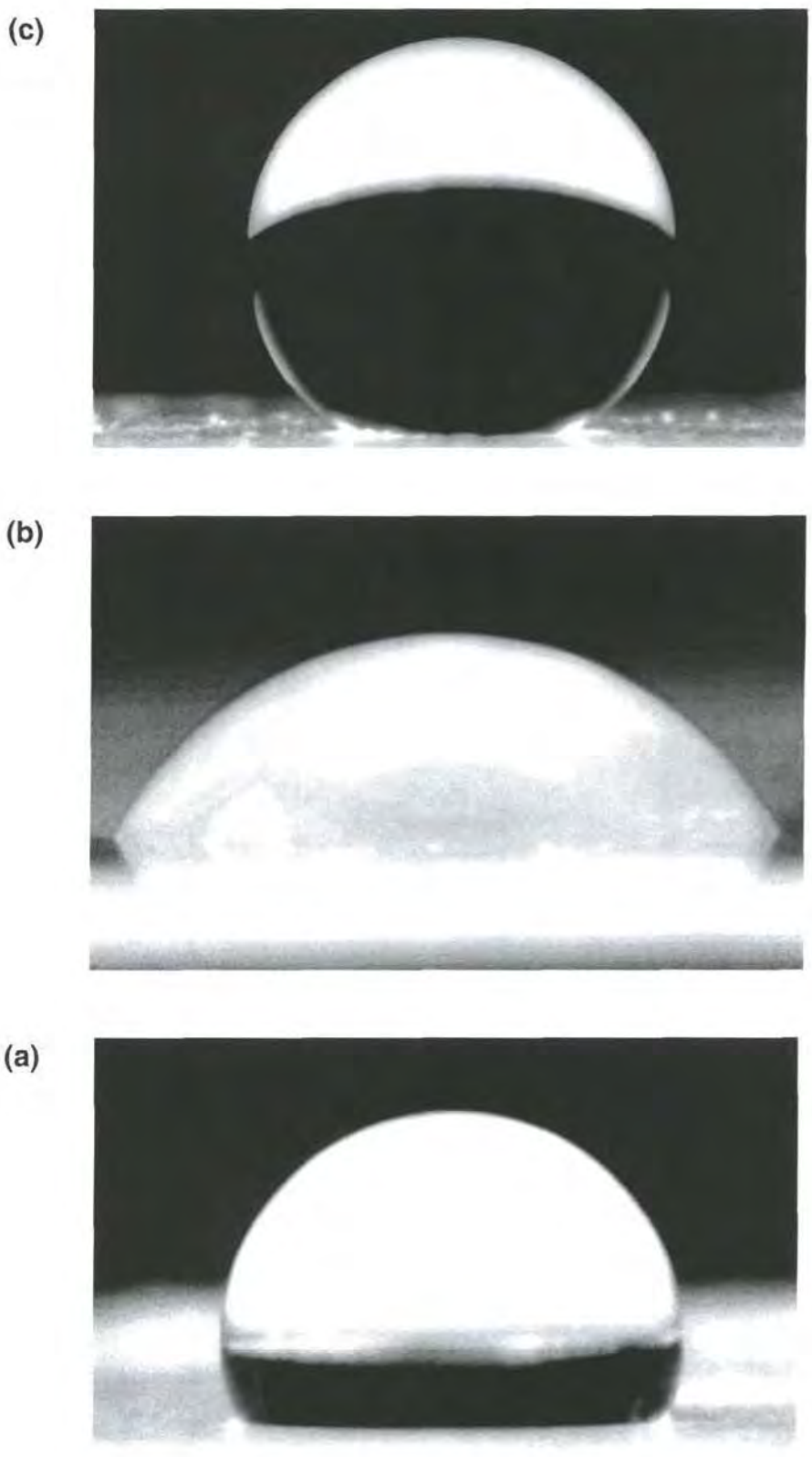

Figure 3.4 Water droplets sitting on: (a) clean polyethylene; (b) silent discharge treated polyethylene; and (c) PFDTCS coupled to silent discharge treated polyethylene.

3.2.4 DISCUSSION

Dielectic barrier discharges are already used for producing ozone, destroying air borne pollutants,[33,34] generating high intensity VUV excimer radiation,[35,36,37] and improving the wettability and adhesive properties of polymer surfaces.[38,39] Therefore existing results may be adapted for chlorosilane chemistry.

Conventional chlorosilane coupling to solid surfaces is understood to occur via a silanol intermediate which subsequently binds to reactive sites, this process is susceptible to being catalysed by surface water, Scheme 3.1.[10,11,40] The observed formation of thick PFDTCS films onto glass is a manifestation of the ability of tri-chlorinated silanes to polymerize into a 3-dimensional network following adsorption.[3,4,6,9] Thicknesses up to 10 monolayers have been observed.[7]

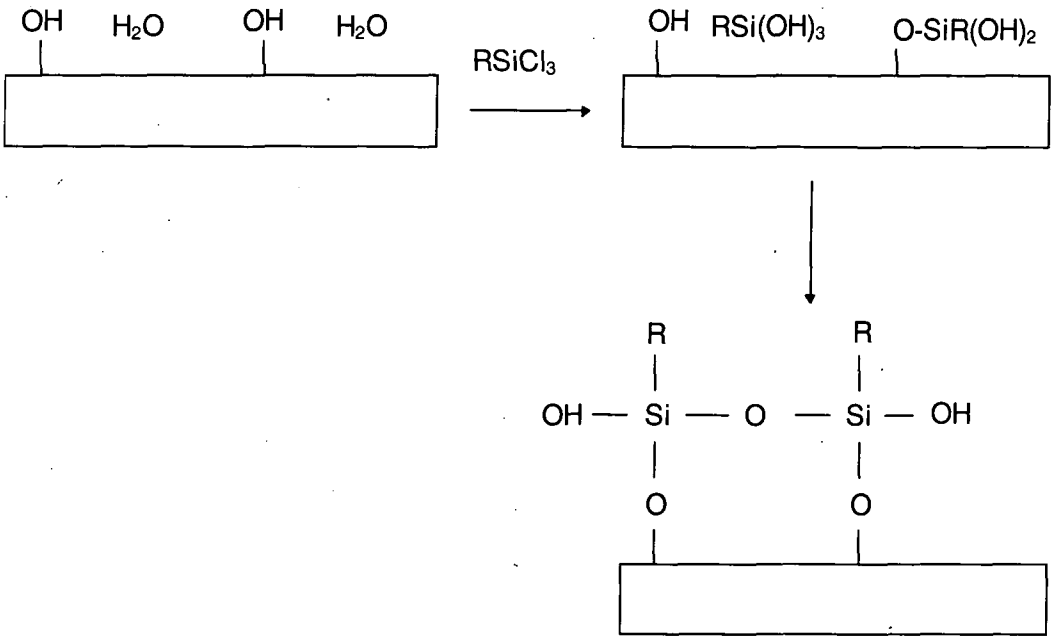

Scheme 3.1 Mechanism for the reaction of a trichlorosilane coupling agent with a silica surface.[10]

Chlorosilane grafting onto silent discharge activated polyethylene may be occurring via surface peroxide groups, as previously observed for corona discharge[42,43] and ozone[41] treated surfaces. Peroxide functionalities are known to be capable of binding poly(N-isopropylacrylamide),[42] poly(vinylamine)[43] and

acrylic-acid.[44] The increase in polymer hydrophilicity with dielectric barrier discharge activation will also have increased the amount of physisorbed water, which is known to play a key role in silane coupling chemistry.[10,11]

The higher water contact angle measured for PFDTCS coupled to silent discharge treated polyethylene, Figure 3.4, compared to the corresponding reaction for glass (despite their identical surface compositions) must be a consequence of the former's surface roughness as predicted by Wenzels law, Equation 1.4.[45] Streamers associated with the plasma discharge result in micron scale roughening,[38] thereby producing an overall increase in hydrophobicity for the PFDTCS coupled overlayer.

The poor coupling performance of PFDMCS can be attributed to the fact that either the concentration of grafting sites is the limiting factor, or alternatively these groups are less reactive towards mono-chlorosilanes. The former seems unlikely on the basis of the gradual rise in grafted material over time for silent discharge activated polyethylene. This is reaffirmed by the observation that the reaction of PFDMCS proceeds much faster with glass due to the higher reactivity of Si-OH groups. Whereas in the case of PFDTCS, film formation is unhindered by the slow production of Si-O-C linkages,[2] since little direct attachment to the substrate is necessary to instigate the rapid formation of a three-dimensional Si-O-Si cross-linked network with perfluoroalkyl side chains.

3.2.5 CONCLUSIONS

Perfluoroalkyltrichlorosilanes are found to undergo coupling reactions with atmospheric dielectric barrier discharge activated polymer substrates much more readily compared to their monochlorinated counterparts. This enhancement can be attributed to the formation of a three-dimensional Si-O-Si cross-linked network with perfluoroalkyl side chains. The resultant surfaces exhibit both hydrophobic and oleophobic behaviour.

3.3 ATMOSPHERIC GROWTH OF POLYSILOXANE LAYERS AND THEIR CONVERSION TO SiO_X

3.3.1 INTRODUCTION

In the previous study (Section 3.2) the attachment of chlorosilane coupling agents to oxidized polyethylene was investigated. However, the methodology was found to be unsuitable for monochlorosilanes, precluding the controlled formation of functionalized monolayers. In this study an alternative approach is used, comprising the deposition and subsequent oxidation of a polydimethylsiloxane-like precursor (itself derived from chlorosilanes).

Polydimethylsiloxane (PDMS) is renowned for its water repellency, chemical inertness, thermal stability,[46] low coefficient of friction, and high gas permeability.[47] Technological applications of PDMS include release coatings,[48] multi-layer resists,[49,50] electrical insulation,[51] fuel combustion systems,[47] and biomedical devices (e.g. body implants,[52] contact lenses,[53] and tissue-culture surfaces[54]). For some of these end-uses, surface wettability is an important criterion. In the past, improvement of the hydrophilicity of polysiloxane surfaces has been achieved by exposure to oxidizing acids,[55] UV-ozone,[56] corona discharge,[51] and low pressure glow discharges of oxygen,[50,52,57] air,[51] carbon dioxide,[53] helium, nitrogen and argon.[54] The improvement in wettability attained by these methods is quite often found to be transitory, with hydrophobicity returning within a matter of days.[46,51,54,57,58,59] Mechanistically, this post-oxidative recovery is understood to be driven by thermodynamic requirements, where mobile low surface energy polysiloxane chains migrate from the bulk towards the air-solid interface. Previous investigations using low pressure[54] and corona discharges[51,60] have shown that a thin silica-like layer formed during plasma oxidation contains cracks which enable polysiloxane species to migrate towards the air-solid interface.

The alternative approach for preparing oxidized polysiloxane surfaces is described here. This consists condensing subsituted chlorodisilanes (SCDS) onto solid surfaces in air to form PDMS-like layers, followed by atmospheric pressure plasma oxidation. The hydrophobic recovery of these layers is

compared with the corresponding behaviour of a conventional PDMS elastomer oxidized under similar conditions. Two types of atmospheric pressure plasma discharge have been chosen because of their low cost and suitability for continuous large scale film processing:[61] dielectric barrier discharge (DBD) and atmospheric pressure glow discharge (APGD). Dielectric barrier discharge (or silent discharge) is an inhomogenous, streamer based plasma which has been described fully in Section 1.2.3.1. APGD, whilst utilising a similar electrode configuration to that for a dielectric barrier discharge, differs in that it requires a higher frequency power supply, and a helium diluent to provide a homogenous glow discharge via a Penning ionization mechanism.[62,63,64,65] Furthermore, APGD systems tend to be much more uniform in nature compared to dielectric barrier discharge (where the reactive species are concentrated into narrow filaments leading to localised surface damage and degradation[38,66]).

The physiochemical nature of the condensed SCDS layers before and after atmospheric plasma oxidation has been examined by X-ray photoelectron spectroscopy (XPS), ATR-FTIR, contact-angle, and gas barrier measurements. Also, since chlorosilane coupling agents are known to readily couple to silica-type surfaces,[1,11,20] the reactivity of the plasma oxidized SDCS films towards 1H, 1H, 2H, 2H - perfluorodecyldimethylchlorosilane (PFDMCS) has been explored. Potentially providing a means of overcoming the difficulties of attaching monochlorosilanes directly to oxidized polyethylene (described in Section 3.2).

3.3.2 EXPERIMENTAL

Polyethylene (LDPE/LLDPE blend, Dowlex 2045A/Dow 5004I) and PDMS (Dow Corning, Sylgard 184 cured elastomer) substrates were cleaned for 30 s in a 1:1 mixture of isopropyl alcohol (BDH, Analar grade) and cyclohexane (BDH, Analar grade) using an ultrasonic bath.

The home-built, parallel-plate dielectric barrier discharge apparatus (Section 2.2) was used to activate the polyethylene substrate prior to exposure to SCDS (substituted chlorodisilanes, Dow Corning, of which at least 80% is $Si_2Me_2Cl_4$ and $Si_2Me_3Cl_3$). Substrate pre-treatment entailed placing a piece of polyethylene film on top of the dielectric and operating the dielectric barrier

discharge at 328 Hz in air for 10 s using a 2 mm inter-electrode gap. Subsequent exposure of the activated polyethylene surface to SCDS vapour was undertaken by placing the treated film in a sealed 60 cm^3 container containing 0.02 ml of SCDS for one hour. Related SCDS exposure experiments were performed in a dry nitrogen glove-box (13 ppm H_2O, and 12 ppm O_2). Any loose condensed SCDS deposited onto the surface was then removed by washing for 60 s in toluene (Fisher, Analytical grade, molecular-sieve dried), since this is a good solvent for polysiloxanes.

Plasma oxidation of the SCDS coatings comprised 60 s treatment using either the dielectric barrier discharge apparatus (328 Hz, 2 mm inter-electrode gap) or an atmospheric pressure glow discharge (APGD) reactor. The latter constituted a high voltage (2.5 kV) 15 kHz ac power supply applied across two aluminium electrodes spaced 6 mm apart, where the lower earthed electrode was shielded by a glass dielectric plate. A piece of coated polymer film was placed on top of this dielectric and the chamber evacuated using a liquid nitrogen trapped mechanical rotary-pump. A 95 % helium (BOC, 99.996%) / 5 % oxygen (BOC, 99.998%) gas mixture was then admitted into the system at a total flow rate of 1900 sccm and 1020 mbar pressure. Following 10 mins of purging, a homogenous glow discharge was ignited in between the electrodes.

The plasma oxidized SCDS films were characterized and reacted with 1H, 1H, 2H, 2H - perfluorodecyldimethylchlorosilane, (PFDMCS, $CF_3(CF_2)_7(CH_2)_2SiMe_2Cl$, Fluorochem) in order to explore their potential suitability as substrates for surface coupling chemistry. Vapour phase exposure of PFDMCS was carried out under a dry nitrogen atmosphere for 18 hours as described in Section 3.2.2.

XPS analysis was performed following each stage of treatment using the methods outlined in Section 1.3.1.

ATR-FTIR spectra of the SCDS coated polyethylene films were recorded using 128 scans at 4 cm^{-1} resolution on a Mattson Polaris spectrometer fitted with an attenuated total reflectance (ATR) accessory (Graseby Specac Golden Gate).

Contact angle values for de-ionized water and decane (Aldrich, 99+%) were obtained using a video capture apparatus, refer to Section 1.3.3. Decane was used because it was shown in Section 3.2 to be a sensitive probe for surface perfluoroalkyl functionalities (i.e. oleophobicity).

The oxygen barrier improvement factor (BIF) of each sample was measured, with reference to the MEPPP of the untreated polyethylene substrate, using the equipment and procedure described in Section 1.3.4.

3.3.3 RESULTS

3.3.3.1 Reaction and Condensation of Substituted Chlorodisilanes onto Polymer Surfaces

XPS analysis of the cleaned polyethylene film confirmed its hydrocarbon nature, (i.e. less than 2% O), Table 3.3. A 10 s dielectric-barrier discharge pre-treatment of polyethylene resulted in a significant level of oxygen incorporation, accompanied by a 50° reduction in water contact angle. Subsequent exposure of this dielectric barrier discharge activated surface to SCDS vapour in air, followed by washing in toluene restored hydrophobicity, yielding films with XPS elemental abundances of 43% C, 27% O, 28% Si, and 1% Cl, which closely resembled those of conventional PDMS (50% C, 25% O, and 25% Si). This structural similarity was confirmed by the fact that a single Si(2p) XPS peak was observed at around 102 eV, which is indicative of a siloxane environment.[51,59] Exposure of both untreated and dielectric barrier discharge activated polyethylene to SCDS vapour in a dry nitrogen glovebox, followed by washing in air also produced complete coverage of the substrate. However, when both SCDS coating and solvent washing steps were executed in the dry nitrogen glovebox, a substrate dependency was noted. SCDS layers deposited onto dielectric barrier discharge activated polyethylene produced the aforementioned PDMS-like characteristics. In contrast, SCDS exposure to just the clean polyolefin substrate showed incomplete coverage. This was evident from the high carbon content together with lower silicon and oxygen levels detected by XPS. Also the water contact angle was greater than that measured for a complete layer of SCDS, and more akin to clean polyethylene, Table 3.3.

Labelling Conditions	Substrate	% C	% O	% Si	% Cl	Contact Angle /°
None	Clean PE	98.4 ±0.3	1.6 ±0.3	0	0	105.8 ±1.5
None	10s DBD PE	82.5 ±1.5	17.5 ±1.5	0	0	65.8 ±1.4
Air, washed in air	Clean PE	45.5 ±0.0	26.6 ±0.3	27.3 ±0.4	0.7 ±0.5	90.6 ±2.2
Air, washed in air	10s DBD PE	43.2 ±2.5	27.4 ±1.1	28.2 ±1.9	1.1 ±0.7	92.4 ±2.0
Dry nitrogen, washed in air	Clean PE	49.2 ±2.0	24.9 ±0.9	25.5 ±1.5	0.4 ±0.4	91.4 ±2.4
Dry nitrogen, washed in air	10s DBD PE	46.0 ±1.3	25.9 ±0.6	27.2 ±1.0	0.9 ±0.9	84.8 ±0.8
Dry nitrogen, washed in dry nitrogen	Clean PE	60.1 ±9.5	18.6 ±5.2	19.1 ±4.6	2.2 ±1.7	104.0 ±5.2
Dry nitrogen, washed in dry nitrogen	10s DBD PE	46.4 ±2.5	25.1 ±2.4	24.6 ±1.3	4.0 ±3.1	90.6 ±4.3

Table 3.3 XPS and water contact angle analysis of SCDS deposited layers.

3.3.3.2 *Atmospheric Pressure Plasma Oxidation of Deposited SCDS, Polyethylene, and PDMS*

The combination of dielectric barrier discharge activated polyethylene and SCDS exposure in air appeared to produce the thickest and best adhered coatings. On this basis, these substrates were chosen for subsequent dielectric barrier discharge and APGD oxidation studies. In both cases, carbon loss was observed at the expense of oxygen incorporation, whilst silicon content remained approximately constant, Table 3.4. A corresponding shift towards higher Si(2p) binding energy confirmed that the condensed polysiloxane network was being converted into an inorganic SiO_x phase.[51,54,57,59] Immediately following plasma oxidation, the SCDS films were found to be fully wettable by water, and retained their hydrophilic nature for a considerable time, Table 3.4 and Figure 3.5. APGD treated SCDS layers performed particularly well in this respect, with an average water contact angle of below 25° over a period of 7 days. This is consistent with the formation of inorganic SiO_x material at the surface.

PDMS elastomer was chosen for comparative purposes. In this case, atmospheric pressure plasma treatment produced SiO_X rich surfaces with elemental abundances similar to those obtained for the corresponding oxidized SCDS layers. However, only APGD treated PDMS was found to be completely wettable, Table 3.4. Dielectric-barrier discharge treated PDMS samples underwent rapid recovery. This initial difference between the APGD and dielectric barrier discharge oxidized PDMS elastomer became less pronounced with storage time. In fact the oxidized PDMS surfaces underwent almost complete recovery after 24 hours of ageing for both types of plasma treatment, Figure 3.5.

Control experiments with a polyethylene substrate showed that atmospheric-pressure plasma oxidation resulted in substantial oxygen incorporation at the surface with a concomitant loss of carbon. Both dielectric barrier discharge and APGD treatment were found to be of almost equal efficacy: yielding water contact angles of ~50° (i.e. not as wettable as the plasma oxidized SCDS layers) and surface elemental abundances of approximately 73 % carbon and 27 % oxygen. These surfaces were found to undergo relatively little hydrophobic recovery: a 10° rise in water contact angle

occurred over a period of 7 days for both APGD and dielectric barrier discharge plasma treated surfaces.

3.3.3.3 Gas Barrier Performance of Films Derived From Condensed SCDS Layers

Surprisingly, condensation of SCDS onto activated polyethylene was found to enhance oxygen permeation through the polyethylene substrate, Table 3.5. Atmospheric pressure plasma oxidation redressed this shortfall, giving a negligible overall change to the polyethylene substrate's gas barrier performance. 10 iterations of the coating-oxidation procedure produced a significant improvement in gas barrier for APGD treatment, Table 3.5. Dielectric barrier discharge treatment was found to be ineffective (probably due to its filamentary nature creating surface defects).

3.3.3.4 ATR-FTIR Analysis

ATR-FTIR has a penetration depth of approximately 0.1 - 10 μm, making it less surface sensitive compared to XPS.[51,67] Coating activated polyethylene with a thick condensed SCDS layer (10 hours SCDS exposure) resulted in the appearance of Si-Me and Si-O-Si/Si-O-C infrared absorption bands at 1260 cm^{-1} and 1090 cm^{-1} respectively, Figure 3.6. In comparison, a film produced using 10 iterations of SCDS and APGD (i.e. 10 x 1 hour SCDS exposure) displayed a much weaker Si-Me absorbance and broader Si-O-Me/Si-O-Si region. Such featureless Si-O-Si infrared absorption bands have previously been assigned to inorganic SiO_x-like material.[56]

Substrate	Treatment	XPS Analysis				Contact Angle /°
		% C	% O	% Si	% Cl	
PE	Washed	98.4 ±0.3	1.6 ±0.3	0	0	105.8 ±1.5
	Dielectric barrier discharge	71.5 ±2.0	28.5 ±2.0	0	0	52.4 ±2.8
	APGD	74.2 ±0.1	25.8 ±0.1	0	0	51.0 ±2.1
Condensed SCDS	Washed	43.2 ±2.5	27.4 ±1.1	28.2 ±1.9	1.1 ±0.7	92.4 ±2.0
	Dielectric barrier discharge	21.3 ±1.2	53.4 ±0.4	25.3 ±0.8	0	wets
	APGD	15.0 ±0.3	57.0 ±1.3	27.8 ±1.3	0.3 ±0.3	wets
PDMS elastomer	Washed	46.4 ±0.4	27.4 ±0.2	25.8 ±0.2	0	119.8 ±1.3
	Dielectric barrier discharge	24.0 ±1.3	48.6 ±1.0	27.3 ±0.3	0	53.6 ±33.4
	APGD	22.2 ±1.6	51.4 ±1.3	26.1 ±0.2	0	wets

Table 3.4 XPS and initial contact angle analysis of atmospheric-pressure plasma oxidized polyethylene, PDMS and SCDS.

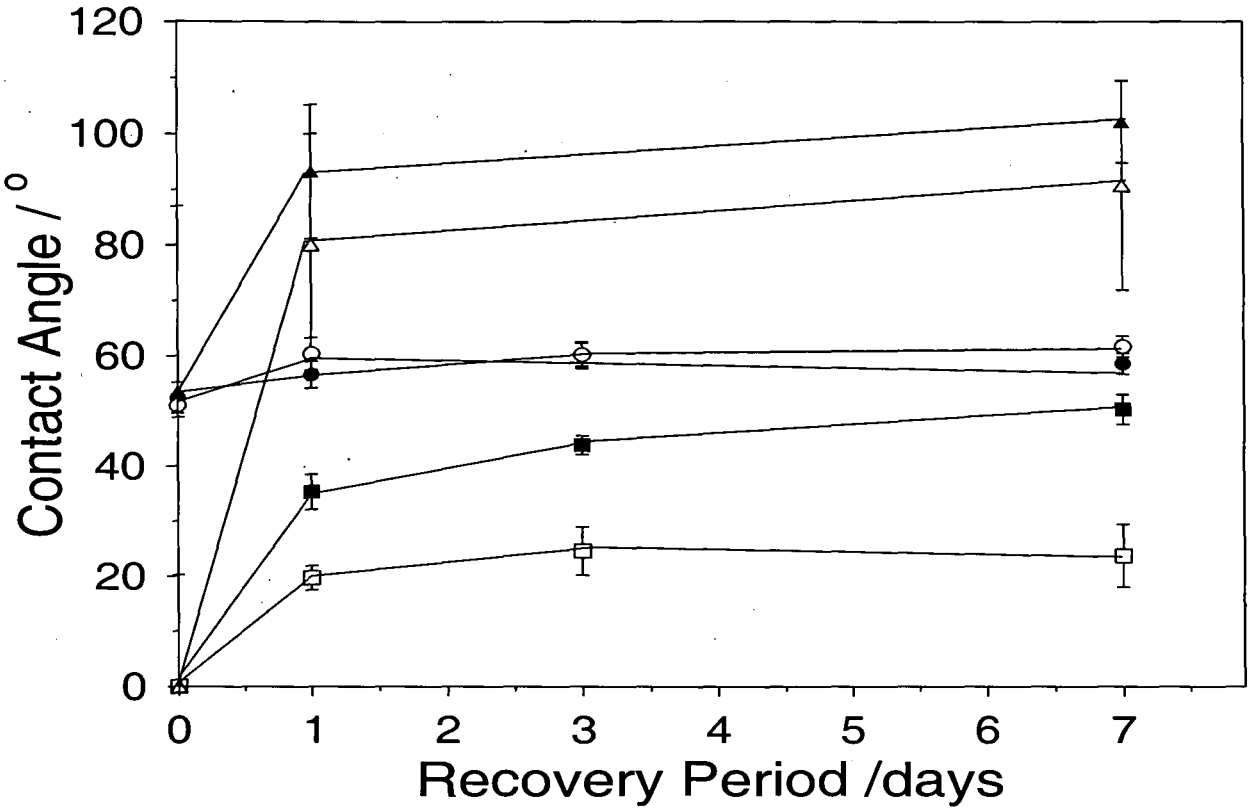

Figure 3.5 Water contact angle recovery of APGD (white) and dielectric barrier discharge oxidized (black) polyethylene (O), PDMS (Δ) and condensed SCDS (□)surfaces.

Sample	Barrier Improvement Factor
Polyethylene substrate (LLDPE/LDPE)	1.0
SCDS coating on activated polyethylene	0.5 ±0.1
Dielectric barrier discharge treated SCDS coating on activated polyethylene	0.9 ±0.2
10 × dielectric barrier discharge treated SCDS coating on activated polyethylene	1.1 ±0.2
APGD treated SCDS coating on activated polyethylene	1.3 ±0.2
10 × APGD treated SCDS coating on activated polyethylene	4.1 ±1.1

Table 3.5 Gas barrier values of plasma oxidized SCDS coatings.

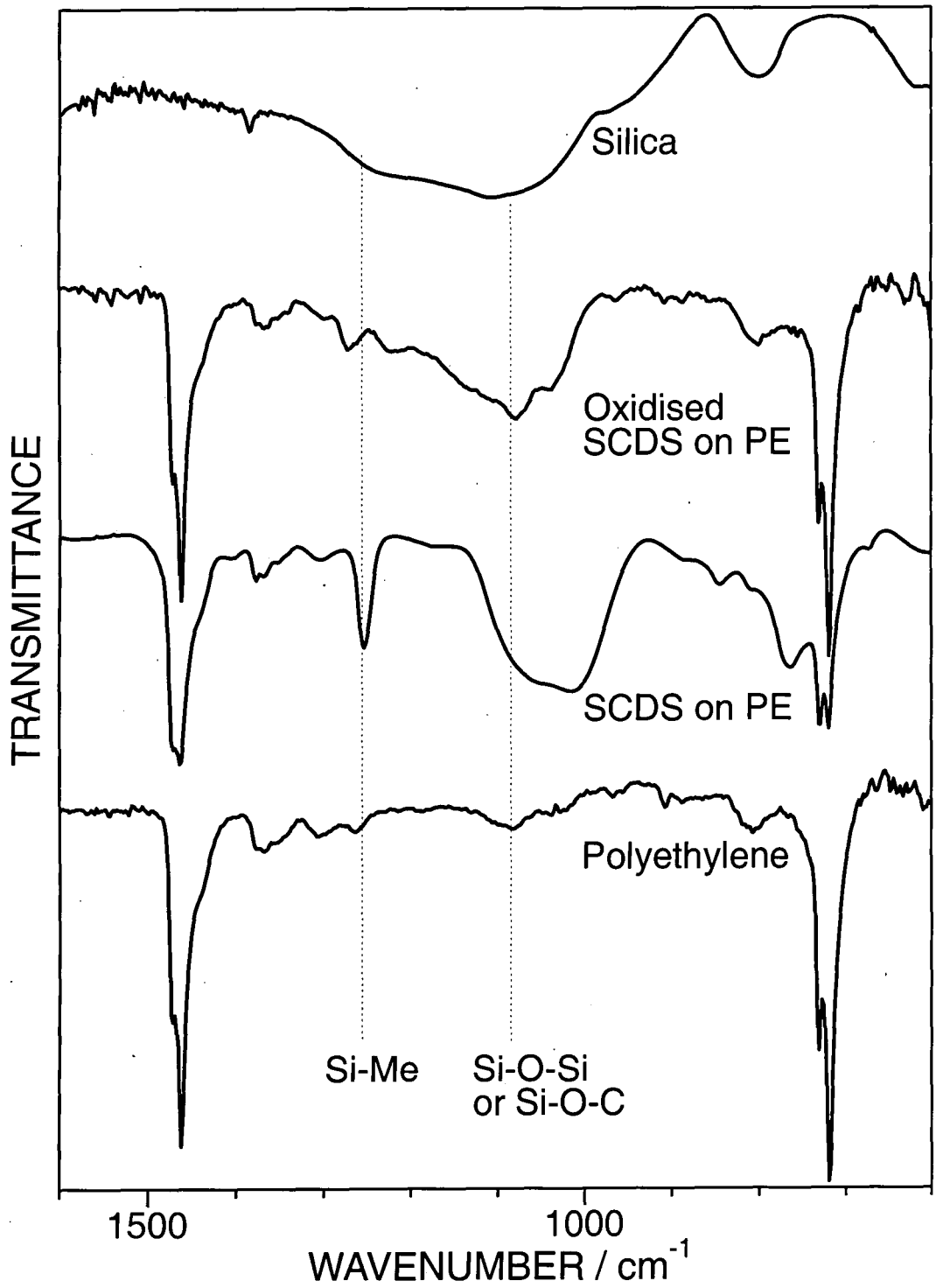

Figure 3.6 ATR-IR spectra of SCDS layers.

3.3.3.5 *Surface Reactivity Towards PFDMCS Coupling Reagent*

The hydrophilic nature of plasma oxidized SCDS layers signifies the presence of silanol groups. Therefore these surfaces should be amenable to conventional chlorosilane coupling chemistry.[11,21] Monochlorosilanes were chosen since they are incapable of undergoing polymerization (unlike trichlorosilanes). On this premise, each coupled PFDMCS molecule can only attach directly to the SiO_x surface. Hence, the extent of derivatization is effectively a measure of the concentration of surface Si-OH groups.[68]

A control experiment comprising exposure of unoxidized SCDS layers to PFDMCS gave rise to negligible coupling at the surface, Table 3.6. This was supported by the absence of oleophobicity. In contrast, dielectric barrier discharge and APGD oxidized SCDS layers were very reactive towards PFDMCS. A substantial increase in both water and decane contact angles was observed, accompanied by a large concentration of fluorine at the surface, and a marked change in the shape of the C(1s) XPS envelope, Figure 3.7. The high binding energy shoulder is characteristic of $\underline{C}F_2$ and $\underline{C}F_3$ groups.[69] A greater number of fluoroalkyl groups were seen in the C(1s) spectrum of the APGD oxidized sample compared to its dielectric barrier discharge counterpart (in spite of their equal concentration of %F). This can be attributed to APGD leaving less residual carbon behind during oxidation of the SCDS layer, Table 3.4, thus making the perfluoroalkyl component appear more prominent relative to the $\underline{C}_xH_y$ component. The absence of significant additional Cl(2p) XPS signal intimated complete hydrolysis of the Si-Cl bond belonging to the PFDMCS coupling reagent.

Sample	% C	% F	% O	% Si	% Cl	C.A. (water) /°	C.A. (decane) /°
Glass	22.9 ±2.7	0	52.9 ±1.3	24.2 ±1.9	0	18.0 ±2.0	wets
PFDMCS coupled to glass	16.3 ±1.0	19.5 ±1.2	43.4 ±0.4	20.9 ±0.1	0	96.0 ±4.7	47.6 ±4.1
Condensed SCDS	43.2 ±2.5	0	27.4 ±1.1	28.2 ±1.9	1.1 ±0.7	92.4 ±2.0	wets
SCDS exposed to PFDMCS	51.3 ±4.3	2.7 ±0.5	22.2 ±1.8	22.7 ±2.0	1.1 ±0.0	99.3 ±4.3	wets
Dielectric barrier discharge oxidized SCDS	21.3 ±1.2	0	53.4 ±0.4	25.3 ±0.8	0	wets	wets
Dielectric barrier discharge oxidized SCDS exposed to PFDMCS	29.3 ±0.3	26.9 ±2.2	30.4 ±2.1	13.4 ±0.4	0	98.6 ±9.2	50.9 ±3.8
APGD oxidized SCDS	15.0 ±0.3	0	57.0 ±1.3	27.8 ±1.3	0.3 ±0.3	wets	wets
APGD oxidized SCDS exposed to PFDMCS	17.4 ±1.8	27.8 ±1.1	36.7 ±0.3	17.5 ±0.3	0.7 ±0.1	113.0 ±1.4	52.5 ±3.9

Table 3.6 XPS and contact angle analysis following exposure of SCDS layers to PFDMCS.

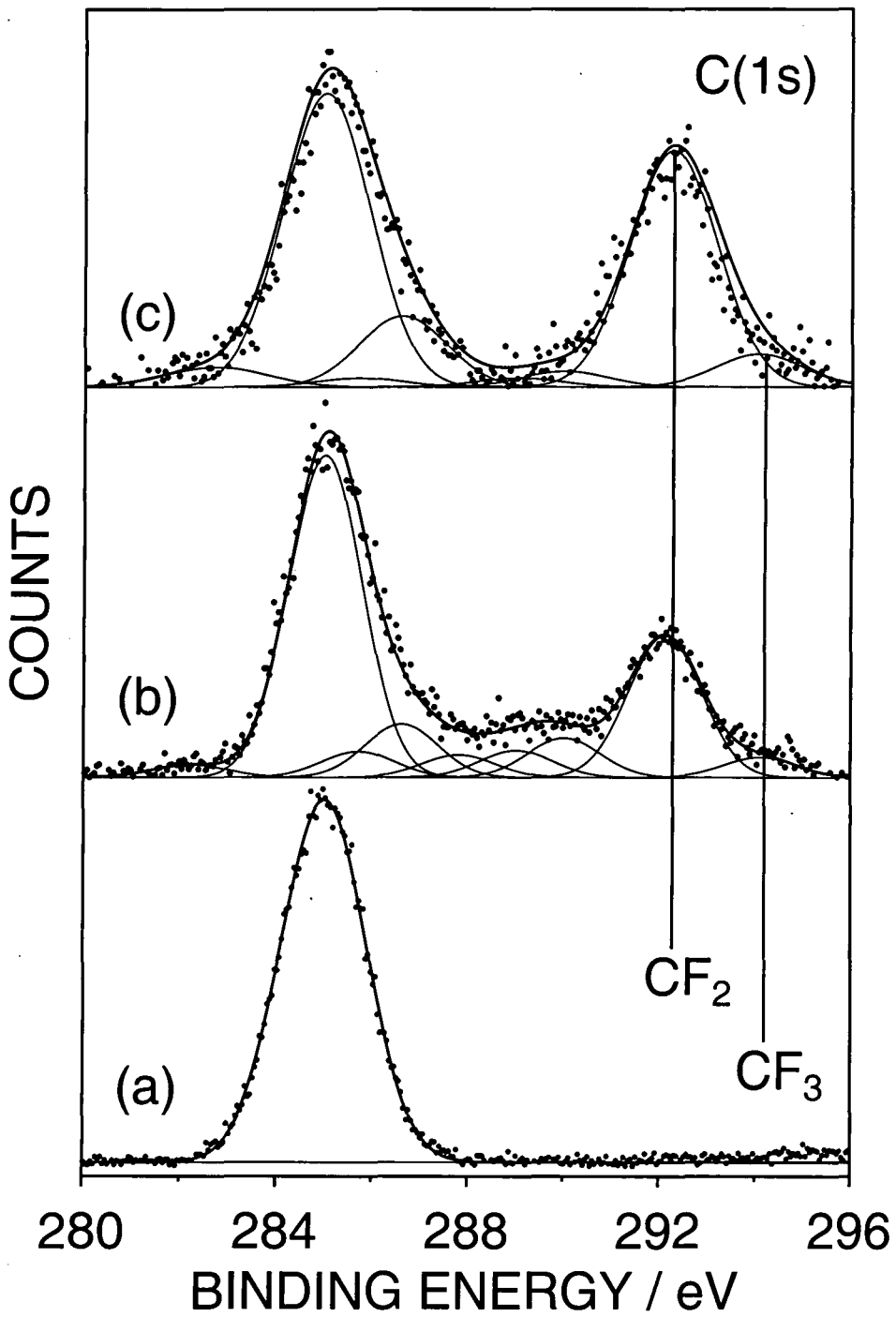

Figure 3.7 C(1s) XPS spectra following exposure of PFDMCS coupling reagent to: (a) unoxidized SCDS layer; (b) dielectric barrier discharge oxidized SCDS layer; and (c) APGD oxidized SCDS layer.

3.3.4 DISCUSSION

It is well known that the formation of Si-OH functionalities from Si-Cl bonds and their subsequent condensation into a Si-O-Si linked network can be catalysed by water adsorbed on a surface.[9,10,11,70] The observed enhancement in SCDS condensation onto dielectric-barrier discharge oxidized polyethylene is most likely to be a combination of two factors. Firstly, polar surfaces, such as those formed by the silent discharge pre-treatment, can absorb a larger amount of atmospheric moisture compared to the relatively clean and dry polyethylene. Also dielectric barrier discharge pre-treated surfaces contain functionalities, namely peroxy groups, which themselves are capable of bonding to reactive molecules,[41,42,43,71] thus enabling some degree of covalent grafting of SCDS to the surface. Furthermore, exposure of these SCDS layers to moist air will promote the condensation reaction. The similar behaviour observed in the case of SCDS exposure under dry nitrogen followed by solvent washing in air, can be explained in terms of SCDS adsorbing onto the activated polyethylene surface under nitrogen to produce a film, which subsequently cross-links upon exposure to moist air, Scheme 3.2. Whereas when both SCDS exposure and solvent washing are performed under dry nitrogen, incomplete films are formed on untreated polyethylene due to the lack of catalytic moisture at the SCDS surface, preventing formation of a wash resistant coating.

A comparison between conventional PDMS elastomer and the condensed SCDS layers shows that they behave very differently following atmospheric plasma discharge treatment, despite possessing similar surface elemental abundances before and after oxidation. PDMS recovers almost completely within 24 hours of plasma modification, whereas the correspondingly treated condensed SCDS layers retain a high degree of hydrophilicity even after 7 days. The post-oxidative re-emergence of hydrophobicity for polysiloxanes is understood to be partly due to the diffusion of low surface energy PDMS material towards the air-solid interface.[51,57,59] The inherent cross-linking of the SCDS layer helps to minimize the amount of available mobile material capable of migrating towards the high energy surface formed during plasma oxidation.

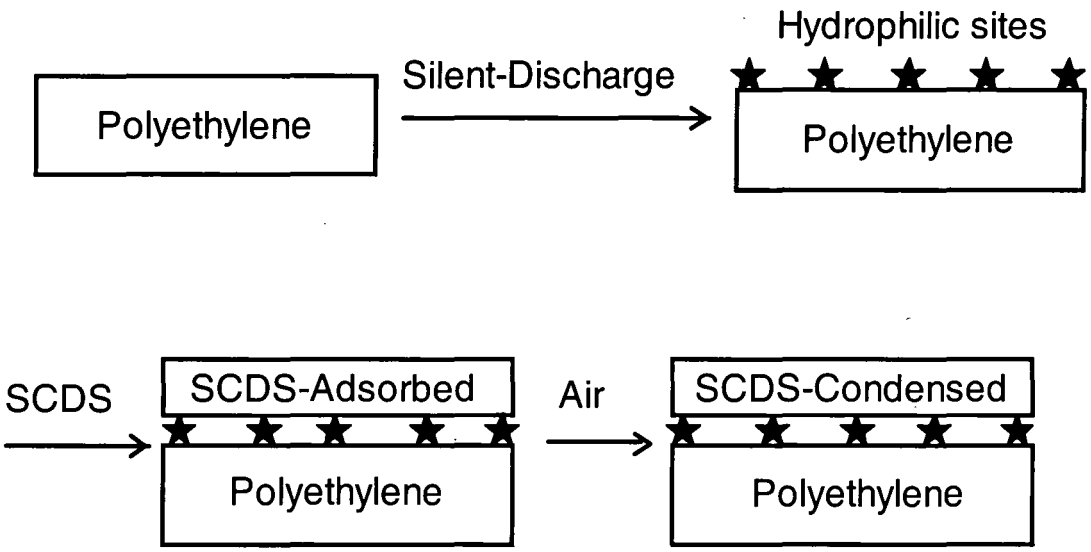

Scheme 3.2 Mechanism for the attachment and condensation of SCDS

The disparity between the rates of hydrophobic recovery for APGD and dielectric barrier discharge treated SCDS layers is most likely to be a consequence of the differing plasma characteristics. The filamentous nature of silent discharge will damage the oxidized SCDS surface, allowing the migration of subsurface unoxidized material, exacerbating hydrophobic recovery. Whilst the homogenous APGD should provide an oxidized layer of greater integrity, which is much better at impeding the migration of sub-surface moieties. This explanation is borne out by gas permeation measurements, which show that reiterative condensation of SCDS followed by APGD treatment yields a significant improvement in gas barrier properties, thus indicating less defects. The observed enhancement in oxygen permeation following deposition of just the SCDS layer onto activated polyethylene can be attributed to either the adsorbed SCDS material swelling the underlying polymer, or greater permeation occurring through the polysiloxane layer. The latter is likely, since polysiloxane materials are renowned for their good permeation properties,[47] i.e. the SCDS layer may improve the oxygen sorption and solvation characteristics of the underlying polyethylene substrate, effectively encouraging the first step of the solution-diffusion mechanism responsible for gas transportation through polymers.[72]

The hydrophobicity of the condensed SCDS layer implies a low concentration of surface silanols. This is supported by the inertness of this surface towards the PFDMCS coupling reagent, Table 3.6. In contrast, the

silanol-rich, oxidized SCDS surfaces readily undergo reaction with the chlorosilane coupling agent. The high degree of fluoroalkylation, and the corresponding enhancements in water and decane repellency illustrate this aspect. Such coatings would be ideally suited for microlithography (e.g. contact printing) and biomedical applications, with the added advantage of being substrate non-specific.

3.3.5 CONCLUSIONS

Substituted chlorodisilanes (SCDS) are found to readily undergo condensation onto activated polymer surfaces to form cross-linked polysiloxane coatings. Subsequent atmospheric-pressure plasma treatment yields highly oxidized layers which display very slow rates of hydrophobic recovery. These oxidized SCDS surfaces also exhibit good gas barrier performance, and have been shown to be highly amenable for conventional chlorosilane coupling chemistry.

3.4 REFERENCES

[1] Revillon, A.; Leroux, D. *Reactive & Functional Polymers* **1995**, *26*, 105

[2] Plueddemann, E.P. Reminiscing on Silane Coupling Agents. In *Silanes and Other Coupling Agents*; Mittal, K.L., Ed.; VSP: Utrecht, The Netherlands, 1992;pp 3-19

[3] Xiao, X.-D.; Liu, G.-Y.; Charych, D.H.; Salmeron, M. *Langmuir* **1995**, *11*, 1600

[4] Wang, D.; Jones, F.R. *Surf. Interface Anal.* **1993**, *20*, 457

[5] Blum, F.D.; Meesiri, W.; Kang, H.-J.; Gambogi, J.E. *J. Adhesion Sci. Technol.* **1991**, *5*, 479

[6] Wang, D.; Jones, F.R.; Denison, P. *J. Adhesion Sci. Technol.* **1992**, *6*, 79

[7] Yee, J.K.; Parry, D.B.; Caldwell, K.D.; Harris, J.M. *Langmuir* **1991**, *7*, 307

[8] Sagiv, J. *J. Am. Chem. Soc.* **1980**, *102*, 92

[9] Wirth, M.J.; Fatunmbi, H.O. *Anal. Chem.* **1993**, *65*, 822

[10] Wasserman, S.R.; Whitesides, G.M.; Tidswell, I.M.; Ocko, B.M.; Pershan, P.S.; Axe, J.D. *J. Am. Chem. Soc.* **1989**, *111*, 5852

[11] Tripp, C.P.; Hair, M.L. *J. Phys. Chem.* **1993**, *97*, 5693

[12] Chaudhury, M.K. *Biosensors & Bioelectronics* **1995**, *10*, 785

[13] Fadeev, A.Y.; McCarthy, T.J. *Langmuir* **1999**, *15*, 3759

[14] Ferguson, G.S; Chaudhury, M.K.; Biebuyck, H.A.; Whitesides, G.M. *Macromolecules* **1993**, *26*, 58707

[15] Tada, H.; Nagayama, N. *Langmuir* **1995**, *11*, 136

[16] Jönsson, U.; Olofsson, G.; Malmqvist, M.; Rönnberg, I. *Thin Solid Films* **1985**, *124*, 117

[17] Grundmeier, G.; Matheisen, E.; Stratmann, M. *J. Adhesion Sci. Technol.* **1996**, *10*, 573

[18] Slavov, S.V.; Chuang, K.T.; Sanger, A.R. *J. Phys. Chem.* **1996**, *100*, 16285

[19] Tsubokawa, N.; Kogure, A. *J. Polym. Sci. Part A: Polym. Chem.* **1991**, *29*, 697

[20] Silver, J.H.; Hergenrother, R.W.; Lin, J.-C.; Lim, F.; Lin, H.-B.; Okada, T.; Chaudhury, M.K.; Cooper, S.L. *J. Biomedical Materials Research* **1995**, *29*, 535

[21] Fadeev, A.Y.; McCarthy, T.J. *Langmuir* **1998**, *14*, 5586

[22] Zhao, B.; Brittain, W.J.; Vogler, E.A. *Macromolecules* **1999**, *32*, 796

[23] Kiaei, D; Hoffman, A. S; Horbett, T.A. *Radiat. Phys. Chem.* **1995,** *46*, 191.

[24] S. K. Stark, US Patent, 6008146, **1999**.

[25] Hwang, S. S.; Ober, C. K.; Perutz, S.; Iyengar, D. R.; Schneggenburger, L. A.; Kramer E.J. *Polymer* **1995,** *36*, 1321.

[26] Hayes, L.; Dixon, D. D. *Textile Res. J.* **1977,** *47,* 277

[27] Wang, J. H.; Chen, J. J.; Timmons R. B. *Chem. Mater.* **1996,** *8*, 2212

[28] Ryan, M.E.; Fonseca, J. L. C.; Tasker, S.; Badyal, J. P. S. *J. Phys. Chem.* **1995,** 99 4261

[29] Schmidt, D. L.; Coburn, C. E.; DeKoren, B. M.; Potter, G. E.; Meyers, G. F.; Fischer, D. A. *Nature* **1994**, *368*, 39.

[30] Hofmann, S. In *Practical Surface Analysis*, 2nd ed.; Briggs, D., Seah, M.P., Eds.; John Wiley & Sons: Chichester, 1990; Vol. 1, pp 143-199

[31] Wang, D.; Leroux, D. *Reactive and Functional Polymers* **1995,** *26*, 105

[32] Beamson, G.; Briggs, D. *High Resolution XPS of Organic Polymers: The Scienta ESCA300 Database*, 1st ed.; John Wiley & Sons Ltd: Chichester, 1992; Appendices 1-2

[33] Sardja, I.; Dhali, S. K. *Appl. Phys. Lett.* **1990,** *56*, 21

[34] Chang, M. B.; Balbach, J. H.; Rood, M. J.; Kushner, M. J. *J. Appl. Phys.* **1991,** *69*, 44

[35] Boyd, I. W. *Appl. Surf. Sci.* **1997**, *109/110*, 538

[36] Bergonzo, P.; Kogelschatz, U.; Boyd, I.W. *Appl. Surf. Sci.*, **1993,** *69*, 393

[37] Kogelschatz, U. *Appl. Surf. Sci.* **1992,** *54*, 410

[38] Greenwood, O. D.; Boyd, R. D.; Hopkins, J.; Badyal, J. P. S. *J. Adhesion Sci. Technol.* **1995,** *9*, 311

[39] Eliasson B.; Egli, W.; Kogelschatz, U. *Pure & Appl. Chem.* **1994,** *66*, 1275

[40] Brunner, H.; Vallant, T.; Mayer, U.; Hoffmann, H. *Langmuir* **1999,** *15*, 1899

[41] Fujimoto, K.; Takebayashi, Y.; Inoue, H.; Ikada, Y. *J. Polym. Sci., Polym. Chem. Ed.* **1993**, *31*, 1035

[42] Seto, F.; Fukuyama, K.; Muraoka, Y.; Kishida, A.; Akashi, M. *J. Appl. Polym. Sci* **1998,** *68*, 1773

[43] Seto, F;.Muraoka, Y.; Akagi, T.; Kishida, A.; Akashi, M. *J. Appl. Polym. Sci.* **1999,** *72*, 1583

[44] Yuhai, G.; Jianchun, Z.; Meiwu, S. *J. Appl. Polym. Sci.* **1999,** *73*, 1161

[45] Padday, J. F. In *Handbook of Adhesion*; Packham, D. E. Ed.; Longman Scientific and Technical: Great Britain, 1994; pp 84-85.

[46] Maksimov, A. I.; Kzotova, G. D.; Bozovikova, I. N.; Kitaev, V. P.; Denisov, A. N. *Elektron Obrab Mater* **1988**, *5*, 52.

[47] Tsutsumi, N.; Mimaki, M.; Nagura, K.; Kiyotsukuri, T. *Polymer Communications* **1990**, *31*, 132.

[48] Bullock, S.; Johnston, E. E.; Willson, T.; Gatenholm, P.; K.J., W. *J. Colloid Interface Sci.* **1999**, *210*, 18.

[49] Namatsu, H.; Yoshikawa, A. Dry Etching Characteristics of Polysiloxane. Presented at Proc, Symp. Dry Process, 1988

[50] Namatsu, H. *J. Electrochem. Soc.* **1989**, *136*, 2676.

[51] Hillborg, H.; Gedde, U. W. *Polymer* **1998**, *39*, 1991.

[52] Klee, D.; Breuers, W.; Bilo-Jung, M.; Mittermayer, C.; Hocker, H. *Die Angewandte Makromolekulare Chemie* **1989**, *166/167*, 179.

[53] Hettlich, H.-J.; Otterbach, F.; Mittermayer, C.; Kaufmann, R.; Klee, D. *Biomaterials* **1991**, *12*, 521.

[54] Owen, M. J.; Smith, P. J. *J. Adhesion Sci. Technol.* **1994**, *8*, 1063.

[55] Hollahan, J. R.; Carlson, G. L. *J. Appl. Polym. Sci.* **1970**, *14*, 2499.

[56] Muisener, R. J.; Koberstein, J. T. *Abstracts of Papers of the American Chemical Society* **1997**, *214*, 653.

[57] Murakami, T.; Kuroda, S.-I.; Osawa, Z. *J. Colloid Interface Sci.* **1998**, *202*, 37.

[58] Bogonosov, A. N.; Kzotova, G. D.; Maksimov, A. I. *Elektron Obrab Mater* **1987**, *4*, 39.

[59] Morra, M.; Occhiello, E.; Marola, R.; Garbassi, F.; Humphrey, P.; Johnson, D. *Journal of Colloid and Interface Science* **1990**, *137*, 11.

[60] Toth, A.; Bertoti, I.; Blazso, M.; Banhegyi, G.; Bognar, A.; Szaplonczay, P. *Appl. Polym. Sci.* **1994**, *52*, 1293.

[61] Pochner, K.; Neff, W.; Lebert, R. *Surface and Coatings Technology* **1995**, *74-75*, 394.

[62] Kanazawa, S.; Kogoma, M.; Moriwaki, T.; Okazaki, S. *J. Phys. D: Appl. Phys.* **1988**, *21*, 838.

[63] Okazaki, S.; Kogoma, M. *Proc. Jpn. Symp. Plasma Chem* **1989**, *2*, 95.

[64] Kanazawa, S.; Kogoma, M.; Okazaki, S.; Moriwaki, T. *Nucl. Instrum. Methods Phys. Res., Sect. B* **1989**, *37/38*, 842.

[65] Yokoyama, T.; Kogoma, M.; Kanazawa, S.; Moriwaki, T.; Okazaki, S. *J. Phys. D: Appl. Phys.* **1990**, *23*, 374.

[66] Massines, F.; Gouda, G. *J. Phys. D.: Appl. Phys.* **1998**, *31*, 3411.

[67] Gaboury, S. R.; Urban, M. W. Analysis of Gas-Plasma Modified Poly(dimethylsiloxane) Elastomer Surfaces. Attenuated-Total-Reflectance-Fourier Transform Infrared Spectroscopy In *Structure-Property Relations in Polymers,* Urban, M. W., Clara, D.C., Eds.; A.C.S., 1993; Vol. 236, pp 778.

[68] Armistead, C. G.; Tyler, A. J.; Hambleton, F. H.; Mitchell, S. A.; Hockey, J. A. *J. Phys. Chem.* **1969**, *73*, 3947.

[69] Clark, D.T.; Shuttleworth, D. *J. Polym. Sci. Chem. Ed.* **1980**, *18*, 27.

[70] Brunner, H.; Vallant, T.; Hoffman, H.; Basnar, B.; Vallant, M.; Friedbacher, G. *Langmuir* **1999**, *15*, 1899.

[71] Fujimoto, K.; Takebayashi, Y.; Inoue, H.; Ikada, Y. *J. Polym Sci.,Polym. Chem. Ed.* **1993**, *31*, 1035.

[72] Rogers, C. E. Permeation of Gases and Vapours in Polymers In *Polymer Permeability,* 1st ed.; J. Comyn, Ed.; Elsevier: New York, 1985; pp 11.

CHAPTER 4

ATMOSPHERIC PRESSURE PLASMA OXIDATION OF POLYDIMETHYLSILOXANE-POLYETHYLENE BLEND SURFACES

4.1 INTRODUCTION

The preparation and uses of surface oxidized PDMS were discussed in Section 3.3.1.[1,2,3,4,5,6,7,8,9,10,11] There it was described how the hydrophilicity concomitant with oxidation is transient.[4,8,9,12,13,14] Hydrophobicity returns within days, effected (at least in part) by the migration of low molecular weight PDMS through defects in the siliceous layer created by oxidation.[4,8,15] This mechanism appeared to explain the slower recovery (and appreciable gas barrier) of APGD oxidized PDMS and condensed-SCDS compared to their dielectric barrier discharge treated counterparts, Section 3.3.

In this study PDMS-rich surfaces were prepared by annealing blends of polyethylene mixed with one of three PDMS containing additives: vinyl terminated PDMS homopolymer, and diblock (AB) or triblock (ABA) copolymers of PDMS and polyethylene. Previous studies concerning polysiloxane and polysiloxane copolymer blend systems have focused on how surface segregation behaviour is influenced by the nature of the PDMS-based constituent,[16,17] its loading,[5] the host homopolymer,[18] its crystallinity,[31] and annealing conditions.[19] The plasma oxidation and subsequent relaxation behaviour of such blend systems has received relatively little attention.

Two types of atmospheric pressure plasma have been utilized: dielectric barrier discharge and atmospheric pressure glow discharge (APGD). The characteristics and applications of both have been described elsewhere, Section 1.2.

Based upon the premise that atmospheric plasma oxidation should lead to the formation of surface silanol groups,[6] the treated polymer blend substrates were subsequently exposed to 1H, 1H, 2H, 2H - perfluorodecyl dimethylchlorosilane (PFDMCS) coupling agent. Chlorosilanes have been successfully used in the past to functionalize silica surfaces,[20,21,22,21,23,24] and also low pressure glow discharge oxidized PDMS substrates.[25]

The physiochemical nature of the polymer blend surfaces following each modification step was examined by X-ray photoelectron spectroscopy (XPS), contact-angle measurements and atomic force microscopy (AFM).

4.2 EXPERIMENTAL

Three different types of PDMS containing additive were mixed with the same polyethylene homopolymer (LLDPE/LDPE blend, Dowlex 2045A/Dow 5004I). These were a vinyl terminated PDMS polymer (M_w~500,000, Dow Corning), a diblock copolymer of PDMS and polyethylene units ($A_{95}B_{65}$ where A is a $-CH_2-$ unit and B a $-SiMe_2O-$ unit, M_w~6200, Dow Corning), and a triblock copolymer ($A_{30}B_{30}A_{30}$, M_w~3100, Dow Corning). The overall PDMS loading of each polymer blend film was kept constant at 2.5 % PDMS by weight.

Prior to any experimentation, adventitious silicone from the polymer blend surfaces was removed by ultrasonic cleaning for 30 seconds in a 1:1 mixture of isopropyl alcohol (BDH, Analar grade) and cyclohexane (BDH, Analar grade). These conditions were found to be sufficient to remove silicone-containing material from just the XPS sampling depth (2-5 nm).[26] Subsequent annealing gave rise to well controlled surface segregation of PDMS from the bulk. This entailed laying pieces of polymer blend film onto a clean glass plate placed in an oven for 30 mins at 353 K. Surface analysis and plasma treatment were then performed on the outward facing side of the annealed polymer film samples.

The home-built, parallel-plate dielectric barrier discharge and APGD reactors were used for plasma modification of the blend surfaces. Dielectric barrier discharge treatment was performed for 60 s (328 Hz, 2 mm inter-electrode gap, see Section 3.3.2). APGD oxidation entailed 60 s plasma treatment in a mixture of 95% helium (BOC 99.996%) and 5% oxygen (BOC, 99.998%) at a total flow rate of 1900 sccm at 1020 mbar pressure, refer to Section 3.3.2 for further details.

The plasma oxidized polymer blend surfaces were reacted for 18 hours with 1H, 1H, 2H, 2H - perfluorodecyldimethylchlorosilane, (PFDMCS, $CF_3(CF_2)_7(CH_2)_2$ $SiMe_2Cl$, Fluorochem) vapour under the conditions used in Section 3.2.2.

XPS surface elemental analysis was performed using the spectrometer and Si(2p) peak-fitting procedures cited in Section 1.3.1.

Contact angle measurements using de-ionised water and decane (Aldrich, 99+%) were used to probe the hydrophobic and oleophobic natures of the samples, see Section 1.3.3 for details.

Tapping mode AFM images were collected under conditions described in Section 1.3.5. As the phase images showed most clearly the changes that occurred upon treatment it is generally these that have been presented.

4.3 RESULTS

4.3.1 SURFACE SEGREGATION OF PDMS SEGMENTS UPON ANNEALING

Solvent washing followed by annealing for all three types of polymer blend system yielded surface enrichment of PDMS at concentrations well in excess of the bulk 0.5% atomic Si loading (ignoring hydrogen for XPS analysis), Table 4.1. Surface segregation was most pronounced for the ABA and AB copolymer blend systems, which exhibited surface silicon abundancies of 19% and 15% respectively. In contrast, the PDMS/PE polymer blend underwent relatively little surface enrichment to give only 5% silicon, Table 4.1. The water contact angles for all three blends were very similar, and did not reflect their differing surface compositions. A control sample of the polyethylene homopolymer film displayed a water contact angle value typical for a polyolefin substrate, Table 4.1.[27]

4.3.2 ATMOSPHERIC PRESSURE PLASMA OXIDATION OF PDMS ENRICHED POLYMER BLEND SURFACES

Atmospheric plasma oxidation of the annealed PDMS/PE films produced a surface containing predominantly oxidized hydrocarbon species, Table 4.1. Contact angle measurements reaffirmed this: the wettability of both silent-discharge and APGD treated surfaces was found to be similar to that achieved following corresponding treatment of pure polyethylene film. The small amount of silicon present displayed a high Si(2p) binding energy (~103.5 eV) compared to the unoxidized PDMS/PE blend (~102 eV). This can be taken as being indicative of a more oxidized, inorganic SiO_x phase being formed.[4,8,9,14] Hydrophobic recovery was comparable to that experienced by oxidised polyethylene, with only a small rise in water contact angle being measured over a period of 7 days, Figures 4.1a and 4.1b.

AFM images showed that dielectric barrier discharge oxidation of both PDMS/PE and polyethylene yielded large droplet-like features (up to 2 μm diameter) characteristic of low-molecular weight oxidized material (LMWOM),[28] Figures 4.2a(ii) and 4.2b(ii). Similarly APGD treatment of polyethylene was found to result in discrete features, Figure 4.2a(iii), which were removed by washing in a mixture of IPA and cyclohexane intimating that they too were LMWOM, Figure 4.2a(iv). However, APGD oxidation of PDMS/PE resulted in a largely wash resistant, reticulated structure, Figures 4.2b(iii) and Figure 4.2b(iv). 3-dimensional topographic plots of APGD treated PDMS/PE appear to show the removal of intervening material, accentuating the unevenness of the sample, Figure 4.3. The absence of such features on equivalently treated polyethylene indicates that the ridged morphology is a legacy of the oxidized PDMS additive observed by XPS.

Plasma treatment of the annealed AB/PE blend system produced greater incorporation of oxygen at the expense of carbon, Table 4.1. The Si(2p) spectra confirmed the formation of oxidized silicon species. In this case SiO_x coverage was sufficient to yield a totally hydrophilic surface following both types of atmospheric plasma modification. However, these fully wettable surfaces were found to undergo hydrophobic recovery, Figure 4.1. After 1 week, the water contact angle had increased to 72°. AFM showed the presence of

defects on the surfaces of both dielectric barrier discharge and APGD oxidized AB/PE blend which may have facilitated this phenomena, Figures 4.2c(ii) and 4.2c(iii). No significant difference in recovery behaviour was observed between the dielectric-barrier and APGD discharge treated samples.

The ABA/PE system displayed the greatest propensity to form SiO_x, (twice as much as the AB/PE blend), Table 4.1. Dielectric barrier discharge modification resulted in a water contact angle of 49°, with recovery almost complete within a day. APGD oxidized samples were found to be completely wettable and retained comparable hydrophilicity to that obtained for the treated AB blend after 1 week, Table 4.1. AFM of dielectric barrier discharge oxidized ABA/PE depicted a heterogeneous surface consisting of small 'plates' interspersed with areas of differing phase, Figure 4.2d(ii). In contrast ABA/PE treated with APGD possessed a fairly homogenous surface, Figure 4.2d(iii).

Sample	Treatment	XPS Atomic %			XPS Si (2p)	Water Contact Angle (Immediate) /°	Water Contact Angle After 7 days /°
		% C	% O	% Si	% $\underline{Si}O_x$		
PE	Washed and annealed	98.4 ±0.3	1.6 ±0.3	0	0	105.8 ±1.5	-
	Dielectric barrier	71.5 ±2.0	28.5 ±2.0	0	0	52.4 ±2.8	58.6 ±1.9
	APGD	74.2 ±0.1	25.8 ±0.1	0	0	51.0 ±2.1	61.7 ±1.9
PDMS/PE	Bulk	99.0	0.5	0.5	0	-	-
	Washed and annealed	88.1 ±1.3	6.6 ±0.7	5.3 ±0.7	0	109.0 ±2.2	-
	Dielectric barrier	64.4 ±1.0	33.2 ±0.8	2.4 ±0.2	6.5 ±0.6	50.6 ±5.7	62.4 ±1.5
	APGD	71.4 ±0.3	25.3 ±0.2	3.4 ±0.1	8.9 ±0.3	46.5 ±5.3	72.3 ±2.8
AB/PE	Bulk	99.0	0.5	0.5	0	-	-
	Washed and annealed	68.3 ±4.2	16.7 ±2.0	15.0 ±2.2	0	107.1 ±1.6	-
	Dielectric barrier	52.5 ±2.3	36.3 ±1.6	11.1 ±0.9	29.0 ±0.5	wets	72.1 ±3.8
	APGD	55.3 ±4.7	34.1 ±4.3	10.6 ±1.2	28.8 ±3.7	wets	72.1 ±3.2
ABA/PE	Bulk	99.0	0.5	0.5	0	-	-
	Washed and annealed	60.2 ±2.9	20.7 ±2.4	19.2 ±0.6	0	109 ±1.4	-
	Dielectric barrier	36.2 ±3.6	44.3 ±2.9	19.5 ±0.8	44.3 ±1.3	49.1 ±5.3	103.9 ±2.3
	APGD	26.5 ±0.5	51.1 ±0.3	22.4 ±0.2	55.6 ±1.7	wets	72.9 ±10.1

Table 4.1 XPS and water contact angle analysis.

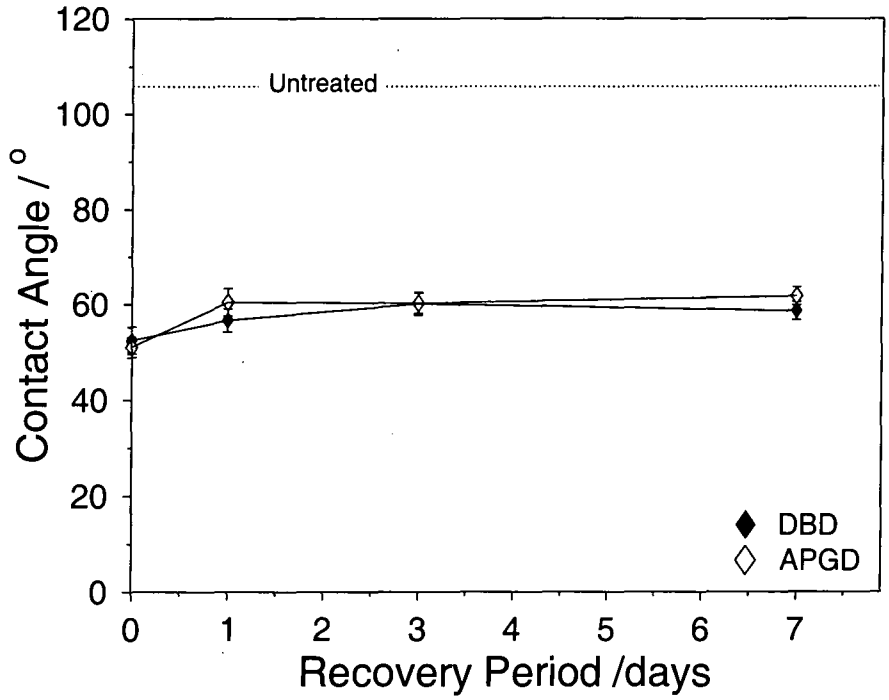

Figure 4.1a Hydrophobic recovery of oxidized polyethylene.

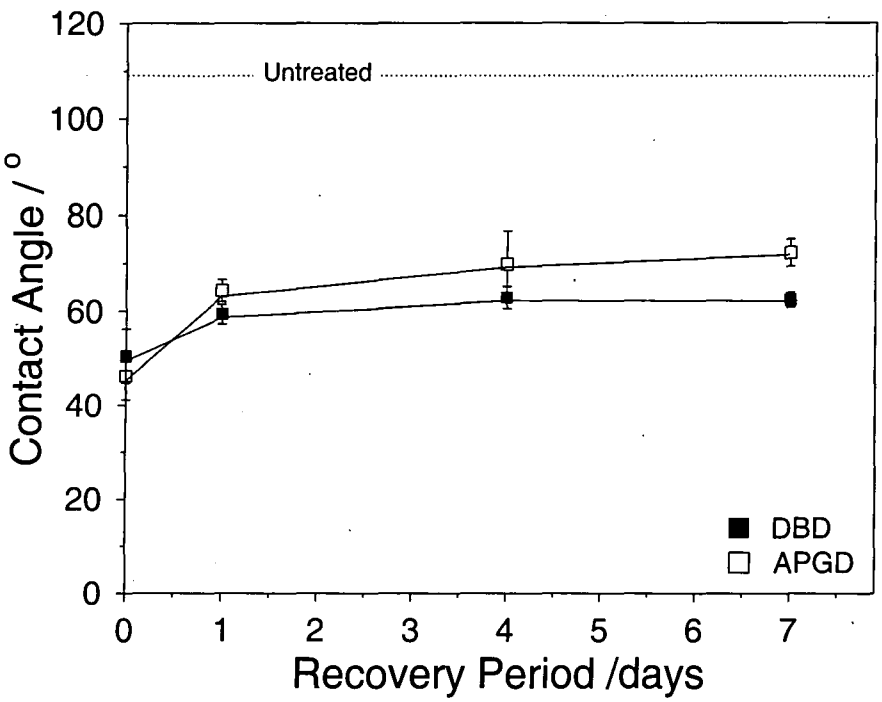

Figure 4.1b Hydrophobic recovery of oxidized PDMS/PE blend.

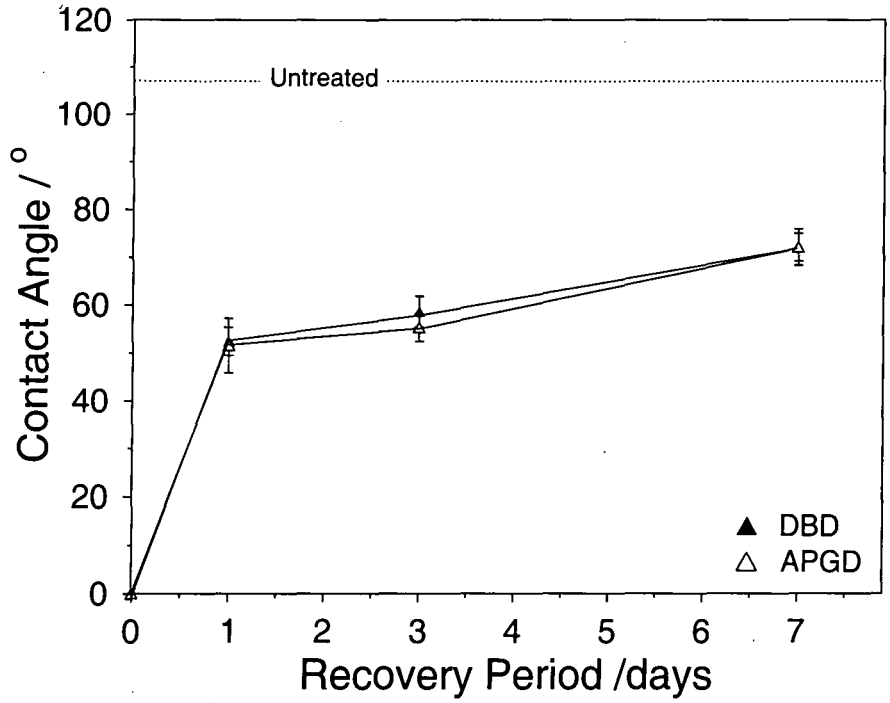

Figure 4.1c Hydrophobic recovery of oxidized AB/PE blend.

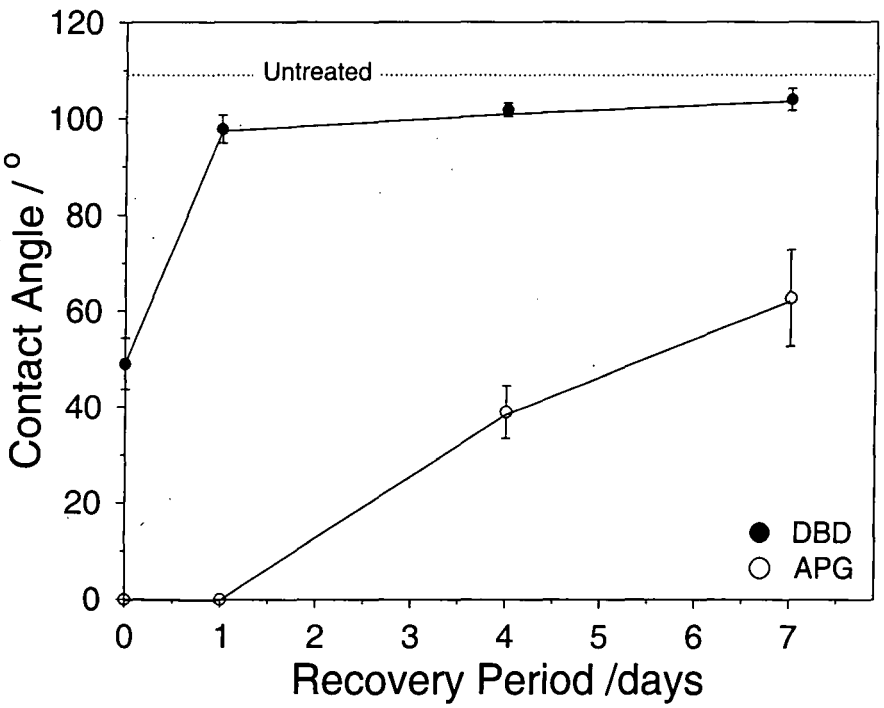

Figure 4.1d Hydrophobic recovery of oxidized ABA/PE blend.

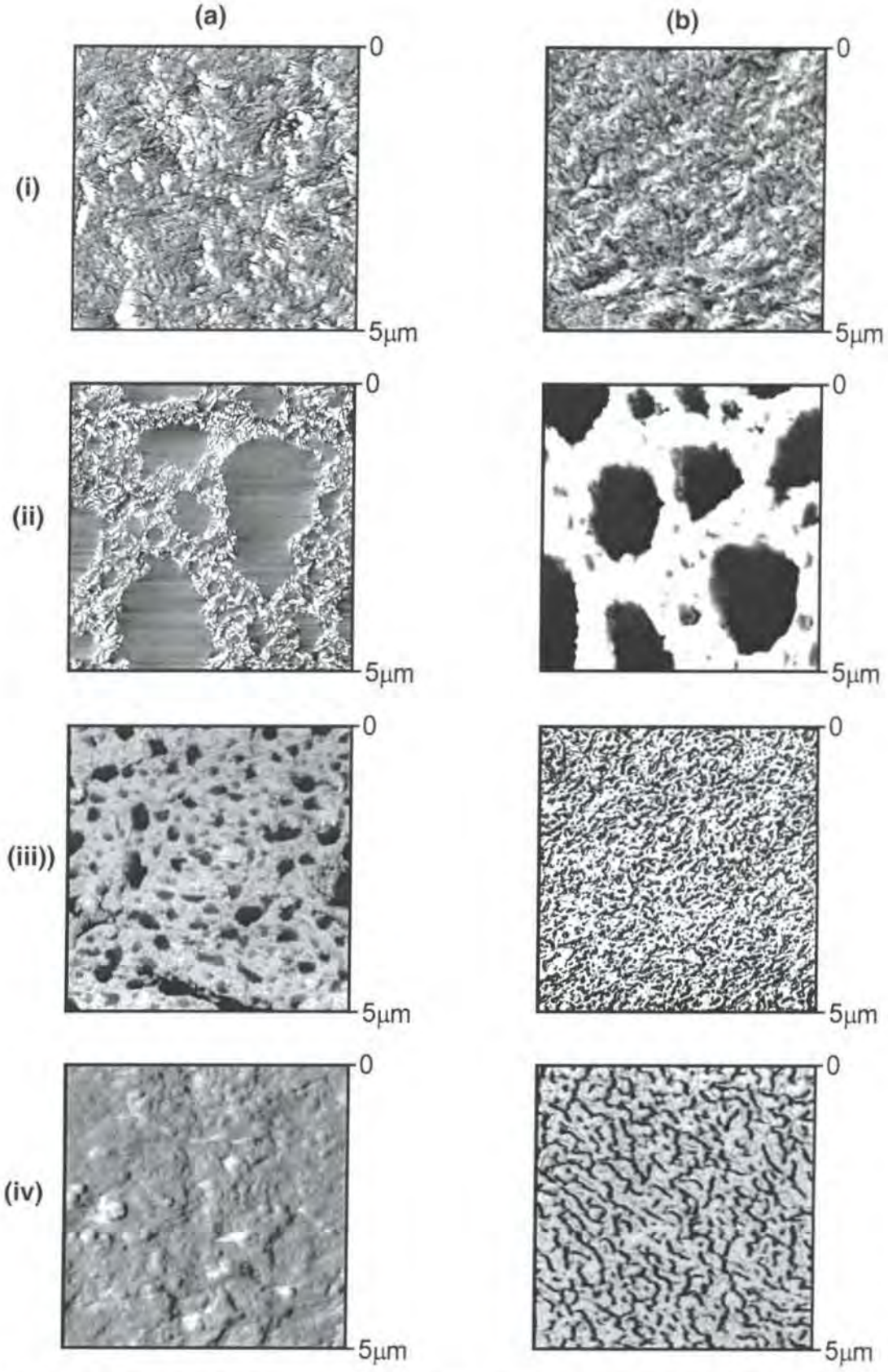

Figure 4.2 AFM phase images of (a) PE and (b) PDMS/PE blend after (i) washing and annealing, (ii) DBD, (iii) APGD and (iv) APGD followed by washing.

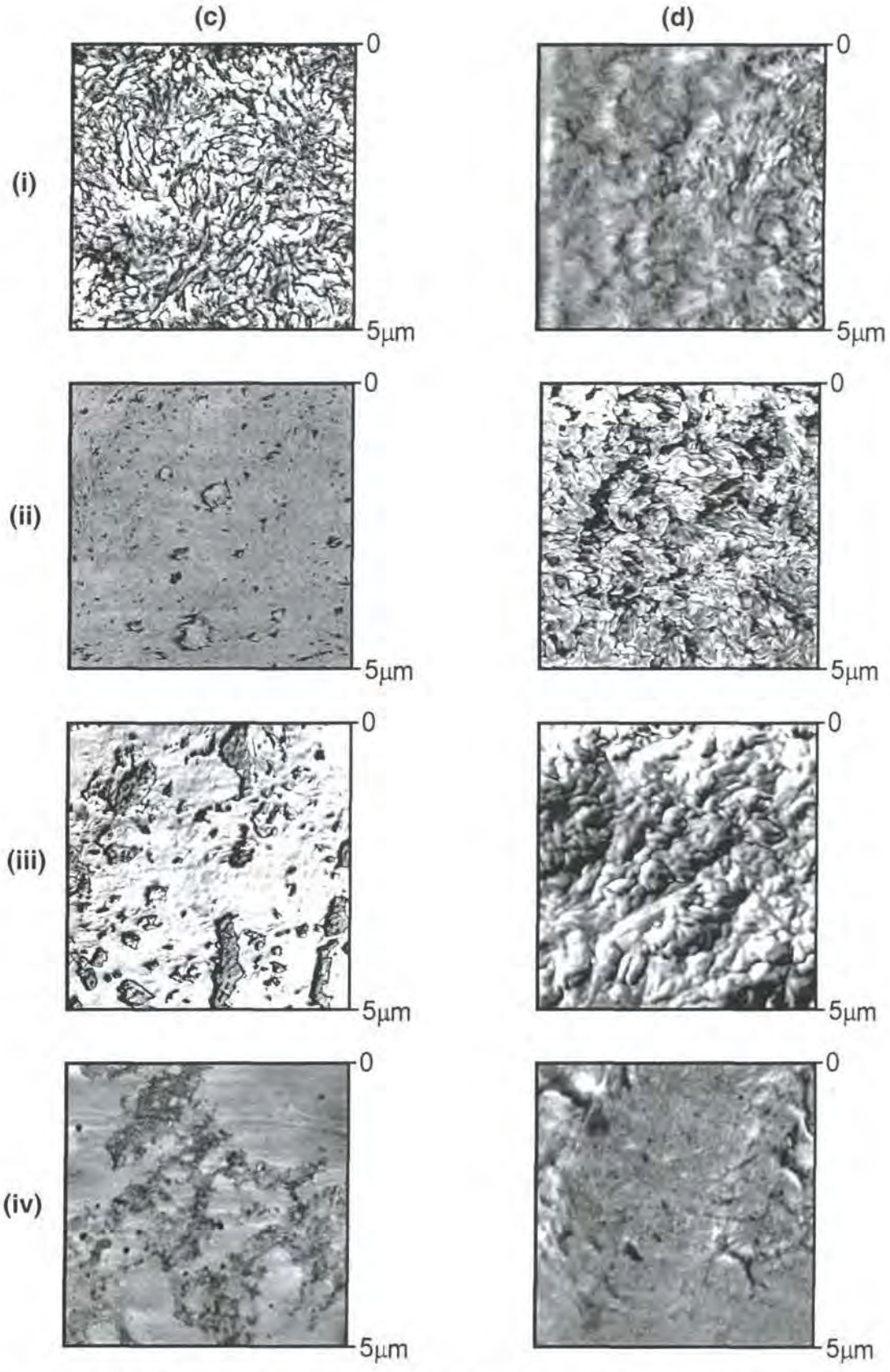

Figure 4.2 AFM phase images of (c) AB copolymer blend and (d) ABA **continued...** copolymer blend after (i) washing and annealing, (ii) DBD, (iii) APGD and (iv) APGD followed by washing.

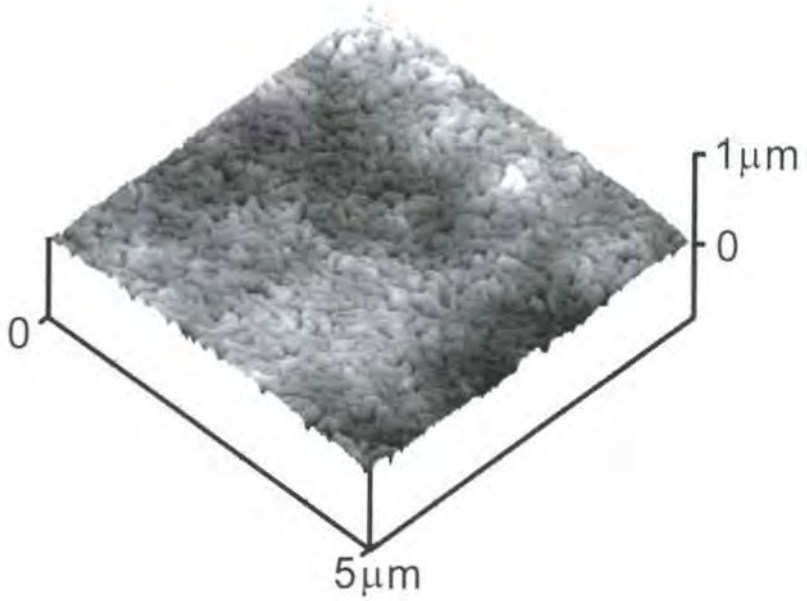

(a)

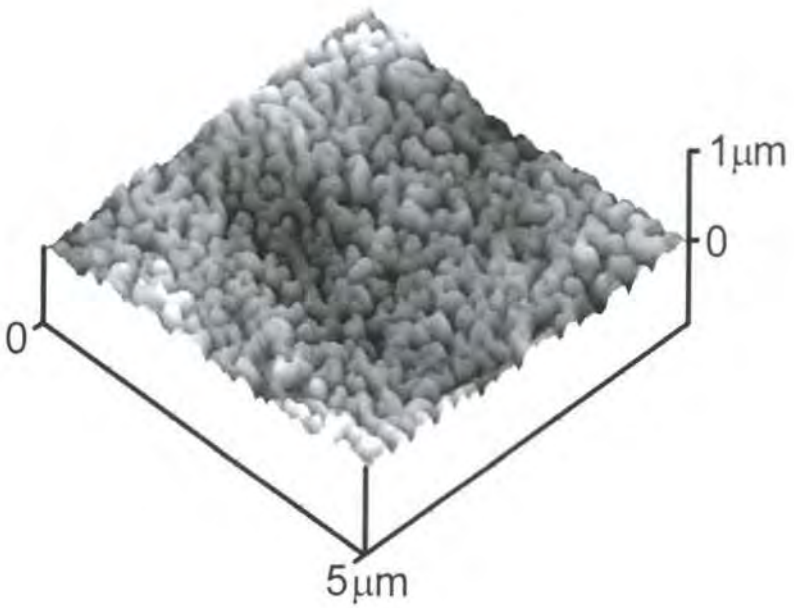

(b)

Figure 4.3 AFM height images of PDMS/PE blend after (a) APGD oxidation, and (b) APGD oxidation followed by washing.

4.3.3 CHLOROSILANE COUPLING TO PLASMA OXIDIZED PDMS BLEND SURFACES

Monochlorosilanes (unlike trichlorosilanes) cannot undergo self-condensation reactions at a surface, and thus each molecule of PFDMCS can only couple directly onto a silica surface. On this basis, the degree of PFDMCS attachment can be taken as a measure of surface reactivity (i.e. number of Si-OH moieties).[29] Exposure of the unoxidized polymer films to PFDMCS vapour resulted in virtually no reaction, Table 4.2. In contrast, the atmospheric pressure plasma oxidized polymer blend surfaces experienced a high degree of perfluoroalkyl group incorporation, as evident from the high %F, and improved water and decane repellency, Table 4.2. Furthermore, the absence of any Cl(2p) signal intimated complete hydrolysis of the Si-Cl bond belonging to the PFDMCS precursor. The coupling efficiency was found to be governed by the amount of oxidized SiO_x at the surface, Figure 4.5. The SiO_X-rich copolymer blends were most susceptible towards derivatization, whilst the oxidized PDMS/PE and polyethylene homopolymer substrates were not as amenable. This was supported by the high C(1s) binding energy shoulder, attributable to $\underline{C}F_2$ (at 291.2 eV) and $\underline{C}F_3$ (at 293.3 eV)[30] groups being significantly more pronounced for plasma oxidized ABA/PE and AB/PE compared to the relatively unreactive PDMS/PE system, Figure 4.4. Dielectric barrier discharge oxidized AB/PE was found to be the most reactive towards PFDMCS coupling. PFDMCS was found to react with atmospheric pressure plasma oxidized PE to only a small extent, Figure 4.4.

Sample	Treatment	% C	% F	% O	% Si	C.A. (water) /°	C.A. (decane) /°
Glass	none	22.9 ±2.7	0	52.9 ±1.3	24.2 ±1.9	18.0 ±2.0	wets
	PFDMCS labelled	16.3 ±1.0	19.5 ±1.2	43.4 ±0.4	20.9 ±0.1	96.0 ±4.7	47.6 ±4.1
PE	PFDMCS labelled	96.6 ±0.0	0.3 ±0.3	2.6 ±0.5	0.6 ±0.2	103.2 ±2.8	wets
	Dielectric barrier, PFDMCS labelled	72.0 ±1.2	2.3 ±2.3	25.1 ±1.3	0.6 ±0.1	57.1 ±2.4	wets
	APGD, PFDMCS labelled	78.2 ±0.9	2.8 ±0.1	18.9 ±0.1	0.1 ±0.1	59.2 ±4.5	wets
PDMS/PE	PFDMCS labelled	84.8 ±0.3	0.2 ±0.2	9.1 ±0.0	6.0 ±0.2	106.2 ±1.3	wets
	Dielectric barrier, PFDMCS labelled	56.7 ±0.5	14.2 ±1.1	26.0 ±0.7	3.1 ±0.1	88.2 ±3.7	35.6 ±3.3
	APGD, PFDMCS labelled	56.0 ±0.8	21.4 ±0.4	18.8 ±0.5	3.9 ±0.1	107.1 ±4.3	39.9 ±4.0
AB/PE	PFDMCS labelled	68.6 ±0.4	1.7 ±0.3	15.9 ±0.2	13.8 ±0.1	108.1 ±1.4	wets
	Dielectric barrier, PFDMCS labelled	31.7 ±0.6	34.9 ±0.9	23.2 ±0.8	10.2 ±0.8	114.3 ±3.1	58.4 ±4.1
	APGD, PFDMCS labelled	29.3 ±1.5	28.7 ±0.7	29.5 ±1.0	12.6 ±1.2	115.0 ±4.6	54.4 ±2.4
ABA/PE	PFDMCS labelled	63.9 ±0.5	0.2 ±0.2	18.8 ±0.5	17.2 ±0.2	106.4 ±1.6	wets
	Dielectric barrier, PFDMCS labelled	26.0 ±2.2	30.2 ±3.6	29.3 ±1.1	14.5 ±0.4	113.8 ±2.7	50.1 ±6.7
	APGD, PFDMCS labelled	25.4 ±1.2	24.1 ±2.7	35.3 ±0.7	15.3 ±0.9	109.6 ±3.7	53.8 ±2.8

Table 4.2 XPS and contact angle analysis following PFDMCS exposure to plasma oxidized surfaces.

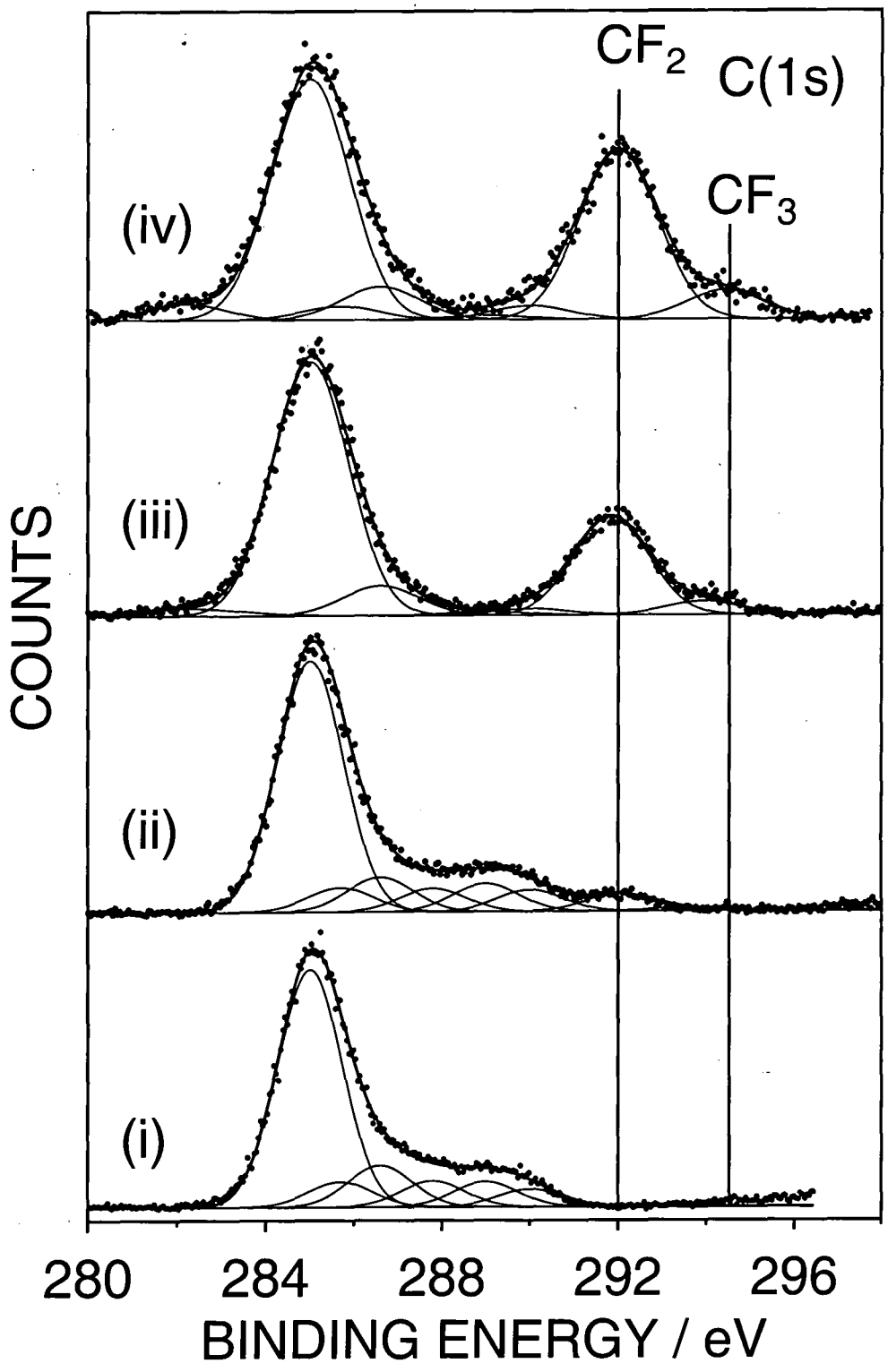

Figure 4.4a C(1s) XPS spectra of (i) PE; (ii) PDMS/PE blend; (iii) AB/PE blend; and (iv) ABA/PE blend following silent-discharge treatment and PFDMCS exposure.

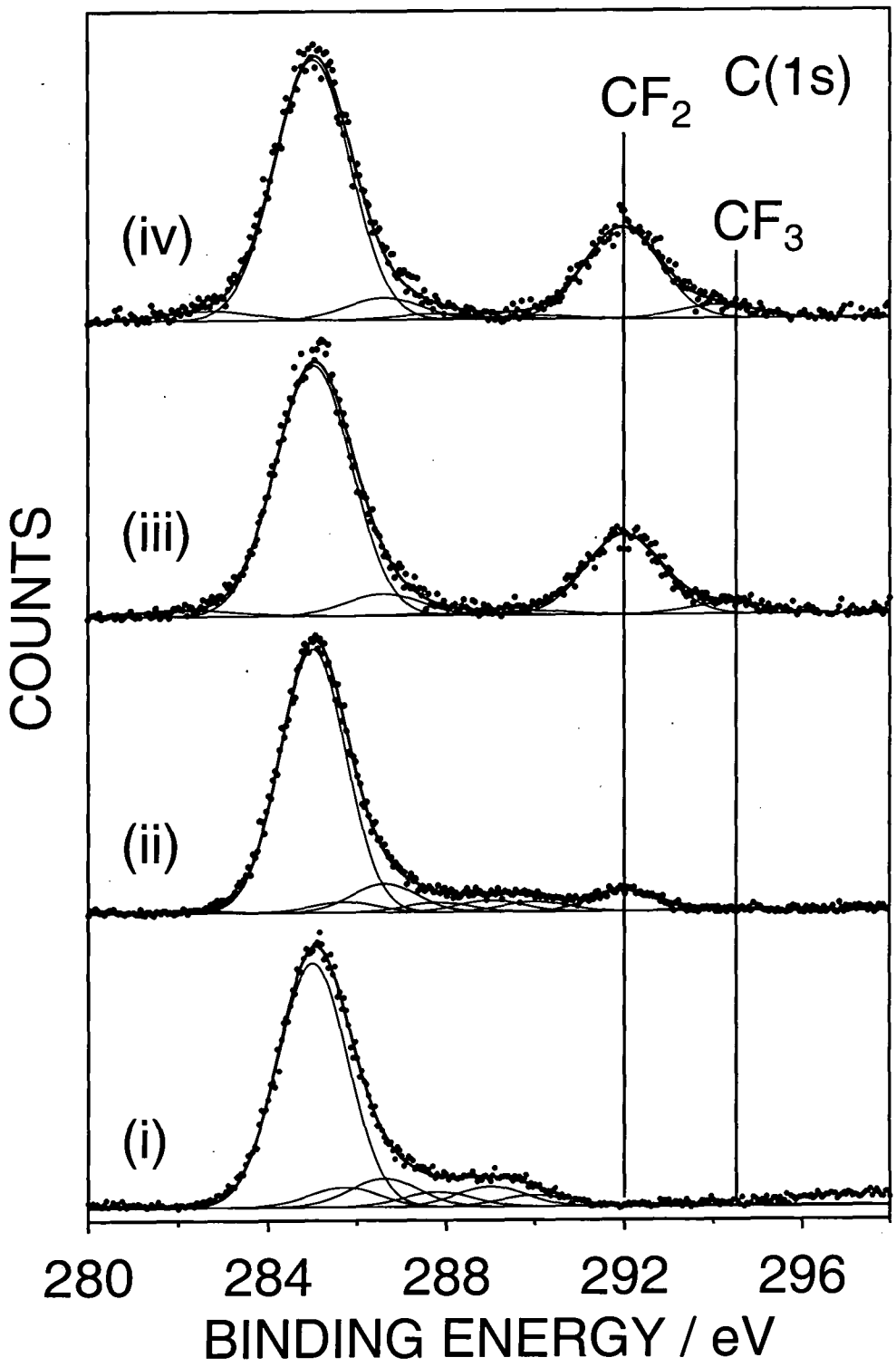

Figure 4.4b C(1s) XPS spectra of (i) PE; (ii) PDMS/PE blend; (iii) AB/PE blend; and (iv) ABA/PE blend following APGD treatment and PFDMCS exposure.

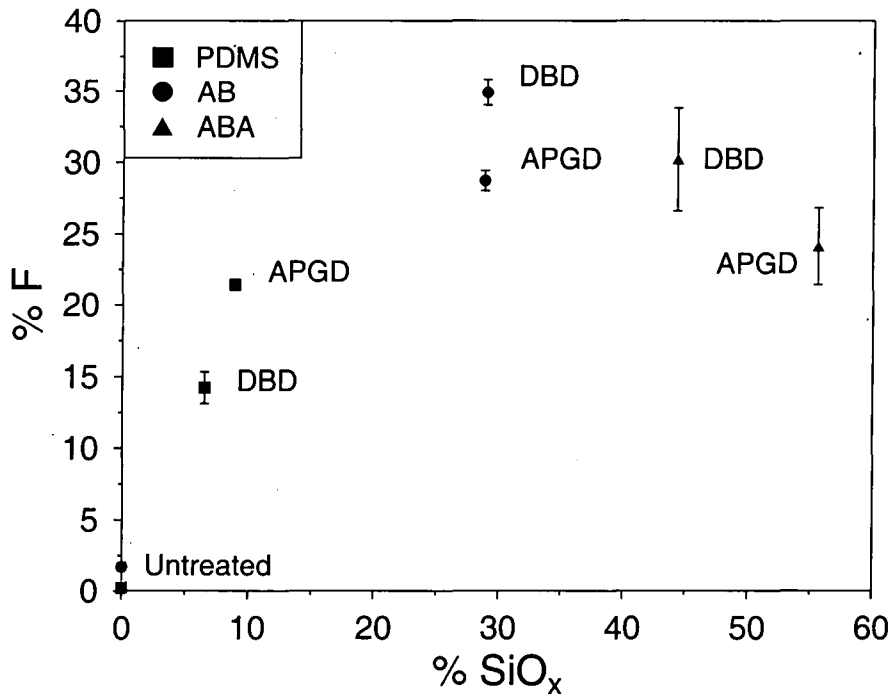

Figure 4.5 The correlation between $\%SiO_x$ and the degree of PFDMCS attachment (%F) for the plasma oxidized surfaces.

4.4 DISCUSSION

Mixing a small quantity of a low surface-energy component (such as a polysiloxane) into a polyolefin matrix can be a highly effective way of altering the surface chemistry, without significantly perturbing the underlying bulk properties.[31] Two factors are considered to contribute towards this phenomenon: minimization of surface energy at the air-solid interface by segregation of the lower surface energy component and the reduction of energetically unfavourable interactions between chemically dissimilar components contained in the blend.[32,33]

In the present study, the triblock additive (ABA) was found to be the most effective at migrating towards the surface of polyethylene during annealing, closely followed by the diblock copolymer (AB), whilst PDMS proved the worst, Table 4.1. This is in marked contrast to a previous investigation which concluded that for a fixed PDMS loading, blends containing a PDMS additive segregate more readily than those where the PDMS is contained within a

copolymer.[16] Furthermore, PDMS containing diblock copolymers have been found to enrich surfaces better than their triblock counterparts.[17,34] Although thermodynamics usually predicts surface segregation of the low surface energy segments towards the surface,[34] exceptions can occur in blend systems where the low surface energy component possesses a high molecular weight. In such cases, confinement of the large low surface energy species at the surface incurs severe entropic penalties; so instead, the surface becomes enriched by the higher surface-energy component.[35] However, this is unlikely to be the case in the present study because the molecular weights of the PDMS-containing moieties are much smaller than the host polyethylene matrix. A more feasible explanation for the observed reversal in additive segregation efficacy would be that the blends do not fully reach thermodynamic equilibrium during annealing. For instance, the PDMS content is likely to be dispersed as discrete domains throughout the host homopolymer, as observed in several previous studies.[5,31] In this situation viscosity will also contribute to surface segregation behaviour.[32] The higher molecular weight pure PDMS component should experience the most difficulty spreading between the dispersed PDMS domains. Whereas the lower molecular weight PDMS segments contained in the block copolymers can diffuse more easily towards the fully segregated thermodynamic-equilibrium surface.[32] Hence, the lighter ABA copolymer (M_w~3100) migrates faster than the relatively heavier AB copolymer (M_w~6200) additive through the polyethylene matrix.

In general, the copolymer blend surfaces were found to be more susceptible towards plasma oxidation than the PDMS/PE system because of their higher surface PDMS content. The observed re-emergence of hydrophobicity following plasma oxidation can be attributed to surface silanol condensation, polar group reorientation into the bulk, and the diffusion of low surface energy material towards the air-solid interface.[9,14] The low hydrophobic recovery observed for the APGD treated ABA/PE film is probably a consequence of the high SiO_X content generated during plasma oxidation, and the homogeneity of the APGD plasma[36,37,38,39] (whereas the filamentous nature of silent discharge is likely to damage the oxidized surface,[40] facilitating the migration of sub-surface unoxidized material, thus exacerbating hydrophobic recovery). This hypothesis was supported by AFM which showed a greater

degree of surface heterogeneity after silent-discharge oxidation compared to APGD.

The oxidized polymer blend surfaces also displayed reactivity towards chlorosilane coupling agents. The high degree of fluoroalkylation and corresponding enhancement in water and decane repellency demonstrated the viability of this approach, Table 4.2. The extent of chlorosilane coupling was found to be dependent on the surface coverage of SiO_X, Figure 4.5. Interestingly, the oxidized AB/PE and ABA/PE copolymer blends were perfluoroalkylated with almost equal efficacy (dielectric barrier discharge oxidized AB/PE was in fact the most functionalised surface), despite the oxidation of ABA/PE blends yielding far higher concentrations of SiO_x within the XPS sampling depth, Table 4.1. This discrepancy may be explained in terms of the oxidized surfaces of both blends consisting of equally oxidized silica-like layers at the very surface, the difference in SiO_x content due to differing depths of oxidation since XPS probes 2-5 nm below the surface.[41] The increased PFDMCS coupling to ABA/PE and AB/PE after dielectric barrier discharge treatment compared to APGD can be attributed to the use of unmodified air in the dielectric barrier discharge gap which may have encouraged greater surface silanol formation than the APGD (which uses relatively dry, pure He and O_2 feed gases). In the case of PDMS/PE the significantly larger amount of SiO_x produced with APGD is probably the overriding factor governing the degree of PFDMCS attachment.

4.5 CONCLUSIONS

Blending polyethylene with PDMS or PDMS-PE block copolymers gives rise to PDMS enrichment at the air-solid interface. These surfaces are found to be highly susceptible towards oxidation by atmospheric-pressure plasmas, with APGD being more effective than dielectric barrier discharge. SiO_X moieties produced at the oxidized polymer blend surfaces improve the wettability of the substrate and also readily undergo reaction with chlorosilane coupling agents. The vast range of available chlorosilane coupling agents means that the surfaces of PDMS containing polymer blend systems can be tailored with a wide range of chemical functionalities.

4.6 REFERENCES

[1] Smith, A. L. Introduction To Silicones In *The Analytical Chemistry of Silicones,* 1st ed.; A. L. Smith, Ed.; John Wiley & Sons, 1991, pp 3.

[2] Hwang, S. S.; Ober, C. K.; Perutz, S.; Iyengar, D. R.; Schneggenburger, L. A.; Kramer, E. J. *Polymer* **1995**, *36*, 1321.

[3] Hettlich, H.-J.; Otterbach, F.; Mittermayer, C.; Kaufmann, R.; Klee, D. *Biomaterials* **1991**, *12*, 521.

[4] Owen, M. J.; Smith, P. J. *J. Adhesion Sci. Technol.* **1994**, *8*, 1063.

[5] Senshu, K.; Furuzono, T.; Koshizaki, N.; Yamashita, S.; Matsumoto, T.; Kishida, A.; Akashi, M. *Macromolecules* **1997**, *30*, 4421.

[6] Hollahan, J. R.; Carlson, G. L. *J. Appl. Polym. Sci.* **1970**, *14*, 2499.

[7] Muisener, R. J.; Koberstein, J. T. *Abstracts of Papers of the American Chemical Society* **1997**, *214*, 653.

[8] Hillborg, H.; Gedde, U. W. *Polymer* **1998**, *39*, 1991.

[9] Murakami, T.; Kuroda, S.-I.; Osawa, Z. *J. Colloid Interface Sci.* **1998**, *202*, 37.

[10] Klee, D.; Breuers, W.; Bilo-Jung, M.; Mittermayer, C.; Hocker, H. *Die Angewandte Makromolekulare Chemie* **1989**, *166/167*, 179.

[11] Namatsu, H. *J. Electrochem. Soc.* **1989**, *136*, 2676.

[12] Maksimov, A. I.; Kzotova, G. D.; Bozovikova, I. N.; Kitaev, V. P.; Denisov, A. N. *Elektron Obrab Mater* **1988**, *5*, 52.

[13] Bogonosov, A. N.; Kzotova, G. D.; Maksimov, A. I. *Elektron Obrab Mater* **1987**, *4*, 39.

[14] Morra, M.; Occhiello, E.; Marola, R.; Garbassi, F.; Humphrey, P.; Johnson, D. *J. Colloid InterfaceSci.* **1990**, *137*, 11.

[15] Toth, A.; Bertoti, I.; Blazso, M.; Banhegyi, G.; Bognar, A.; Szaplonczay, P. *Appl. Polym. Sci.* **1994**, *52*, 1293.

[16] Pertsin, A. J.; Gorelova, M. M.; Levin, V. Y.; Makarova, L. I. *J. Appl. Polym. Sci.* **1992**, *45*, 1195.

[17] Chen, X.; Gardella, J. A.; Kumler, P. L. *Macromolecules* **1992**, *25*, 6631.

[18] Chen, X.; Gardella, J. A. *Macromolecules* **1994**, *27*, 3363.

[19] Wen, J.; Somorjai, G.; Lim, F.; Ward, R. *Macromolecules* **1997**, *30*, 7206.

[20] Revillon, A.; Leroux, D. *Reactive & Functional Polymers* **1995**, *26*, 105.

[21] Tripp, C. P.; Hair, M. L. *J. Phys. Chem.* **1993**, *97*, 5693.

[22] Silver, J. H.; Hergenrother, R. W.; Lin, J.-C.; Lim, F.; Lin, H.-B.; Okada, T.; Chaudhury, M. K.; Cooper, S. L. *J. Biomed. Mater. Res.* **1995**, *29*, 535.

[23] Wasserman, S. R.; Whitesides, G. M.; Tidswell, I. M.; Ocko, B. M.; Pershan, P. S.; Axe, J. D. *J. Am. Chem. Soc* **1989**, *111*, 5852.

[24] Wirth, M. J.; Fatunmbi, H. O. *Anal. Chem.* **1993**, *65*, 822.

[25] Ferguson, G. S.; Chaudhury, M. K.; Biebuyck, H. A.; Whitesides, G. M. *Macromolecules* **1993**, *26*, 5870.

[26] Spanos, C.; Goodwin, A. J.; Merlin, P.; Badyal, J. P. S *To be published.*

[27] *Contact Angle, Wettability and Adhesion*; Mittal, K.; Ed.; VSP: Utrecht, The Netherlands, 1993; pp 3-36

[28] Boyd, R.D.; Kenwright, A.M.; Badyal, J.P.S.; Briggs, D. *Macromolecules* **1997**, *30*, 5429

[29] Armistead, C. G.; Tyler, A. J.; Hambleton, F. H.; Mitchell, S. A.; Hockey, J. A. *J. Phys. Chem.* **1969**, *73*, 3947.

[30] Clark, D.T.; Shuttleworth, D. *J. Polym Sci., Chem. Ed.* **1980**, *18*, 27.

[31] Chen, X.; Gardella, J. A.; Cohen, R. E. *Macromolecules* **1994**, *27*, 2206.

[32] Volkov, I. O.; Gorelova, M. M.; Pertsin, A. J.; Filimonova, L. V.; Torres, M. A. P. R.; Oliveira, C. M. F. *J. Appl. Polym. Sci.* **1998**, *68*, 517.

[33] Chen, X.; Lee, H. F.; Gardella, J. A. *Macromolecules* **1993**, *26*, 4601.

[34] Hariharan, A.; Harris, J. G. *J. Phys. Chem.* **1995**, *99*, 2788.

[35] Kajiyama, T.; Tanaka, K.; Takahara, A. *Macromolecules* **1998**, *31*, 3746.

[36] Kanazawa, S.; Kogoma, M.; Moriwaki, T.; Okazaki, S. *J. Phys. D: Appl. Phys.* **1988**, *21*, 838.

[37] Okazaki, S.; Kogoma, M. *Proc. Jpn. Symp. Plasma Chem* **1989**, *2*, 95.

[38] Kanazawa, S.; Kogoma, M.; Okazaki, S.; Moriwaki, T. *Nucl. Instrum. Methods Phys. Res., Sect. B* **1989**, *37/38*, 842.

[39] Yokoyama, T.; Kogoma, M.; Kanazawa, S.; Moriwaki, T.; Okazaki, S. *J. Phys. D: Appl. Phys.* **1990**, *23*, 374.

[40] Greenwood, O. D.; Boyd, R. D.; Hopkins, J.; Badyal, J.P.S. *J. Adhesion Sci. Technol.* **1995**, *9*, 311.

[41] *Handbook of Surface and Interface Analysis*; Rivière, J.C., Myhra, S., Eds.; Marcel Dekker: New York, 1998

CHAPTER 5

ATMOSPHERIC PRESSURE GLOW DISCHARGE DEPOSITION OF POLYSILOXANE AND SiO_x FILMS

5.1 INTRODUCTION

Silicon-containing films find many technological applications in the packaging,[1,2,3,4] biomedical,[5,6] automotive,[7,8] and microelectronics[9,10,11] industries. Chemical vapour deposition (CVD)[12,13,14,15] and the pyrolytic degradation[16] of silicon containing precursors are often used in this context. Due to their inherently high operating temperatures (typically over 673 K) these techniques are often unsuitable for treating temperature sensitive materials such as polymers and semi-conductors[17] (e.g. GaAs, InP and a-Si:H). One way of overcoming this limitation is to use low pressure glow discharge methods such as plasma enhanced CVD (PECVD)[18,19] and remote plasma enhanced CVD (RPECVD).[20,21] However, the prerequisite vacuum makes these processes expensive and limited to batch treatments. UV irradiation[22] and UV/ozone[23] treatment are viable alternatives operating at atmospheric pressure and low temperature although film growth tends to be slow.

In this study, an atmospheric pressure glow discharge (APGD) fitted with an ultrasonic atomiser was used to deposit coatings from octamethylcyclotetrasiloxane (OMCTS) and tetramethylcyclotetrasiloxane (TMCTS) precursors, Figure 5.1. The APGD is a homogenous, atmospheric pressure plasmas described fully elsewhere (Section 1.2.4).[24,25,26,27] Ultrasonic nozzles employ a piezo-electric transducer to convert a liquid feed into an atomized spray.[28] This permits the vaporisation of even non-volatile precursors, leading to extremely high deposition rates since the monomer flux is not limited by vapour pressure (as in conventional low pressure plasma systems). Octamethylcyclotetrasiloxane and tetramethylcyclotetrasiloxane have been chosen as precursors since they consist of cyclic Si-O structures, which should easily ring open to provide polysiloxane networks. The physicochemical nature of the deposited films has been examined by X-ray photoelectron spectroscopy (XPS), ATR-FTIR, contact-angle, and gas permeability measurements.

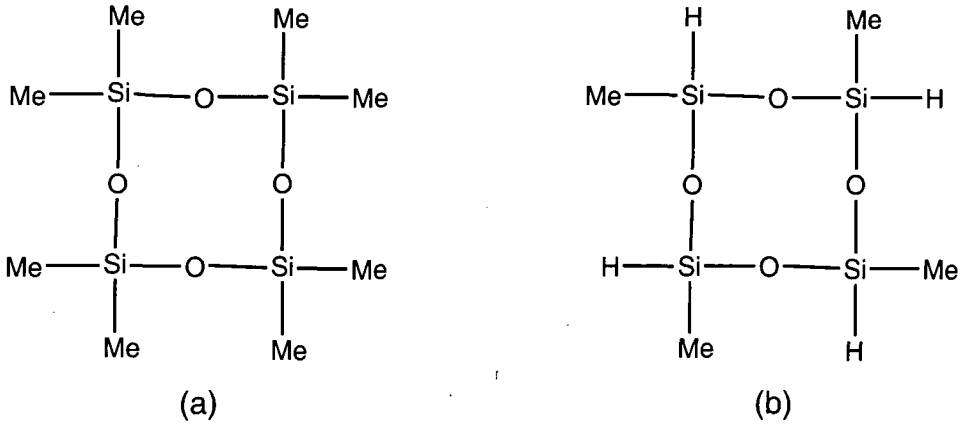

Figure 5.1 The structures of (a) octamethylcyclotetrasiloxane and (b) tetramethycyclotetrasiloxane.

5.2 EXPERIMENTAL

The atmospheric pressure glow discharge (APGD) deposition reactor constituted a high voltage 15 kHz ac power supply applied across two aluminium electrodes spaced 12 mm apart, with the lower live electrode shielded by a glass dielectric plate, Figure 5.2. An ultrasonic nozzle (Sono-tek, 8700-120) was embedded flush within the upper, earthed electrode and powered by a broad-band ultrasonic generator (Sono-tek, 06-05108). Octamethylcyclotetrasiloxane, OMCTS, (Fluka >99%) and tetramethylcyclotetrasiloxane, TMCTS (Fluorochem 95% min.) were introduced into the ultrasonic nozzle using a syringe pump (Harvard Apparatus) via a non-lubricated ball-valve.

Plasma deposition entailed placing a piece of polyethylene film (ultrasonically washed for 30 s in a 1:1 mixture of isopropyl alcohol (BDH, Analar grade) and cyclohexane (BDH, Analar grade)) on top of the glass dielectric plate and evacuating the chamber with a liquid nitrogen trapped rotary-pump. The process gas was then admitted at a flow-rate of 1900 sccm and a pressure of 1020 mbar. Two compositions were used: helium (BOC, 99.996%) and a 99% helium / 1% oxygen (BOC, 99.998%) mixture. After 10 mins of purging, the monomer reservoir syringe pump was switched on at a flow of 0.12 ml/hr. When the liquid OMCTS or TMCTS reached the ultrasonic nozzle, the ultrasonic generator was switched on (2.5 W) to initiate atomisation of the

precursor. Subsequently, the APGD plasma was ignited by applying 1.5 kV across the electrodes. Following 10 mins of deposition, any labile material was pumped off by placing the samples under vacuum for 20 mins.

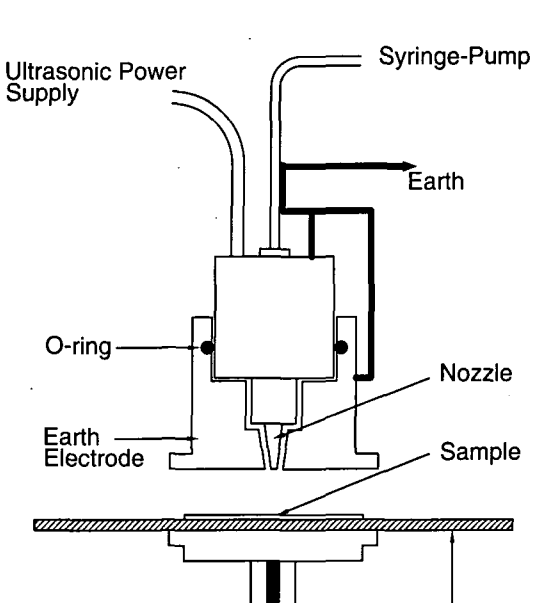

Figure 5.2 *Schematic of the APGD deposition reactor.*

ATR-FTIR spectra of the deposited films were recorded using 100 scans at 4 cm^{-1} resolution on a Mattson Polaris spectrometer fitted with an attenuated total reflectance (ATR) accessory (Graseby Specac Golden Gate).

A spectrophotometer (Aquila Instruments, nkd-6000) was used to determine film thickness. Transmittance-reflection curves over the 350-1000 nm range were fitted to a Drude-Lorentz model using a modified Levenburg-Marquardt procedure.[29] Repeatability and sample homogeneity were assessed by recording multiple readings from several different samples.

XPS and contact angle analysis (de-ionised water) were performed using the apparatus and procedures described in Section 1.3.1 and Section 1.3.3 respectively.

Oxygen gas permeation measurements were acquired using a mass spectrometric device, Section 1.3.4. The barrier improvement factor (BIF) for each sample was determined by referencing with respect to the MEPPP value measured for the untreated polyethylene substrate (Dowlex 2045A / Dow 5004I blend).

5.3 RESULTS

5.3.1 OCTAMETHYLCYCLOTETRASILOXANE DEPOSITION

APGD deposition of OMCTS in the presence of helium carrier gas yielded hydrophobic coatings with surface elemental abundances resembling those of the monomer, Table 5.1. Mixing oxygen with the helium feed gas produced a hydrophilic, oxidised surface containing a small amount of carbon. A corresponding increase in the Si(2p) binding energy, intimated the formation of a more inorganic, SiO_x rich environment,[30,31,32,33] Figure 5.3. Spectrophotometric thickness measurements indicated that the films deposited in pure He and the He/O_2 mixture were 279 ± 36 nm and 286 ± 38 nm thick respectively, Table 5.1.

ATR-FTIR has a penetration depth of approximately 0.1 - 10 μm,[32,34] it thereby provides an insight into the bulk chemical structure of the coating (whereas XPS is only sensitive to outermost 2-5 nm). Films deposited onto polyethylene substrate using a OMCTS/He APGD displayed similar IR spectral features to those seen for the liquid OMCTS precursor, Figure 5.4. The main differences were an enhancement of the peak at ~850 cm^{-1} and the emergence of a shoulder on the band at 1100-1000 cm^{-1} (Si-O-Si stretch[18,35,23]). The precise nature of the polymerised product is difficult to determine since absorbances due to $Si-CH_2-Si$ and Si-O-C coincide with Si-O-Si (1020-1090 cm^{-1}),[36,37] and Si-O, Si-C, Si-H and $Si-Me_3$ features all overlap in the 880-800 cm^{-1} region.[21,36,42] The absence of polyethylene bands at 1450 cm^{-1}, 2850 cm^{-1} and 2950 cm^{-1} indicated that the deposited films were sufficiently thick to preclude infrared sampling of the underlying substrate.

OMCTS coatings deposited in the presence of a helium/oxygen mixture exhibited several new infrared spectral features, Figure 5.4. The Si-O-Si stretch (1100-1000 cm^{-1}) broadened, and shifted towards higher wavenumber, this can be taken as being representative of quartz-like material.[23] In contrast the Si-Me band at 1260 cm^{-1} became attenuated, intimating the oxidative removal of methyl groups.[13,23] Bands at ~910 cm^{-1} and 3500-3000 cm^{-1} also emerged, indicative of Si-OH and SiOH-H_2O/absorbed H_2O respectively.[18,20,38,39] The absence of the C-H stretch at 2950 cm^{-1},[40] (a band seen for both liquid OMCTS and the helium deposited polymer) provided further evidence to support the preferential loss of organic material.

Oxygen gas permeability measurements of the coating obtained from the OMCTS/helium APGD were comparable to the untreated polyethylene substrate, Table 5.2. In contrast, OMCTS films deposited in a helium/oxygen mixture gave rise to a marked improvement in the gas barrier characteristics of the substrate.

Sample	XPS				Contact angle /°	Deposition rate /nm min^{-1}
	% C	% O	% Si	% SiO_x		
OMCTS, theoretical monomer	50	25	25	0	-	-
OMCTS, 100% He	43.3 ±2.5	29.3 ±0.8	25.8 ±0.6	35.7 ±6.5	107.8 ±9.2	28 ±4
OMCTS, 99% He, 1% O_2	25.5 ±5.2	48.5 ±4.5	26.0 ±0.7	74.4 ±2.8	56.4 ±9.8	29 ±4
TMCTS, theoretical monomer	33.3	33.3	33.3	-	-	-
TMCTS, 100% He	32.5 ±0.3	39.1 ±1.0	28.4 ±0.6	65.4 ±1.3	102.3 ±2.8	82 ±11
TMCTS, 99% He, 1% O_2	9.2 ±0.2	61.4 ±2.2	29.5 ±2.0	81.5 ±5.9	wets	244 ±38

Table 5.1 Summary of XPS, contact angle, and deposition rate measurements for OMCTS and TMCTS deposition.

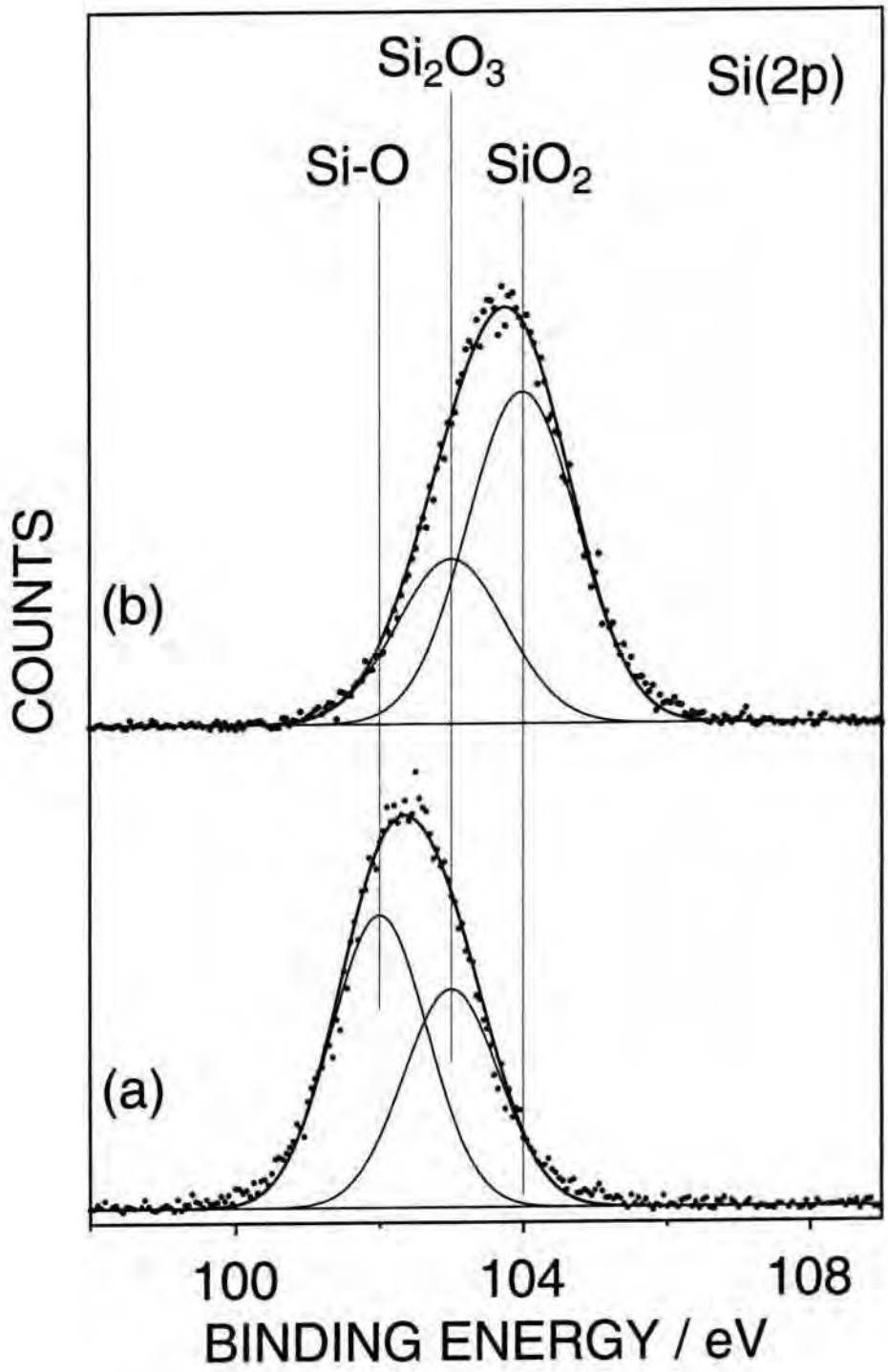

Figure 5.3 Si(2p) XPS spectra of OMCTS films deposited in: (a) helium APGD; and (b) helium / oxygen APGD.

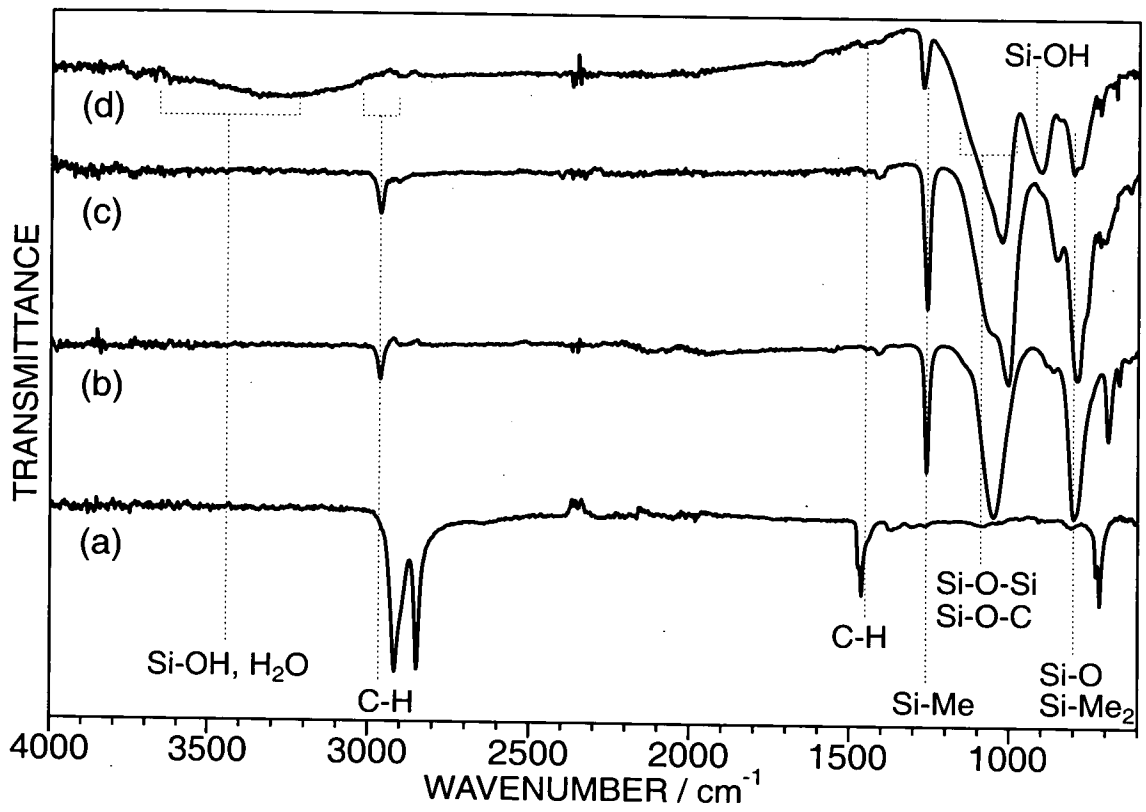

Figure 5.4 ATR-FTIR spectra of (a) polyethylene substrate; (b) OMCTS liquid; (c) helium APGD deposited OMCTS; and (d) helium / oxygen APGD deposited OMCTS.

Deposition Conditions	Barrier Improvement Factor
Polyethylene substrate	1.0
OMCTS, 100% He	0.9 ±0.2
OMCTS, 99% He, 1% O_2	6.8 ±3.5
TMCTS, 100% He	0.9 ±0.1
TMCTS, 99% He, 1% O_2	4.5 ±1.6

Table 5.2 Oxygen permeation measurements for APGD deposited OMCTS and TMCTS coatings

5.3.2 TETRAMETHYLCYCLOTETRASILOXANE DEPOSITION

XPS analysis showed that the hydrophilic TMCTS films deposited in helium contained more oxygen than predicted from the monomer structure, Table 5.1. The Si(2p) binding energy was also higher than expected, exhibiting a value (~102.8 eV) akin to a cross-linked structure such as a silisesquioxane (Si(2p) B.E. ~103 eV), Figure 5.5.[41] Addition of oxygen to the plasma resulted in carbon removal and a corresponding increase in oxygen concentration. This, with an increase in the Si(2p) binding energy, intimated the formation of oxidised coatings more SiO_X rich than those deposited from OMCTS and He / O_2. The films deposited from TMCTS were also far thicker than their OMCTS counterparts, especially those deposited from He/O_2 which had thicknesses of ~2.4 μm.

ATR-IR spectra of the films deposited from TMCTS/He APGD displayed similar features to the liquid monomer, Figure 5.6. The main differences were a broadening of the Si-O-Si stretch (1100-1000 cm^{-1}), and a diminishment of the Si-H band at ~2200 cm^{-1}.[36,42,43] These features can be attributed to Si-O-Si cross-linking with a corresponding partial loss of Si-H functionality. Addition of oxygen to the APGD plasma appeared to augment this phenomena; films

deposited in a He/O_2 mixture possessed a larger, broader Si-O-Si stretch, a weaker Si-Me band (1260 cm^{-1}) and an almost extinct Si-H peak. A broad band at 3500-3000 cm^{-1} also emerged, indicative of $SiOH-H_2O$/absorbed H_2O; the presence of which explains the enhanced hydrophilicity of this system

TMCTS coatings deposited from helium APGD did not significantly alter the oxygen permeability characteristics of the polyethylene substrate, Table 5.2. In contrast, TMCTS films deposited from a helium / oxygen mixture gave rise to a marked improvement in the gas barrier characteristics of the substrate.

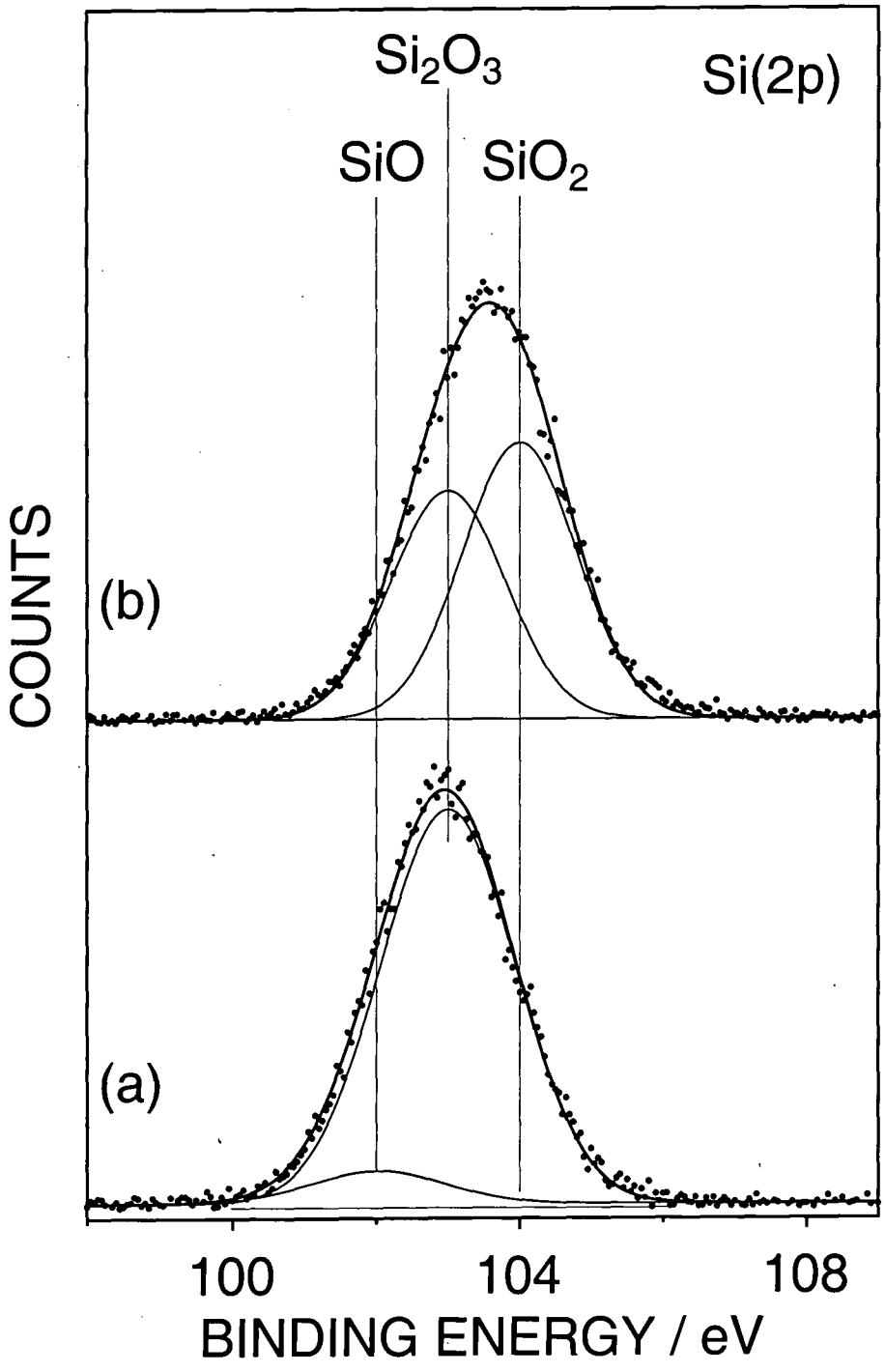

Figure 5.5 Si(2p) XPS spectra of TMCTS films deposited in: (a) helium APGD; and (b) helium / oxygen APGD.

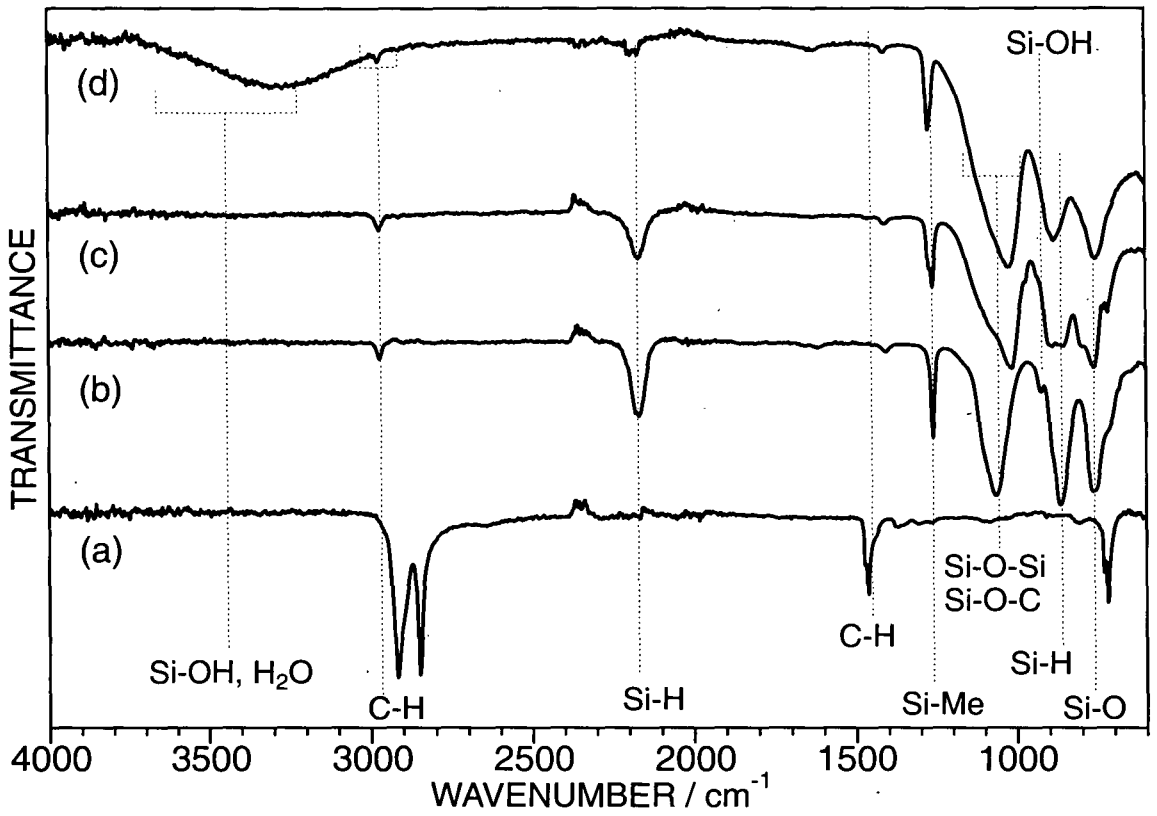

Figure 5.6 ATR-FTIR spectra of (a) polyethylene substrate; (b) TMCTS liquid; (c) helium APGD deposited TMCTS; and (d) helium/oxygen APGD deposited TMCTS.

5.4 DISCUSSION

Siloxane coatings deposited from OMCTS in a helium APGD displayed many XPS and IR spectral features expected for the OMCTS monomer. The observed differences were attributable to the opening and polymerisation of the siloxane ring. The high organic content and low degree of cross-linking (shown by the low Si(2p) binding energy characteristic of linear siloxanes) were responsible for the negligible improvement in gas barrier.[42] However gas absorption by such plasma polymerised OMCTS films may find application in selective gas sensors.[44,45] Also surface hydrophobicity was noted to be comparable to that obtained for conventional low pressure plasma deposited water repellent polysiloxane films.[46]

The high deposition rate and enhanced cross-linking observed for TMCTS films could be attributable to the Si-H bonds contained in the precursor. These were shown by ATR-IR to be particularly labile, probably leading to the formation of Si-O-Si linkages. This phenomena can be explained by considering the weakness of the Si-H bond relative to the Si-O bond (average bond dissociation enthalpies: Si-H=318 kJ $mol^{-1}$and Si-O=466 kJ mol^{-1}).[47]

The introduction of oxygen into the OMCTS and TMCTS helium APGD mixtures gave rise to a significant level of oxygen incorporation at the expense of carbon and hydrogen removal, yielding an inorganic SiO_x cross-linked structure. The corresponding attenuation in oxygen permeation is most likely to be a consequence of the increase in film density[42] (i.e. decrease in free volume) and hindrance in segmental mobility associated with an oxidised siliceous phase. A similar drop in oxygen transmission has previously been reported for SiO_x films deposited by CVD and low pressure PECVD.[42]

5.5 CONCLUSIONS

Introduction of substituted cyclotetrasiloxane precursors into a helium atmospheric pressure glow discharge using an ultrasonic atomiser gave rise to the rapid deposition of hydrophobic polysiloxane films. The addition of oxygen

resulted in SiO_x rich coatings which displayed a marked improvement in hydrophilicity and gas barrier.

5.6 REFERENCES

[1] Inagaki, N.; Tasaka, S.; Makino, M. *J. Appl. Polym. Sci.* **1997**, *64,* 1031

[2] Frisk, P.; Jaccoud, B.; Roulin, A.; Johansson, H. U.S. Patent 5,721,027 Feb. 24, 1998

[3] Frisk, P. U.S. Patent 5,916,685 June 29, 1999

[4] Fukugami, N.; Nishino, H.; Yanaka, M.; Tomiyama, K.; Tsukahora, Y. *J. Vac. Sci. Technol., A* **1999**, *17*, 1840

[5] Hettlich, H.-J.; Otterback, F.; Mittermoyer, C.; Kaufmann, R.; Klee, D. *Biomaterials* **1991**, *12*, 521

[6] Fox, C. L.; Modak, S. M.; Sampath, L. A. U.S. Patent 5,616,338 April 1, 1997

[7] Gordon, N. U.S. Patent 5,098,745 March 24, 1992

[8] Inokuchi, Y.; Kuwata, S. U.S. Patent 5,760,109 June 2, 1998

[9] Engle, G. M. U.S. Patent 4,223,048 Sept. 16, 1980

[10] Dory, T. S. U.S. Patent 4,877,651 Oct. 31, 1989

[11] Batey, J.; Tierney, E. U.S. Patent 5,068,124 Nov. 26, 1991

[12] Gill, W.N.; Ganguli, S. *J. Vac. Sci. Technol. B* **1997**, *15*, 948

[13] Fujino, K., Nishimoto, Y.; Tokumasu, N.; Maeda, K. *Jpn. J. Appl. Phys.* **1994**, *33*, 2019

[14] Ikeda, K,; Maeda, M. *Jpn. J. Appl. Phys.* **1996**, *35,* 1573

[15] Fujino, K.; Nishimoto, Y.; Tokumasu, N.; Maeda, N. *J. Electrochem. Soc.* **1990**, *137*, 2883

[16] Seyferth, D. *Adv. Chem. Ser.* **1990**, *224*, 565

[17] Bergonzo, P.; Kogelschatz, U.; Boyd, I.W. *Appl. Surf. Sci.* **1993**, *69,* 393

[18] Nguyen, S.; Dobuzinsky, D.; Harmon, D.; Gleason, R.; Fridman, S. *J. Electrochem. Soc.* **1990**, *7*, 2209

[19] Rats, D.; Hajek, V.; Martinu, L. *Thin Solid Films* **1999**, *340, 33*

[20] Regnier, C.; Tristant, P.; Demaison, J. *Surface and Coatings Technology* **1996**, *80*, 18

[21] Wrobel, A.M.; Walkiewicz-Pietrzykowska. A.; Wickramanayaka, S.; Hatanaka, Y. *J. Electrochem. Soc.* **1998**, *145*, 2866

[22] Niwano, M.; Kinashi, K.; Kazuhiko, S.; Miyamoto, N. *J. Electrochem. Soc.* **1994**, *141*, 1556

[23] Muisener, R.J.; Koberstein, J.T. *Abstracts of Papers of the American Chemical Society* **1997**, *214,* 56

[24] Kanazawa, S.; Kogoma, M.; Moriwaki, T.; Okazaki, S. *J. Phys. D: Appl. Phys.* **1988**, *21*, 838.

[25] Okazaki, S.; Kogoma, M. *Proc. Jpn. Symp. Plasma Chem* **1989**, *2*, 95.

[26] Kanazawa, S.; Kogoma, M.; Okazaki, S.; Moriwaki, T. *Nuclear Instruments and Methods in Physics Reseach* **1989**, *B37/38*, 842.

[27] Yokoyama, T.; Kogoma, M.; Kanazawa, S.; Moriwaki, T.; Okazaki, S. *J. Phys. D: Appl. Phys.* **1990**, *23*, 374.

[28] Ultrasonic-nozzle Product Information, *Sono-tek*, U.S.A.

[29] Technical Information, *Aquila Instruments,* Cambridge, U.K.

[30] Owen, M. J.; Smith, P. J. *J. Adhesion Sci. Technol.* **1994**, *8*, 1063.

[31] Murakami, T.; Kuroda, S.-I.; Osawa, Z. *J. Colloid Interface Sci.* **1998**, *202*, 37.

[32] Hillborg, H.; Gedde, U. W. *Polymer* **1998**, *39*, 1991.

[33] Morra, M.; Occhiello, E.; Marola, R.; Garbassi, F.; Humphrey, P.; Johnson, D. *Journal of Colloid and Interface Science* **1990**, *137*, 11.

[34] Gaboury, S. R.; Urban, M. W. Analysis of Gas Plasma Modified Poly(dimethylsiloxane) Elastomer Surfaces. Attenuated-Total-Reflectance-Fourier Transform Infrared Spectrscopy In *Structure-Property Relations in Polymers*; Urban, M. W., Craver, D.C., Eds.; A.C.S., 1993; Vol. 236, pp 778.

[35] Fujii, T.; Hiramatsu, M.; Nawata, M. *Thin Solid Films* **1999**, *343-344*, 457

[36] Bogart, K.H.A.; Ramirez, S.K.; Gonzales, L.A.; Bogart, G.R. *J. Vac. Sci. Technol. A* **1998**, *16,* 3175

[37] Kim, M.T. *Thin Solid Films* **1999**, *347,* 99

[38] Zajickova, L.; Janca, J.; Perina, V. *Thin Solid Films* **1999**, *338*, 49

[39] Veprek-Heijman, M.G.J.; Boutard, D. *J. Electrochem. Soc.* ***1991***, *138*, 2042

[40] Okimura, K.; Maeda, N. *J. Vac. Sci. Technol. A* **1998**, *16,* 3157

[41] Greenwood, O.D. Ph.D. Thesis, University of Durham, U.K., 1997

[42] Agres, L.; Segui, Y.; Delsol, R.; Raynaud, P. *J. Appl. Polym. Sci.* **1996**, *61*, 2015

[43] Lin, C.-F.; Tseng, W.-T.; Feng, M.S. *J. Appl. Phys.* **2000**, *87*, 2808

[44] Janca, J.; Sodomka, L. *Surface and Coatings Technology* **1998**, *98,* 851

[45] Guo, S.; Rochotzki, R.; Lundstrom, I.; Arwin, H. *Sensors and Actuators B* **1997**, 44, *243*

[46] Mahlberg, R.; Niemi, H.E.-M.; Denes, F.; Rowell, R.M. *International Journal of Adhesion and Adhesives* **1998**, *18*, 283

[47] Atkins, P.W. *Physical Chemistry*, 5th ed.; Oxford University Press: Oxford, U.K.,1994; p C7

CHAPTER 6

ATMOSPHERIC PRESSURE PLASMA DEPOSITION OF STRUCTURALLY WELL-DEFINED POLYACRYLIC ACID AND 1H, 1H, 2H - PERFLUORO-1-OCTENE FILMS

6.1 INTRODUCTION

Low pressure glow discharges are a well established means of polymerizing volatile, organic molecules to produce thin, pin-hole free coatings.[1] However, they suffer from a number of drawbacks which include the requirement for vacuum, low deposition rates, and often poor control of reaction selectivity. The high energy of plasmas enables reactive processes such as UV irradiation and ion bombardment to ablate the growing film, often leading to the elimination of the desired surface moiety.[1,2]

In this investigation an atmospheric pressure glow discharge (APGD) deposition reactor equipped with an ultrasonic atomising nozzle has been used to deposit polymeric coatings from acrylic acid and 1H, 1H, 2H - perfluoro-1-octene, Structures 6.1 and 6.2.

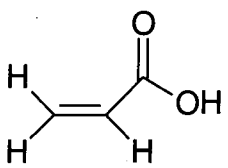

Structure 6.1 Acrylic acid

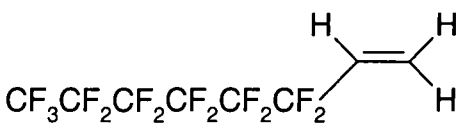

Structure 6.2 1H, 1H, 2H - Perfluoro-1-octene

The polymerisation of acrylic acid using low pressure plasmas has been extensively investigated. Applications of this technology include adhesion,[3,4] biocompatibility,[5] membranes,[6,7] and wettability enhancement.[8] The proportion of carboxylic acid groups in these plasma polymers, often of critical importance, is usually low (~20% c.f. 33% in the monomer).

Perfluoroalkyl chains are renowned for their liquid repellency, a useful property in biomedical layers, protective coatings and stain resistant textiles.[9,10,11] The low pressure plasma polymerization of monomers, such as 1H, 1H, 2H - perfluoro-1-octene, which combine long perfluoroalkyl chains and a polymerizable functionality, has previously been found to result in hydrophobic surfaces.[12,13]

The APGD / ultrasonic nozzle reactor has been previously described in Chapter 5. Here it is shown how this apparatus' combination of high monomer flux and favourable discharge characteristics can overcome the monomer fragmentation traditionally associated with plasma methods .

6.2 EXPERIMENTAL

The APGD / ultrasonic nozzle deposition reactor was used to polymerize the two monomers under the conditions stated in Section 5.2. The process gas in all experiments was pure helium (BOC, 99.996%).

XPS analysis was performed using the equipment and procedures cited in Section 1.3.3. Complete coverage was confirmed by the absence of a N(1s) signal from the nylon 6,6 substrate (Goodfellow, 0.15 mm thick).

All FT-IR spectra were recorded in transmission mode using 100 scans at 4 cm^{-1} resolution on a Mattson Polaris spectrometer. Plasma polymer films were deposited onto KBr disks (Aldrich, analytical reagent), whilst the reference monomer spectrum were acquired by placing neat liquid between two NaCl plates. Commercial polyacrylic acid (Aldrich) was mixed with KBr powder and pressed into a disk.

Film thickness was measured with the spectrophotometer used in Section 5.2. Transmittance-reflection curves spanning the 350-1000 nm range were fitted to the Cauchy model using a modified Levenburg-Marquardt procedure.[14] As before, repeatability and sample homogeneity were assessed by recording multiple readings from several different samples.

De-ionized water contact-angle values were measured using the video capture apparatus (Section 1.3.3). The critical surface tension (γ_c) of the perfluoroalkene films was calculated by the Zisman method, Section 1.3.3. The contact angle of the plasma polymer surface was measured using a homologous series of liquids (n-alkanes). A graph of the cosine of the contact angle versus the surface tension of the liquid then yielded a Zisman plot. Extrapolation of the line of best fit to $\cos\theta=1$ resulted in a value for γ_c.[15] The surface tensions of the probe liquids are given in Table 6.1.[16]

Liquid	Surface Tension /mN m^1 (at 20 °C)
Hexadecane	27.5
Tetradecane	26.6
Dodecane	25.4
Decane	23.8
Octane	21.6

Table 6.1 Surface tensions of n-alkane probe liquids.[16]

Oxygen permeation through APGD deposited polyacrylic acid was assessed using the mass spectrometric device described in Sections 1.3.4. The barrier improvement factor (BIF) for the coated sample was referenced to the MEPPP value of an untreated polyethylene substrate (LLDPE/LDPE blend, Dowlex 2045A/Dow 5004I).

Evaluation of the adhesive characteristics of the acrylic acid plasma polymer layer was undertaken by single lap shear tests.[17] Polyacrylic acid layers were deposited onto 10 mm wide nylon strips (Goodfellow, 0.15 mm thick). Two opposing faces were then overlapped to create a joint covering 1 cm^2 area. Curing was performed for 60 minutes under a 2 kg weight at 343 K. The strength of the joints was then determined by pulling apart at a rate of 5 mm min^{-1} using a tensilometer (Instron, 5543, 500 N static load cell) and noting the maximum load reached prior to failure. Control joints fabricated from pieces of uncoated nylon displayed no adhesive properties.

6.3 RESULTS

6.3.1 APGD POLYMERIZATION OF ACRYLIC ACID

The elemental abundances of the deposited films were consistent with polyacrylic acid, Table 6.2. This similarity was corroborated by peak-fitting the C(1s) XPS spectra and comparing with conventional polyacrylic acid. The binding energies of the oxidized carbon functionalities were fitted as follows: **C**-CO_2H at 285.4 eV, **C**-O at 286.6 eV, **C**=O or O-**C**-O at 287.8 eV and **C**O_2H at 289.2 eV.[18] A large well-resolved feature at 289.2 eV was indicative of high carboxylic acid group retention (26.4 %, compared to a theoretical maximum of 33 %), Figure 6.1. The wettability of the plasma polymer surface towards water further corroborated the presence of hydrophilic CO_2H groups, Table 6.2.

FT-IR spectroscopy showed that acrylic acid monomer possessed absorption bands due to C=C and $=CH_2$ at 1637 cm^{-1} and 984 cm^{-1} respectively, Figure 6.2.[19,20] These disappeared upon APGD polymerisation, and can be taken as evidence for the reaction of the carbon-carbon double bond. The hydroxyl vibrational stretch also broadened towards >3500 cm^{-1}, which is most likely to be indicative of water absorption.[21] Several other aspects of the monomer FT-IR spectra were lost or modified by deposition: the C-OH bend at 1430 cm^{-1}, the C-O stretching doublet at ~1260 cm^{-1} and the O-H out of plane bend at 920 cm^{-1}.[22] Overall, the strong similarity between the IR spectra of the plasma polymer and commercial polyacrylic acid confirms that APGD deposition has led to the formation of a polymeric material which resembles its conventional counterpart, Figure 6.2.

The plasma deposited polyacrylic acid layers also exhibited appreciable gas barrier characteristics. A 2.3 μm coating reduced oxygen permeation through polyethylene film by a factor of 7, Table 6.3.

Lap-shear tests demonstrated the considerable adhesive powers of APGD deposited polyacrylic acid. Self-adhered films withstood a maximum load of 74 ±11 N before failure of the joint.

	% C	% O	% CO_2H	% CO_2H retention	Contact Angle /°	Deposition Rate nm min^{-1}
Theoretical (from monomer)	60.0	40.0	33.3	100	-	-
Polyacrylic acid (commercial)	63.3 ±0.2	36.7 ±0.2	29.9 ±0.2	89.6 ±0.5	wets	-
APGD plasma polymer	62.6 ±0.6	37.4 ±0.6	26.4 ±1.9	79.3 ±5.6	wets	231.0 ±95.0

Table 6.2 XPS, contact angle and deposition rate measurements for acrylic acid polymers.

Sample	Barrier Improvement Factor
Polyethylene substrate	1.0 (by definition)
APGD plasma polymer	7.2 ±0.9

Table 6.3 Gas barrier measurements for the acrylic acid plasma polymer.

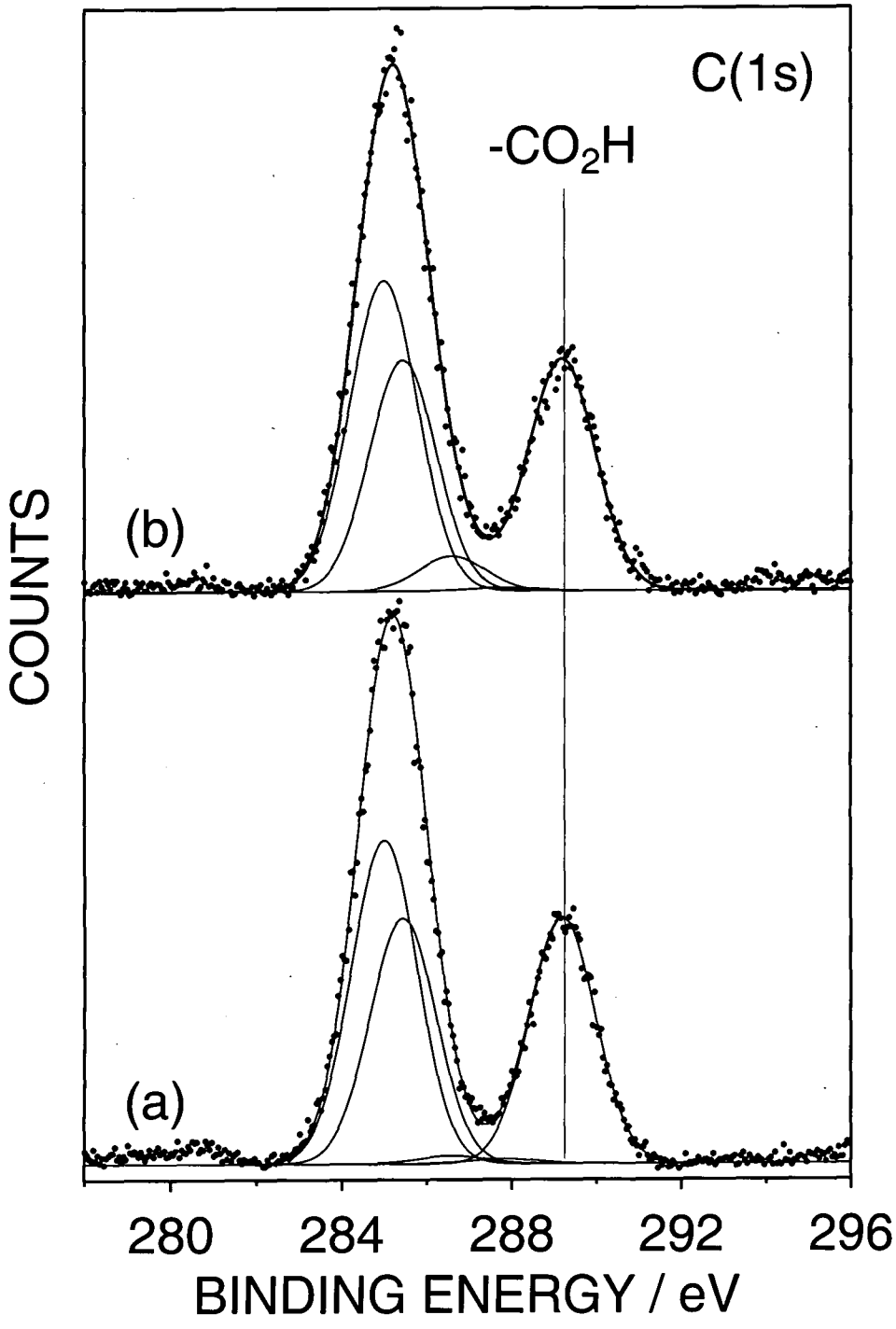

Figure 6.1 C(1s) XPS spectra of (a) conventional polyacrylic acid, and (b) APGD deposited plasma polymer.

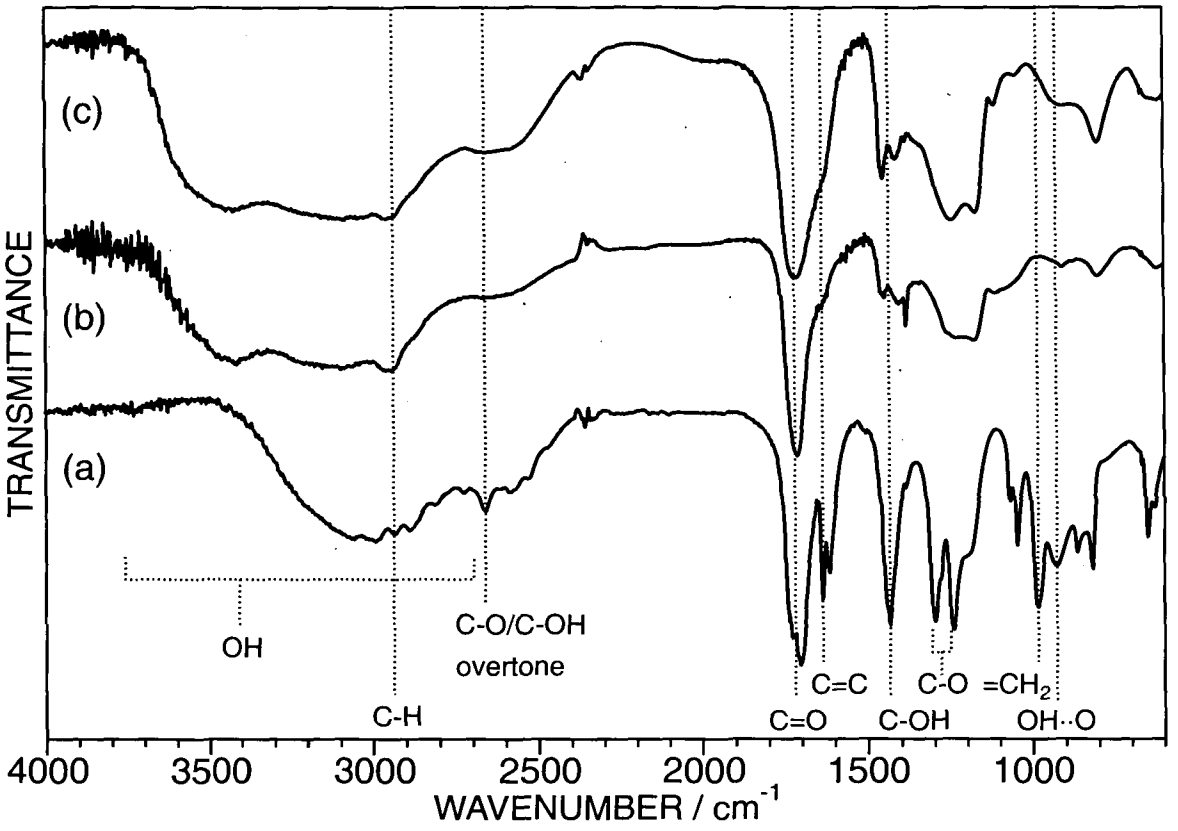

Figure 6.2 Transmission FT-IR spectra of: (a) acrylic acid monomer; (b) APGD polymerized acrylic acid; and (c) conventional polyacrylic acid.

6.3.2 APGD POLYMERIZATION OF 1H, 1H, 2H - PERFLUORO-1-OCTENE

Aside from a small amount of oxygen, the elemental abundances of plasma polymerized 1H, 1H, 2H - perfluoro-1-octene were in accordance with the monomer, Table 6.4. A high degree of monomer retention was confirmed by the C(1s) spectra, the large feature at high binding energy unambiguously announcing the presence of fluoroalkyl functionalities, Figure 6.3.

The plasma polymer structure was quantitatively investigated by peak-fitting using the following scheme: $\underline{C}$-CF_n (and C-O) at 286.6 eV, $\underline{C}$-F (and C=O) at 287.8 eV, $\underline{C}F$-CF_n (and CO_2R) at 289.0 eV, $\underline{C}F_2$ at 291.2 eV and $\underline{C}F_3$ at 293.3 eV, Table 6.5.[18,23] Allowance was also made for the corresponding Mg $K\alpha_{3,4}$ peaks which were shifted to ~9 eV lower binding energy.[24] This analysis indicated that whilst the total amount of perfluoroalkyl functionality was similar to that of the monomer some rearrangement has occurred, creating additional $\underline{C}$-CF_n, $\underline{C}$-F, and $\underline{C}F$-CF_n environments at the expense of $\underline{C}F_2$. The apparent increase in $\underline{C}F_3$ may be an artefact of these groups being aligned at the solid-air interface, creating an artificially intense XPS signal.[25]

Upon APGD deposition the FT-IR spectra of the 1H, 1H, 2H - perfluoro-1-octene monomer experienced the loss of the in plane $=CH_2$ deformation (1415 cm^{-1} and 1310 cm^{-1}) and the out of plane $=CH_2$ deformation (990 cm^{-1} and 910 cm^{-1}), Figure 6.4.[19,20] This suggests that, like acrylic acid, the perfluoroalkene is plasma polymerized via its carbon-carbon double bond. The presence in the polymer spectra of the sharp spectral features associated with the wide C-F band of the monomer (1350-1100 cm^{-1}) intimated retention of the perfluoroalkyl chain.[26,27]

Contact angle measurements demonstrated that the APGD deposited surfaces were hydrophobic, Table 6.4. A Zisman plot performed using a homologous series of n-alkanes yielded a critical surface tension (γ_c) value of 14 mN m^{-1}, Figure 6.5 and Table 6.4. This γ_c is below that of the benchmark hydrophobic surface PTFE (γ_c=18 mN min^{-1}) and characteristic of a surface possessing CF_3 functionalities.[28,29]

	% C	% F	% O	C.A. (water) /°	C.A. (decane) /°	γ_c /mN m^{-1}	Deposition Rate /nm min^{-1}
Theoretical	38.1	61.9	0	-	-	-	-
APGD polymer	38.0 ±0.1	60.0 ±0.1	2.1 ±0.1	118.9 ±3.0	61.1 ±2.2	14.3	159 ±15

Table 6.4 XPS, contact angle and deposition rate measurements for the APGD polymer of 1H, 1H, 2H - perfluoro-1-octene.

	% $\underline{C}_xH_y$	% $\underline{C}$-CF_n	% $\underline{C}$-F	% CF-CF_n	% $\underline{C}F_2$	% $\underline{C}F_3$	% ($\underline{C}F_2$+$\underline{C}F_3$) retention
Theoretical	12.5	12.5	0	0	62.5	12.5	100
APGD polymer	10.7 ±0.7	19.5 ±1.3	3.8 ±1.5	8.2 ±1.6	43.5 ±1.8	14.3 ±0.2	77.0 ±2.7

Table 6.5 Comparison of the actual and expected distribution of chemical environments within the 1H, 1H, 2H - perfluoro-1-octene plasma polymer films, as determined by C(1s) XPS peak-fitting.

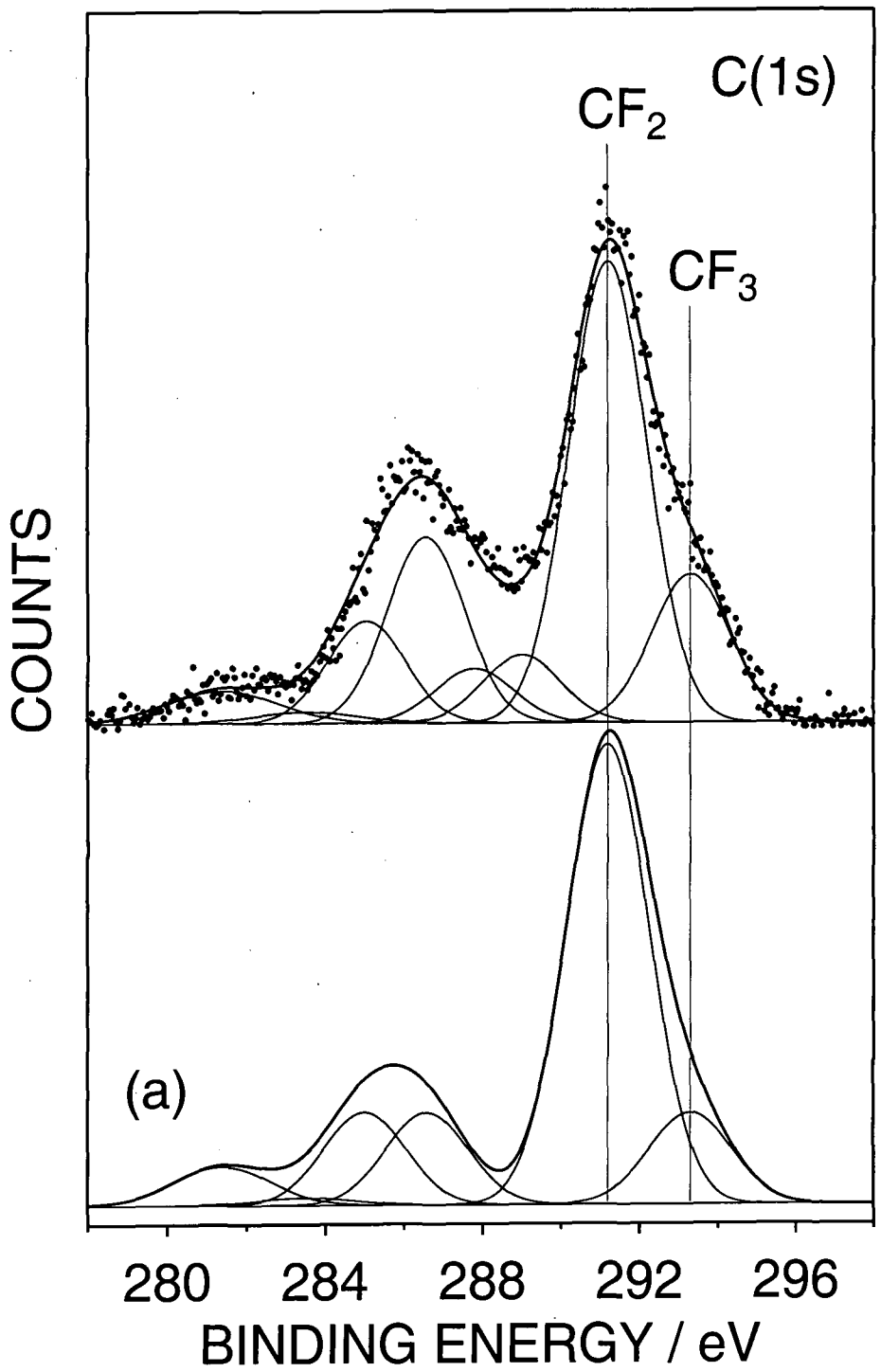

Figure 6.3 C(1s) spectra of (a) theoretical polymer of 1H, 1H, 2H - perfluoro-1-octene (b) APGD deposited polymer of 1H, 1H, 2H - perfluoro-1-octene.

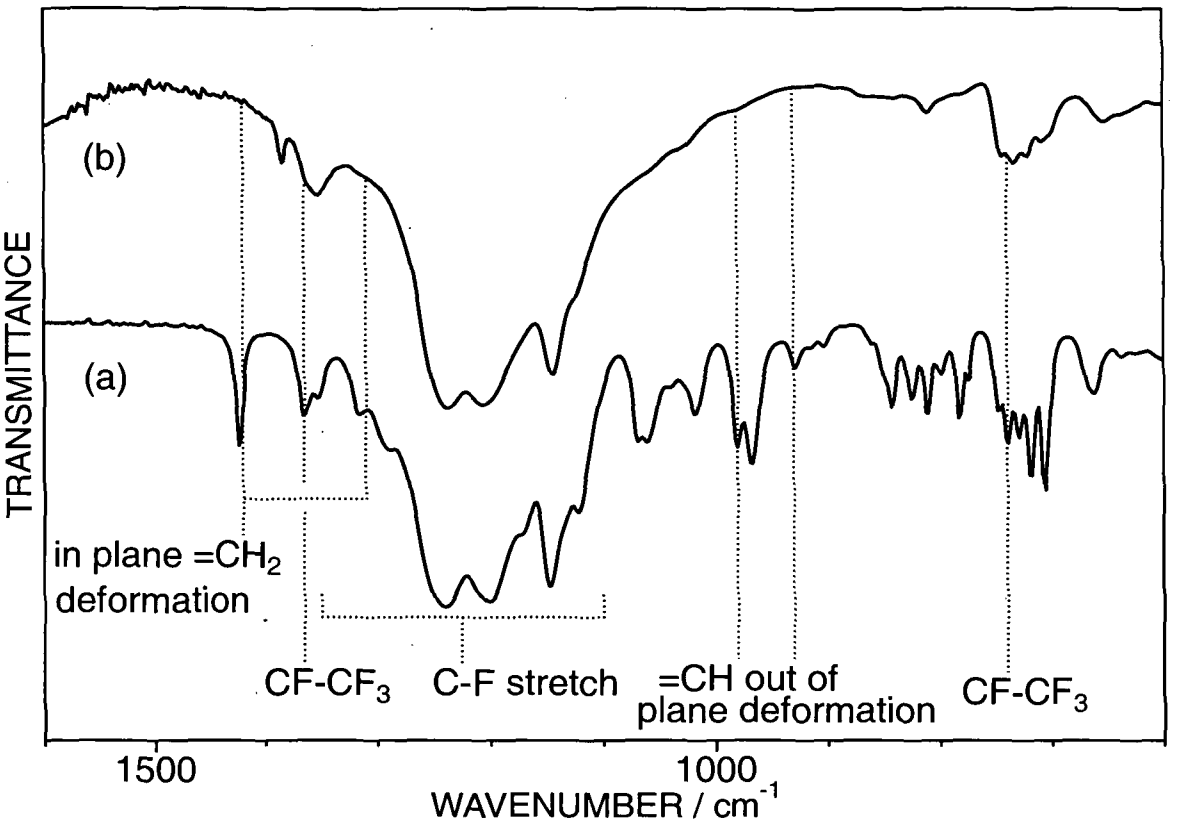

Figure 6.4 FT-IR spectra of (a) 1H, 1H, 2H - perfluoro-1-octene monomer (b) APGD plasma polymer of 1H, 1H, 2H - perfluoro-1-octene.

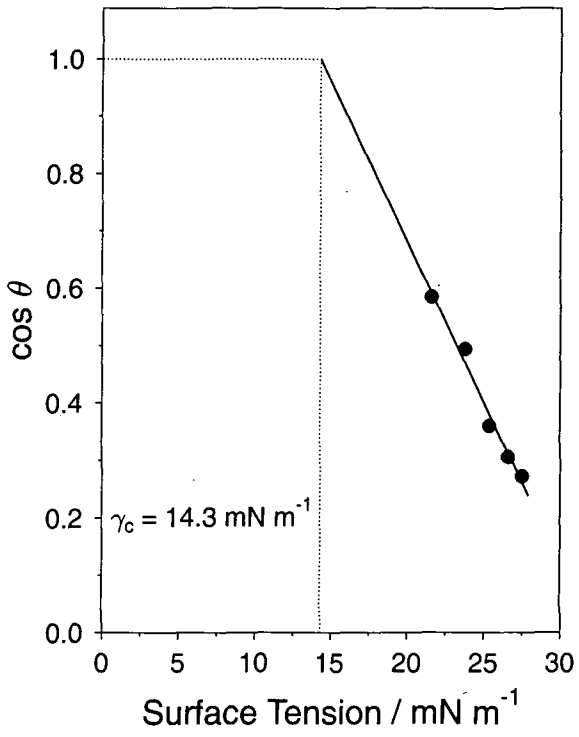

Figure 6.5 Zisman plot of the 1H, 1H, 2H - perfluoro-1-octene APGD plasma polymer.

6.4 DISCUSSION

Ultrasonic atomization of acrylic acid and 1H, 1H, 2H - perfluoro-1-octene into an APGD gave rise to the rapid deposition of highly functionalized plasma polymer layers. XPS and FT-IR analysis indicated that polymerization proceeds predominantly via the C=C bond.

The principle mechanism for activation within an APGD is the Penning reaction involving metastable helium.[30] These excited species possess high internal energies (2^3S: 19.8 eV, 2^1S: 20.7 eV)[30] and would be expected to be highly destructive as most molecules undergo dissociation at approximately 5-10 eV.[31] The deleterious effect of metastable helium upon organic surfaces is in fact utilized in techniques such as CASING (cross-linking via activated species of inert gases),[32,33] neutral atom lithography[34] and atomic beam imaging.[35] The high level of structural retention and low degree of cross-linking

within the deposited plasma polymers is hence somewhat surprising. A possible reason for this phenomena is the inherent surface specificity of APGD. Metastable helium atoms are immediately quenched upon interaction with a surface, leaving an inert ground state species which cannot cause further damage.[35] In addition electrons released within a polymer by Penning ionization have short inelastic scattering lengths (<1 nm, assuming an electron energy of 10 eV), minimising their potential for subsurface damage.[34] These factors limit the damage capability of APGD to the outermost layers of the growing film. The rapid deposition rate would augment this effect, screening the growing plasma polymer and protecting it from post-deposition degradation. An additional plasma property which may further encourage structural retention is the low ion velocity within an APGD, meaning that the effects of ion bombardment can be neglected.[36] In contrast, the ion bombardment and VUV radiation instrumental in low pressure plasmas can induce profound changes deep within deposited films.[1,37]

The slight loss of structural retention experienced by the perfluoroalkene may be attributable to its lower deposition rate (159 nm min^{-1} c.f. 231 nm min^{-1} for acrylic acid) conferring a reduced degree of shielding from metastable helium. An alternative explanation is provided by the possible presence of free fluorine atoms. These highly reactive species are known to cause chain scission and subsequent rearrangements in low pressure discharges.[1]

The appreciable gas barrier of plasma deposited polyacrylic acid is most likely a consequence of inter-chain bonding between carboxylic acid groups. Polar interactions are known to increase the cohesive energy of polymers, decreasing their segmental mobility and consequently the transmission of permeants, Table 6.3.[38]

Polar interactions are also thought to be the source of polyacrylic acid's adhesive powers. The ability of carboxylic acid group functionalized materials to improve inter-polymer bonding is well known and finds application in pressure sensitive adhesives.[39] Additionally, the soft and flexible nature of the polyacrylic acid will have maximized the contact between the two pieces of nylon, compensating for any asperities.

6.5 CONCLUSIONS

An APGD reactor equipped with an ultrasonic nozzle was used to deposit thick, highly functionalized films from organic precursors. The polyacrylic acid plasma polymer possessed adhesive and gas barrier characteristics whilst the 1H, 1H, 2H - perfluoro-1-octene polymer was hydrophobic.

6.6 REFERENCES

[1] Yasuda, H. *Plasma Polymerisation*; Academic Press: Orlando, 1985.

[2] Morosoff, N. An Introduction to Plasma Polymerization In. *Plasma Deposition, Treatment, and Etching of Polymers*; d'Agostino, R., Ed.; Academic Press: San Diego, CA, 1990; Chapter 1

[3] Adamson, D.V. U.S. Patent 4902590, Feb. 20, 1990

[4] Novis, Y.; Chaib, M.; Caudana, R.; Lutgen, P.; Feyder, G. *Brit. Polym. J.* **1989**, *21*, 171

[5] Ko, T.-M.; Cooper, S.L. *J. Appl. Polym. Sci.* **1993**, *47*, 1601

[6] Huang, R.Y.M. U.S. Patent 4,892,661 Jan. 9, 1990

[7] Chapiro, A.; Seidler, P. U.S. Patent 3,839,172 Oct. 1, 1974

[8] Saotome, K. U.S. Patent 5,026,596 June 25, 1991

[9] Klinger, L.; Griffith, J.R.; Rall, C.J.N. *Org. Coat. Appl. Polym. Sci. Proc.* **1983**, *48*, 407

[10] Bonardi, C. Eur. Patent Appl. EP 426530 May 8, 1991

[11] DeMarco, C.G.; Macquade, A.J.; Kennedy, S.J. *J. Mod. Text. Mag.* **1960**, *2*, 50

[12] Morita, S.; Ikeda, S.; Ishibashi, S.; Ieda, M.; Norimatsu, T.; Tamanaka, C. *International Symposium on Plasma Chemistry* **1981**, *5, 272*

[13] Chen, W.; Fadeev, A.Y.; Hsieh, C.; Oner, D.; Youngblood, J.; McCarthy, T.J. *Langmuir* **1999**, *15,* 3395

[14] Technical Information, *Aquila Instruments,* Cambridge, U.K.

[15] Shafrin, E.G.; Zisman, W.A. *J. Phys. Chem.* **1960**, *64*, 519

[16] Jasper, J.J. *J. Phys. Chem. Ref. Data* **1972**, 1, *841*

[17] Comyn, J. *Adhesion Science;* RSC: Cambridge, 1997; Chapter 9

[18] Beamson, G.; Briggs, D. *High resolution XPS of Organic Polymers: The Scienta ESCA300 Database*; 1st ed.; John Wiley & Sons: Chichester, 1992.

[19] Lin-Vien, D.; Colthup, N.B.; Fateley, W.G.; Grasselli, J.G. *The Handbook of Infrared and Raman Characteristic Frequencies of Organic Molecules*; Academic: San Diego, CA, 1991; Chapter 6

[20] Bellamy, L.J. *The Infrared Spectra of Complex Molecules*; Chapman and Hall: London, 1986; Chapter 3

[21] Bellamy, L.J. *The Infrared Spectra of Complex Molecules*; Chapman and Hall: London, 1986; Chapter 6

[22] Wilson, M.D.; Whitesides, G.M. *J. Am. Chem. Soc.* **1988**, *110*, 8718

[23] Clark, D. T.; Shuttleworth, D. *J. Polym. Sci. Chem. Ed.* **1980**, *18*, 27.

[24] *Practical Surface Analysis Volume 1 - Auger and X-ray Photoelectron Spectroscopy*, 2nd ed.; Briggs, D., Seah, M.P., Eds.; Wiley: Chichester, U.K., 1990

[25] Coulson, S.R. PhD. Thesis ,University of Durham, 1999

[26] Bellamy, L.J. *The Infrared Spectra of Complex Molecules*; Chapman and Hall: London, 1986; Chapter 19

[27] Lin-Vien, D.; Colthup, N.B.; Fateley, W.G.; Grasselli, J.G. *The Handbook of Infrared and Raman Characteristic Frequencies of Organic Molecules*; Academic: San Diego, CA, 1991; Chapter 3

[28] Adamson, A.W.; Gast, A.P. *Physical Chemistry of Surfaces*, Wiley: New York, 1997; Chapter 10

[29] Zisman, W.A. Influence of Constitution on Adhesion. In *Handbook of Adhesives;* 2nd ed. Skeist, I., Ed.; VNR: New York, 1977; Chapter 3

[30] Sawada, Y.; Ogawa, S.; Kogoma, M. *J. Phys. D: Appl. Phys.* **1995**, *28*, 1661

[31] Yokoyama, T.; Kogoma, M.; Moriwaki, T.; Okazaki, S. *J. Phys. D.: Appl. Phys.* **1990**, *23*, 1125

[32] Massines, F.; Gouda, G. *J. Phys. D.:Appl. Phys.* **1998**, *31*, 3411.

[33] Egitto, F.D.; Vukanovic, V.; Taylor, G.N. Plasma Etching of Organic Polymers In. *Plasma Deposition, Treatment, and Etching of Polymers*; d'Agostino, R., Ed.; Academic Press: San Diego, CA, 1990; Chapter 5

[34] Bell, A.S.; Brezger, B.; Drodofsky, U.; Nowak, S.; Pfau, T.; Stuhler, J.; Schulze, T.; Mlynek, J. *Surface Science* **1999**, *433-435*, 40

[35] Bard. A.; Berggren, K.K.; Wilbur, J.L.; Gillaspy, J.D.; Rolston, S.L.; McClelland, J.J.; Phillips, W.D.; Prentiss, M.; Whitesides, G.M. *J. Vac. Sci. Technol. B.* **1997**, *15*, 1805

[36] Prat, R.; Koh, Y.J.; Babukutty, Y.; Kogoma, M.; Okazaki, S.; Kodama, M. *Polymer* **2000**, *41*, 7355

[37] Biederman, H.; Martinû, L. Plasma Polymer-Metal Composite Films In. *Plasma Deposition, Treatment, and Etching of Polymers*; d'Agostino, R., Ed.; Academic Press: San Diego, CA, 1990; Chapter 4

[38] Rogers, C.E. In *Polymer Permeability*; Comyn, J., Ed.; Elsevier Applied Science: Barking, UK, 1985; Chapter 2

[39] Gross, M.E.; Weber, C.D. Carboxylic Polymers in Adhesives. In *Handbook of Adhesives;* 2nd ed. Skeist, I., Ed.; VNR: New York, 1977; Chapter 20

CHAPTER 7

CONCLUSIONS AND FUTURE WORK

7.1 CONCLUSIONS

The primary aim of this project was an efficient, atmospheric pressure means of creating siliceous gas-barrier films. There have, however, been departures from this theme such as the development of a chlorosilane coupling methodology and the deposition of functionalized organic polymers. The following is a summary of each chapter's findings, highlighting where applicable their influence upon subsequent work.

Chapter 2 examined the plasma oxidation of three spin-coated, organo-silicon polymers: a polysilane and two polysilsesquioxanes. Air dielectric barrier discharge (DBD) treatment caused the rapid loss of organic functionality and the formation of a shallow, SiO_x rich layer (1-20 nm thick). The extent of surface elemental change (detected by XPS), depth of oxidation and the degree of morphological disruption were found to be linked. Experimental factors such as total plasma on-time, applied voltage and the gap between successive voltage pulses were also important.

Unfortunately the shallow oxidation depth and cracking observed in DBD oxidized organo-silicon polymers rendered them unsuitable for gas barrier applications. In order to overcome these deficiencies an alternative methodology using chlorosilanes and the atmospheric pressure glow discharge (APGD) plasma was developed (Chapter 3). The vapour-phase condensation of substituted chlorodisilanes (SCDS) upon a DBD pre-treated polymer substrate was found to yield a coating akin to slightly cross-linked polydimethylsiloxane (PDMS). Upon plasma oxidation this condensed-SCDS developed a thin, SiO_x rich, surface layer, amenable to further iterations of SCDS deposition and oxidation. When oxidized using the more homogenous APGD plasma the resultant stratified coatings, containing several layers of SiO_x, were possessed of significantly enhanced gas barrier and slower hydrophobic recovery than their DBD treated counterparts. In addition, the silanol rich surfaces exhibited the capacity for further functionalization with conventional chlorosilane coupling agents (e.g. R_FSiMe_2Cl).

A contrasting approach to the vapour-phase deposition methodology described above was to bring the organo-silicon oxidation precursor out from within the polymer substrate (Chapter 4). Annealing films consisting of a PDMS

based additive within a polyethylene homopolymer yielded surfaces enriched in silicon, the degree of enhancement depending upon the additive structure. Upon oxidation these disparities in surface PDMS concentration yielded differences in surface SiO_x content. This allowing, in turn, the surface attachment of different quantities of chlorosilane coupling agent. The greater homogeneity of APGD was again manifested by the slower hydrophobic recovery of the APGD oxidized films compared to those treated with the DBD.

However, the laborious SCDS multi-layer method was, as yet, the only approach to yield significant gas barrier behaviour. A more efficient approach, requiring only one treatment cycle, was to deposit a continuous SiO_x coating by oxidising the precursor in the gas phase. This was achieved using a specially built APGD / ultrasonic-nozzle reactor (Chapter 5). The delivery of siloxanes into an oxygen containing APGD plasma resulted in the rapid deposition of a highly oxidised, hydrophilic, siliceous gas barrier material. Conversely, deposition within a non-oxidative APGD was found to yield hydrophobic, polysiloxane-like films.

The discretionary retention of siloxane functionality in the previous study intimated the possibility of depositing functionalised organic polymers. The successful deposition of acrylic acid and perfluoro-1-octene with the APGD / ultrasonic nozzle apparatus confirmed this. The rapid deposition rate facilitated by the ultrasonic nozzle and the low ion velocity within the plasma appearing to protect the growing polymer from the damage often witnessed in low pressure plasma deposition (Chapter 6).

In summary, atmospheric pressure plasmas were shown to be an effective means of oxidizing surfaces. However, only the more homogenous APGD plasma yielded SiO_x rich coatings of sufficient integrity to significantly reduce oxygen transmission (and to a lesser extent hydrophobic recovery). APGD, in conjunction with an ultrasonic nozzle was also shown to be a novel and effective means of depositing both SiO_x rich barrier layers and polymeric materials (organic and inorganic) retaining much of the monomer's characteristics.

7.2 FUTURE WORK

The limited duration of this research left several topics relatively unexplored. The APGD / ultrasonic-nozzle reactor which was built late in the project is a prominent example. The results obtained so far, whilst promising much, may only partially reflect its capability. A possible instrumental improvement is the installation of a heated substrate holder. This would extend the range of usable, involatile, monomers and facilitate the removal of organic contaminants from SiO_x films. Additionally, a more advanced high-voltage supply would allow the effects of different electronic parameters upon product structure to be fully explored. Of particular interest would be pulsing the plasma on-time, a technique known to enhance monomer retention in low pressure plasmas.

The rapid pace of this project also left a number of specific queries unanswered. Several questions awaiting future work are listed below:

The oxidation of PMSQ (Chapter 2) was thought to result in the especially rapid formation of a thin, highly oxidized SiO_x crust, the depth of which may have been dependent on the off-time between pulses. This explanation whilst supported by argon-ion depth profiling and peak-fits of the Si(2p) XPS envelope remained contentious (especially as argon-ion depth profiling is unreliable at short sputter times). A more surface sensitive technique than XPS, such as SIMS (secondary ion mass spectroscopy) would confirm the presence of a well-defined SiO_x surface layer of sub-XPS sampling depth thickness. Similarly SIMS analysis may verify the explanations given for the greater degree of PFDMCS attachment to (a) oxidized AB/PE blends compared to ABA/PE (inspite of AB/PE's lower $\%SiO_x$) and (b) DBD oxidized ABA/PE and AB/PE rather than their APGD treated counterparts (Chapter 4).

The assumed homogeneity of APGD treatment (compared to that of DBD) has been repeatedly cited as a cause of enhanced gas barrier properties (Chapter 3, SCDS multi-layers) and slower hydrophobic recovery (Chapters 3 and 4). This postulate could be investigated with AFM, the roughness measuring methods contained within the AFM software enabling quantitative analysis.

APPENDIX

COLLOQUIA, SEMINARS, PRESENTATIONS AND LECTURE COURSES

UNIVERSITY OF DURHAM
BOARD OF STUDIES IN CHEMISTRY

COLLOQUIA AND SEMINARS FROM INVITED SPEAKERS

1997

October 15 — Dr R M Ormerod, Keele University ,
Studying catalysts in action.

October 22 — Professor R J Puddephatt, University of Western Ontario.
Organoplatinum chemistry and catalysis.

October 23 — Professor M R Bryce, University of Durham.
New Tetrathiafulvalene Derivatives in Molecular, Supramolecular and Macromolecular Chemistry: controlling the electronic properties of organic solids.

November 12 — Dr J Frey, Department of Chemistry, Southampton University.
Spectroscopy of liquid interfaces: from bio-organic chemistry to atmospheric chemistry.

December 2 — Dr C J Ludman, University of Durham.
Explosions.

1998

January 14 — Professor D Andrews, University of East Anglia
Energy transfer and optical harmonics in molecular systems

March 11 — Professor M J Cook, Dept of Chemistry, UEA
How to make phthalocyanine films and what to do with them.

October 21 — Professor P Unwin, . Warwick University
Dynamic Electrochemistry: Small is Beautiful.

October 23	Professor J C Scaiano, Department of Chemistry, University of Ottawa, Canada In Search of Hypervalent Free Radicals, RSC Endowed Lecture
October 28	Professor J P S Badyal, University of Durham. Tailoring Solid Surfaces, Inaugural Lecture.
November 3	Dr C J Ludman, University of Durham. Bonfire night Lecture.
November 18	Dr R Cameron, Department of Materials Science & Metallurgy, Cambridge University Biodegradable Polymers

1999

January 20	Dr A Jones, University of Edinburgh. Luminescence of Large Molecules: from Conducting Polymers to Coral Reefs.
January 27	Professor K Wade, Department of Chemistry, University of Durham. Foresight or Hindsight? Some Borane Lessons and Loose Ends.
February 10	Dr C Bain, University of Oxford Surfactant Adsorption and Marangoni Flow at Expanding Liquid Surfaces
February 17	Dr B Horrocks, Department of Chemistry, Newcastle University Microelectrode techniques for the Study of Enzymes and Nucleic Acids at Interfaces

October 27	Dr. C. Braddock, Imperial College Novel catalysts for Atom Economic Transformations
November 3	Professor D.W. Smith, University of Waikato, NZ The Strengths of C-C and C-H Bonds in Organic and Organometallic Molecules: Empirical, Semi-empirical and Ab Initio Calculations
November 10	Dr. I. Samuel, Department of Physics, University of Durham Improving Organic Light Emitting Diodes by Molecular, Optical and Device Design
November 24	Professor T. Jones, Imperial College Atomic and Molecular Control of Inorganic and Organic Semiconductor Thin Films
November 30	Rev. R. Lancaster Principles and Practice
2000	
January 19	Dr. P.R. Fielden, UMIST Miniaturised Chemical Analysis (Lab-on-a-Chip): Functional or Merely Fashionable?
February 23	Dr. N. Clarke, UMIST The Flow of Polymer Blends
March 1	Professor D. Tildsley, Unilever (Head of Research) Computer Simulation of Interfaces: Fact and Friction

EXAMINED LECTURE COURSES

Mass Spectrometry, M. Jones

Electron Microscopy, K. Durose

Experimental Design and Instrumentation, J. P. Badyal

CONFERENCES ATTENDED

February 1998: IEEE Colloquium on Atmospheric Discharges for Chemical Synthesis

PRESENTATIONS

September 2000: Dow Corning Technical Forum, Barry, U.K.